THÈSE

PRÉSENTÉE À

L'UNIVERSITÉ BORDEAUX 1

ÉCOLE DOCTORALE DE

SCIENCES PHYSIQUES ET DE L'INGÉNIEUR

par Mlle KAMILA SIEJA

POUR OBTENIR LE GRADE DE

DOCTEUR DE L'UNIVERSITÉ BORDEAUX 1

SPÉCIALITÉ : PHYSIQUE NUCLÉAIRE

———————————————

EXTENDED APPROACH TO CORRELATIONS BEYOND MEAN-FIELD IN ATOMIC NUCLEI

———————————————

Soutenue le 26 fevrier 2007

Après avis de MM. J.-F. Berger Rapporteurs
J. Dobaczewski

Devant la commission d'examen formée de :

M.	A. Gozdz,	Professeur, Université de Lublin (Pologne)	Président
MM.	J.-F. Berger,	Physicien, CEA Bruyères-le-Châtel	Examinateurs
	J. Dobaczewski,	Professeur, Université de Varsovie (Pologne)	
	B. Pomorska,	Professeur, Université de Lublin (Pologne)	
	K. Pomorski,	Professeur, Université de Lublin (Pologne)	
	P. Quentin,	Professeur, Université Bordeaux 1	

Centre d'Etudes Nucléaires de Bordeaux – Gradignan

Pour vous seuls, fils de la doctrine et de la sapience, nous avons écrit cette oevre. Scrutez le livre, recueillez-vous dans cette intention que nous y avons dispersée et placée en plusieurs endroits; ce que nous avons occulté dans un endroit, nous l'avons manifesté dans un autre, afin que votre sagesse puisse le comprendre.

Heinrich Cornelius Agrippa von Nettesheim, *De occulta philosophia*, 3.65.

Contents

List of Figures

List of Tables

Chapter 1

Introduction

Any attractive interaction between fermions at low temperatures generally leads to a fermion pairing analogous to the Cooper pairing of electrons in superconducting metals. Thus it is not surprising that pairing lies at the heart of nuclear physics. It is present in finite nuclei, in the nuclear matter of neutron stars (nucleonic pairing) and it is believed to exist in quark-gluon plasma (color superconductivity).

While the concept of the nuclear pairing was introduced at a very early stage of the nuclear structure studies [1, 2], there are still questions regarding this fundamental many-body mode, *e.g.* what is the microscopic origin of many-body pairing in finite nuclei, what part of the effective interaction comes directly from the bare force and what part is induced [3].

Pairing can determine the stability of nuclei. A classic example is the chain of helium isotopes among which only the N-even ones are bound. Such an odd-even effect in nuclear binding energies is well known and particulary important near the drip lines, where the mean-field approximation is no longer a viable approach.

Since the number of nucleons can be precisely controlled, atomic nuclei are wonderful laboratories of pairing in finite many-body systems. Extremely proton or neutron rich nuclei are supposed to form various superconducting phases with Cooper pairs carrying different spin, isospin and angular momenta. In proton-rich nuclei the coupled proton and neutron fields may lead to a rise of deuteron-like (S=1) pairs.

The concept of such pairing, *i.e.* the proton-neutron (pn) pairing, was envisaged over fourty years ago [4]. Theoretical models with the inclusion of proton-neutron pairs like BCS approaches [5, 6, 7, 8, 9, 10, 11], quasi-spin formalism [12, 13], Independent Boson Models [14, 15] etc. have arised and have been constantly developed giving some idea of the importance of such correlations in the theoretical treatment and yielding sometimes a picture more consistent with experimental data as compared to the models excluding the possibility of pn pairs.

Recently a revival of the interest on the subject of the pn pairing is taking place due to the new experimental possibilities. In last years international research has focused on exotic nuclei. The first synthesized elements revealed unexpected deformations and new radioactivities [16, 17, 18, 19, 20]. New facilities using Rare

Isotopes Beams are still to come (*e.g.*, SPIRAL 2 (Système de Production d'Ions Radioactifs en Ligne) [21], EURISOL (European Isotope Separation On-Line) [22]). They would allow to perform experiments on a wide range of neutron and proton-rich nuclei far from the stability line using different production mechanisms and techniques to create unprecedented high intensity beams. Gamma ray detectors of new generation which can be exploited with radioactive and stable beams and with much improved capabilities and much higher sensitivity than existing instruments are as well under construction (AGATA (Advanced Gamma Tracking Array) [23], GRETA (Gamma Ray Tracking Array) [24]).

However, it is fair to say that so far there is no direct experimental evidence for *pn* pairing. The distinctive existence of the deuteron is a proof that the $T = 0$ channel is an important part of the nuclear interaction but not that a deuteron-like condensate can be created in heavier, open-shell systems. It was argued based on a phenomenological analysis of nuclear binding energies of $N = Z$ systems that there is a strong evidence for the isovector *pn* pairing while there is little room, if at all, for the existence of $T = 0$ pair correlations [25, 26].

It goes without saying, that in view of new experiments with exotic nuclei planned, a fair theoretical description of them is required. On the proton-rich side, where the proton-neutron pairing may play a role, a reliable approach can not exclude such correlations. On the other hand, future experiments may lead to a clear answer on what is the role of the *pn* pairing in the description of ground and excited states of exotic nuclei and in decay processes, and what is the interplay between $T = 0$ and $T = 1$ forces in the particle-particle channel.

It is our belief that a fully microscopic theory of nuclei should include explicitely the proton-neutron coupling already in the particle-hole channel and then be taken into account in the residual interaction. A step towards has been already done in Ref. [27] where the general Hartree-Fock-Bogoliubov (HFB) formalism which fully incorporates the proton-neutron mixing on the mean-field level was derived. In the present work, since we use different forces in the particle-hole and particle-particle channels, the terms arising in the effective interaction when densities mix protons and neutrons were not introduced. We focus here on the proton-neutron correlations beyond the mean-field, namely on the role of the *pn* pairing in the description of medium mass proton-rich nuclei ($A \sim 64$). First, we revisit and develop BCS and Lipkin-Nogami (LN) approaches to be able to describe isovector and isoscalar pairing correlations with the use of state-dependent forces. Most calculations of that type carried out so far based on schematic interactions, *i.e.* monopole pairing forces (see *e.g.* [11, 28, 29]). A density-dependent δ force has been already applied in the cranked HFB calculations with the proton-neutron pairing in high spin states (*e.g.* [30]), however no particle-number projection was done in such a case. Then, we discuss the method known as the Higher Tamm-Dancoff Approximation (HTDA), developed recently [31], which gives a possibility to study ground state correlations and excited states in a shell model-like framework. It is free of deficiencies of pairing

approaches of the Bogoliubov type (particle number non-conservation). A generalization of the HTDA method to deal with isovector and isoscalar pairs on the same footing is performed.

We start our considerations with reminding shortly the foundations of the mean-field theory (Chapter 2), *i.e.* the outline of the Hartree-Fock method is presented. We also discuss briefly phenomenological effective interactions and commonly used parametrizations. In Chapter 3 a short overwiev of experimental evidence and possible signatures of the proton-neutron pairing is presented. The phenomenological quantities for nuclei under consideration are derived from experimental data. In Chapter 4 the correlations of the pairing type are studied in the independent quasi-particle theory (BCS) with the use of an approximate particle projection (Lipkin-Nogami) and a realistic two-body contact force to describe the residual interaction and the possible extensions of the pairing interactions are studied. The generalization of models and numerical tools to account for the *pn* pairing is carried out. The problem of the Wigner term and its connections with the proton-neutron pairing is also addressed. In Chapter 5 we perform the study of the correlations beyond the mean-field in the HTDA approach. This method is used to describe ground state properties of considered nuclei and then extended to take into account as well proton-neutron pairs. The role of different types of particle-hole excitations in the ground states of considered nuclei is discussed. The connections of the HTDA results with the Hartree-Fock plus BCS calculations are indicated.

The main conclusions and perspectives for further research are presented in Chapter 6.

Chapter 2

Hartree-Fock method

The Hartree-Fock (HF) method, like many other ideas in nuclear physics, was genuinely introduced in another division of many-body theory, namely in atomic physics. Although the nucleus has much in common with an atom, nucleons are bound solely by their mutual interaction and, unlike the electrons, they do not feel any central field. Straightforward applications of many-body theories created for atomic or solid-state physics to nuclei usually pose difficulties as the nucleus has its own distinctive features, let us point out the short-range repulsive character of the nuclear force or the finite number of nucleons. Nevertheless, the Hartree-Fock method applied the first time to nuclear physics by Kelson in 1963 [32], remains a great advantage and many of other, more refined models, are only extensions of the basic HF ideas.

The Hartree-Fock self-consistent field method is an approximation for reducing the problem of many interacting nucleons to the description of non-interacting particles in a field. It is a great simplification but as well a harsh approximation which neglects a large part of the nucleon-nucleon force. Including the residual interaction ignored in the mean-field approximation is a major dillema of nuclear structure. The methods of treating the correlations beyond the mean-field are the main subject of this work, nonetheless let us first have a closer look to the self-consistent field theory in the present chapter.

2.1 Mean-field approximation

The assumption of the mean-field approach is that nucleons move independently in an average potential produced by all of nucleons. Such a potential can be determined empirically, which is the principle behind the shell model. Historically, the shell model potential was constructed to reproduce the magic numbers. A central field with a crucial spin-orbit interaction suggested the first time by Jensen and Goeppert-Mayer in 1949 [33], succeded with the requirements of reproducing shell closures. The most widely used empirical potentials are

- The Nilsson potential [34, 35], historically the first single-particle (sp) model taking into account nuclear deformations. It consists of the axially-deformed harmonic oscillator potential, a term related to the spin-orbit interaction and of a correction proportional to $\vec{l}^2$ that allows to lower the states with high angular momenta

$$V_{\text{Nilsson}} = \frac{m}{2} \left[\omega_\perp (x^2 + y^2) + \omega_z z^2 \right] - 2\kappa\hbar\omega_{00} \left(\vec{l} \cdot \vec{s} + \mu(\vec{l}^2 - < \vec{l}^2 >) \right), \quad (2.1)$$

where κ, μ are the potential parameters adjusted separately for protons and neutrons, ω_{00} is the spherical harmonic oscillator constant $\hbar\omega_{00}$=41 $A^{1/3}$ MeV that reproduces the nuclear radius.

- The Woods-Saxon potential [36], which represents a more realistic potential well that is consistent with our knowledge of nuclear density distributions:

$$V_{\text{WS}}(r) = -\frac{V_0}{1 + e^{(r-R)/a}}, \quad (2.2)$$

where the constant V_0 is the depth of the potential well. For a fixed angular direction, this potential depends on two additional parameters: the radius R and the surface diffusion a. Together with the spin-orbit term

$$V_{\text{so}} \sim \frac{1}{r} \frac{\mathrm{d}V_{\text{WS}}(r)}{\mathrm{d}r} \vec{l} \cdot \vec{s}. \quad (2.3)$$

it meets the requirements of reproducing the shell structure of nuclei.

The above potentials can be used to construct single-particle wave functions and energies. Yet, the single-particle potential can be as well derived from two-body interactions by a variational principle which is accomplished in the Hartree-Fock method. The phenomenological potentials are often used to initiate the self-consistent process of extracting the average field.

2.2   Variational principle. Hartree-Fock equations

The fundamental assumption of the HF theory is that the nuclear wave function Ψ_A is an antisymmetrized product of A independent particle wave functions Φ. The antisymmetrization operation leads to the normalized Slater determinant form of this function

$$\Psi_A = \frac{1}{\sqrt{A!}} \begin{vmatrix} \Phi_1(1) & \Phi_2(1) & \cdots & \Phi_A(1) \\ \Phi_1(2) & \Phi_2(2) & \cdots & \Phi_A(2) \\ \vdots & & & \\ \Phi_1(A) & \Phi_2(A) & \cdots & \Phi_A(A) \end{vmatrix}. \quad (2.4)$$

The best possible wave function of this type is found by application of the variational principle[1].

---

[1]An alternative understanding of the HF theory is not directly based on the variational method applied to the Slater determinant but rather on the assumption that the ground-state energy can be approximated by a functional of the one-body density matrix [37].

2.2.1   Variational principle

Consider the A-body system described by a Hamiltonian $\hat{H}$ and its eigenfunction $|\Psi_A\rangle$ which obeys the standard Schrödinger equation

$$\hat{H}|\Psi_A\rangle = E|\Psi_A\rangle \,. \tag{2.5}$$

The variational principle of Ritz states that the Eq. (2.5) is equivalent to the variational equation

$$\delta E[\Psi_A] = 0 \,, \tag{2.6}$$

with

$$E = \frac{\langle \Psi_A|\hat{H}|\Psi_A\rangle}{\langle \Psi_A|\Psi_A\rangle} \,. \tag{2.7}$$

The variational method is especially well suited for the determination of the ground state of the system. One can show for any trial function $|\Psi_i\rangle$ that

$$E[\Psi_i] \geq E_0 \,, \tag{2.8}$$

E_0 is always lower than the variational solution.

The variational approximation is based on the fact that $|\Psi_i\rangle$ can be usually restricted to a set of mathematically simple trial wave functions. If the true solution is not included in this set, the minimal solution is not the eigenfunction but only an approximation. Thus the quality of the variational approach depends on the choice of the set of trial wave functions. In order to decide which set is better to describe the ground state we have two criteria:
(i) if one set of the wave functions is a subset of the other, it is usually better to chose the larger one as it contains the first's set minimum;
(ii) out of the two trial wave functions the one for which the corresponding energy is lower should be better, since the exact E_0 is a lower bound.

2.2.2   Hartree-Fock equations

Deriving the Hartree-Fock equations one assumes that there exist an average potential (Hartree-Fock potential) whose eigenfunction corresponding to the lowest energy is an approximation of the exact ground state. This eigenfunction is a Slater determinant (2.4) that can be as well expressed as

$$|\Psi_A\rangle = \Pi_{i=1}^{A} a_i^{\dagger}|0\rangle \,, \tag{2.9}$$

where operators $a_i^{\dagger}$ correspond to single-particle wave functions Φ_i of an A-particle system and $|0\rangle$ is the particle vacuum. A Slater determinant is uniquely characterized by its hermitian, projective density matrix

$$\rho_{ij} = \langle \Psi_A|a_j^{\dagger}a_i|\Psi_A\rangle \,. \tag{2.10}$$

In the trial class of Slater determinants $\{\Psi_i\}$ consisting of A arbitrary but orthogonal single-particle wave functions, we want to minimize the expectation value of the many-body Hamiltonian

$$\hat{H} = \hat{K} + \hat{V} \tag{2.11}$$

where $\hat{K}$ is the kinetic energy operator and $\hat{V}$ an effective two-body interaction. In the second quantization formalism it reads

$$\hat{H} = \sum_{ij} k_{ij} a_j^\dagger a_i + \frac{1}{4} \sum_{ijkl} \tilde{V}_{ijkl} a_i^\dagger a_j^\dagger a_l a_k \,, \tag{2.12}$$

where $\tilde{V}_{ijkl}$ is the antisymmetrized matrix element of $\hat{V}$. The HF energy

$$E_{\mathrm{HF}} = \langle \Psi_A | \hat{H} | \Psi_A \rangle \tag{2.13}$$

with the use of Wick's thorem (Appendix C) can be given as a functional of the single-particle density

$$\begin{aligned}
E_{\mathrm{HF}}[\rho] &= \sum_{ij} k_{ij} \rho_{ji} + \frac{1}{2} \sum_{ijkl} \rho_{kj} \tilde{V}_{ijkl} \rho_{li} \\
&= \mathrm{Tr}(\hat{K}\rho) + \frac{1}{2} \mathrm{TrTr}(\rho \tilde{V} \rho) \,.
\end{aligned} \tag{2.14}$$

The variation of the energy (2.14) leads to the expression (for details see *e.g.* [38, 39])

$$\delta E_{\mathrm{HF}} = E_{\mathrm{HF}}[\rho + \delta\rho] - E_{\mathrm{HF}}[\rho] = \sum_{ij} h_{ij} \delta \rho_{ij} \,, \tag{2.15}$$

with the hermitian matrix

$$h_{ij} = \frac{\partial E_{\mathrm{HF}}[\rho]}{\partial \rho_{ij}} \,, \tag{2.16}$$

connected with the single-particle (Hartree-Fock) Hamiltonian

$$\hat{h}_{\mathrm{HF}} = \hat{k} + \hat{V}_{\mathrm{HF}} \,. \tag{2.17}$$

It is seen from Eq. (2.14) that $\hat{V}_{\mathrm{HF}} = \mathrm{Tr}(\rho \tilde{V})$ is a self-consistent field obtained by folding the two-body potential with a density distribution. In the canonical basis, *i.e.* in the basis where ρ is diagonal, the matrix elements of $\hat{V}_{\mathrm{HF}}$ for any single-particle states i, j are given as

$$\langle i | \hat{V}_{\mathrm{HF}} | j \rangle = \sum_k \langle ik | \hat{V} | jk \rangle \,, \tag{2.18}$$

where the summation runs *e.g.* over all the occupied states k.

The condition $\delta E_{\mathrm{HF}} = 0$ is equivalent to

$$[\hat{h}_{\mathrm{HF}}, \rho] = 0 \,. \tag{2.19}$$

This is a nonlinear equation since $\hat{H}_{\mathrm{HF}}$ depends on the density ρ. It also tells us that $\hat{h}_{\mathrm{HF}}$ and ρ have common eigenstates and can be diagonalized simultaneously. The

eigenstates of ρ are either the occupied states (eigenvalue 1) or unoccupied states (eigenvalue 0). We may use the freedom of choice of the canonical basis to define the HF basis and to diagonalize the Hartree-Fock Hamiltonian. This converts (2.19) into an eigenvalue problem

$$\hat{h}_{\mathrm{HF}}|\Phi_i\rangle = e_i|\Phi_i\rangle\,, \tag{2.20}$$

where e_i are called self-consistent single-particle energies.

The way to find the solution of the coupled, nonlinear equations (2.19) is to find iteratively the self-consistent mean-field. We start by choosing the single-particle Hamiltonian with a reasonable nuclear potential (*e.g.* the potential of the shell model, within this work we use the Woods-Saxon potential to initiate the calculations). Then, we diagonalize the Hamiltonian to find its eigenvectors. These eigenvectors allow to determine the density matrix and construct the self-consistent HF potential corresponding to the effective interaction. Within this new mean-field a new HF Hamiltonian is obtained and the iterative procedure can be restarted. The convergence is achieved when the potentials stay constant in two consecutive steps.

2.3 Numerical aspects

The Hartree-Fock method gives the answer to the question how the single-particle potential can be extracted out of the sum of two-body interactions. Nonetheless, another difficulty arises here: the bare nucleon-nucleon interaction is very ill behaved from the numerical point of view. A necessary condition for the success of the HF method is that the two-nucleon interaction has no infinities. Unfortunately, the interaction between two free nucleons is strongly repulsive at a distance ~ 0.4 fm. Thence the calculations of matrix elements of such an interaction are vastly problematic. However, a nucleon within the nucleus does not feel the bare nucleon-nucleon force but interact with another nucleon in the presence of many other particles. It then justifies replacing the realistic interaction with the hard core by a well behaved effective nucleon-nucleon interaction.

An effective interaction can be obtained microscopically by solving the Bethe-Goldstone equation [40]. Yet, solving it in finite nuclei presents many technical and formal problems. The way out is introducing the so-called reaction matrix G (Brueckner G-matrix) [41] which in diagrammatic language represents the sum over all ladder type of diagrams. This sum is meant to renormalize the repulsive short-range part of the interaction. With a given effective interaction one may work out the Hartree-Fock equations and then use the HF orbitals to obtain the effective interaction by resolving the Bethe-Goldstone equation. Such a doubly self-consistent procedure is called Brueckner-Hartree-Fock method. An approximative scheme that has become successful in connection with Brueckner-Hartree-Fock theory is the local density approximation [42, 43, 44] which relies on the assumption that the G-matrix

at any place in a nucleus is the same as for the nuclear matter of the same density, so locally one can determine the G-matrix as in nuclear matter calculations.

Determining microscopically effective interactions is non-trivial as well as getting with them the agreement with experiment. From the opposite point of view it may be asked if we can figure out the nuclear interaction from empirical binding energies and spectra. Consequently, phenomenological effective interactions with a number of parameters adjusted to reproduce experimental data are widely used. There exists an enormous quantity of different phenomenological interactions that have been applied to various aspects in nuclear physics. They are employed in specific problems on which their range of validity depend very much. A bunch of such interactions is suitable for the case of Hartree-Fock type of calculations, *i.e.* Gogny forces [45] and Skyrme forces described in the next section.

2.3.1   Skyrme interaction

In 1956 Skyrme [46, 47] proposed an effective interaction with a three-body term

$$V = \sum_{i<j} V(i,j) + \sum_{i<j<k} V(i,j,k) \,, \tag{2.21}$$

$$V(1,2,3) = t_3 \delta(\vec{r}_1 - \vec{r}_2)\delta(\vec{r}_2 - \vec{r}_3) \,. \tag{2.22}$$

The three-body term, purely local and repulsive, favours parallel spin alignement which contradicts the observed spin saturation and pairing properties of nuclei. Therefore, to avoid this difficulty the three-body term was replaced by Vautherin and Brink [48, 49] with a density-dependent two-body interaction

$$V(1,2,3) \longrightarrow V(1,2) = \frac{1}{6}t_3(1 + x_3 P^\sigma)\rho_{00}^\gamma(\frac{\vec{r}_1 + \vec{r}_2}{2})\delta(\vec{r}_1 - \vec{r}_2) \,. \tag{2.23}$$

Nowadays, the most commonly used form of the Skyrme interaction is the following

$$
\begin{aligned}
V_{\text{Sky}}(1,2) \;=\;& t_0(1 + x_0 P^\sigma)\delta(\vec{r}_1 - \vec{r}_2) \\
&+ \frac{1}{2}t_1(1 + x_1 P^\sigma)\left[\delta(\vec{r}_1 - \vec{r}_2)\boldsymbol{k}^2 + \boldsymbol{k'}^2\delta(\vec{r}_1 - \vec{r}_2)\right] + t_2(1 + x_2 P^\sigma)\boldsymbol{k'}\delta(\vec{r}_{12})\boldsymbol{k} \\
&+ iW_0(\vec{\sigma}_1 + \vec{\sigma}_2) \cdot \boldsymbol{k'} \times \delta(\vec{r}_1 - \vec{r}_2)\boldsymbol{k} \\
&+ \frac{1}{6}t_3(1 + x_3 P^\sigma)\rho_{00}^\gamma(\frac{\vec{r}_1 + \vec{r}_2}{2})\delta(\vec{r}_1 - \vec{r}_2) \,,
\end{aligned}
\tag{2.24}
$$

where $\boldsymbol{k}$ is the operator of the relative momentum

$$\boldsymbol{k} = \frac{1}{2i}(\vec{\nabla}_1 - \vec{\nabla}_2) \,, \tag{2.25}$$

$\boldsymbol{k'}$ acts on the left and $\hat{P}^\sigma = \frac{1}{2}(1 + \vec{\sigma}_1 \cdot \vec{\sigma}_2)$ is the standard spin exchange operator. The first parameter in (2.24), t_0, describes a pure δ-force with a spin exchange, the next two terms simulate the effective range and non-locality, the fourth term is the spin-orbit interaction in the form suggested by Skyrme. The parameters t_0, t_1, t_2, t_3,

x_0, x_1, x_2, x_3 W_0, γ are adjusted to experimental data, usually binding energies and radii of spherical nuclei and to reproduce properties of symmetric nuclear matter.

There are several sets of parameters called Skyrme I, II, etc. The first two, dubbed SI and SII, were introduced by Vautherin and Brink [48]. Within SII parametrization they were able to reproduce the binding energies over the whole periodic table and at the same time, the nuclear radii. This had not been possible with the usual density independent forces. Next parametrizations, SIII-SVI were found by Beiner *et al.* [50] by fitting the masses and charge radii of spherical nuclei. All these forces yielded similar results, however the one called SIII realized a reasonable compromise between the deeply-bound levels and those around the Fermi surface. The capability of reproducing overall level spectra in a satisfactory agreement with experiment and at the same time total binding energies and charge radii with a good accuracy, makes this force the most popular among SI-SVI parametrizations.

In addition to the 'classical' parametrizations SI-SVI, there exist a variety of others: the SkM of Krivine [51] fitted to reproduce well the mulitipole moments and charge radii, which gives however too low fission barriers, the improved version of SkM, called SkM* [52], modified to give a correct fission barrier of ^{240}Pu, the T6 of Tondeur *et al.* [53] which takes into account the width of the neutron skin in ^{208}Pb and assumes that the effective nucleon mass is equal to the mass of a free particle. A very special case was the SkP force [54] which was the first attempt to reproduce as well the data in the particle-particle channel. It is worth noting here the group of parametrizations introduced by Chabanat *et al* [55], with the most widely used SLy4 force, which is said to be suitable to reproduce well spectroscopic properties of nuclei far from the β-stability line.

In Table 2.1 we list the widely used parametrizations of the Skyrme force, beginning with the SIII one applied in this work.

Due to its zero-range force form that simplifies significantly all the calculations and its capacity to reproduce the masses and radii over the entire periodic table within a reasonable set of parameters, the Skyrme-force remains extensively used in Hartree-Fock calculations. However, despite the success of different Skyrme forces, it has been argued that the zero-range force might not be able to simulate the long range or even the intermediate range parts of the realistic effective interaction and, regardless of several encouraging attempts, fails to reproduce properly the pairing correlations in nuclei.

2.3.2 Skyrme energy functional

The total energy of a nucleus is given as a sum of kinetic energy, potential energy and Coulomb energy. Because of the zero-range of the Skyrme force (2.24) it is possible to express the energy by an integral over the energy density [48]

$$E = \langle \Psi_i | \hat{H} | \Psi_i \rangle = \int d\boldsymbol{r} \mathcal{H}_{\text{tot}}(\boldsymbol{r}) \,, \tag{2.26}$$

Table 2.1: Common parametrizations of the phenomenological Skyrme effective force.

	t_0 (MeVfm^3)	t_1 (MeVfm^5)	t_2 (MeVfm^5)	t_3 (MeVfm$^{3+3\gamma}$)	W_0 (MeVfm^5)
SIII	-1128.75	395.00	-95.00	14000.0	120.0
SkM*	-2645.00	410.00	-135.00	15595.0	130.0
SLy4	-2488.91	486.82	-546.39	13777.0	123.0

	x_0	x_1	x_2	x_3	γ
SIII	0.450	0.0	0.0	1.0	1
SkM*	0.090	0.0	0.0	0.0	$\frac{1}{6}$
SLy4	0.834	-0.344	-1.0	1.354	$\frac{1}{6}$

where the total energy functional $\mathcal{H}_{\text{tot}}(\boldsymbol{r})$ is the sum of Skyrme functional, kinetic and Coulomb energies:

$$\mathcal{H}_{\text{tot}}(\boldsymbol{r}) = \mathcal{H}_{\text{Sky}}(\boldsymbol{r}) + \mathcal{H}_{\text{kin}}(\boldsymbol{r}) + \mathcal{H}_{\text{Coul}}(\boldsymbol{r}) \,. \tag{2.27}$$

For the Slater determinant even due to the time-reversal symmetry (which is the case of the calculations performed in this work) $\mathcal{H}_{\text{Sky}}(\boldsymbol{r})$ can be decomposed as

$$\mathcal{H}_{\text{Sky}}(\boldsymbol{r}) = \mathcal{H}_{\text{vol}}(\boldsymbol{r}) + \mathcal{H}_{\text{surf}}(\boldsymbol{r}) + \mathcal{H}_{\text{so}}(\boldsymbol{r}) \,. \tag{2.28}$$

The $\mathcal{H}_{\text{tot}}(\boldsymbol{r})$ is an algebraic function of three quantities:
(i) the nucleon density

$$\rho(\boldsymbol{r}) = \sum_{i,\sigma} |\Phi_i(\boldsymbol{r}, \sigma)|^2 \tag{2.29}$$

(ii) the kinetic energy density

$$k(\boldsymbol{r}) = \sum_{i,\sigma} |\vec{\nabla} \Phi_i(\boldsymbol{r}, \sigma)|^2 \tag{2.30}$$

(iii) the so-called spin-orbit currents

$$\vec{J}(\boldsymbol{r}) = (-i) \sum_{i,\sigma\sigma'} |\Phi_i^\star(\boldsymbol{r}, \sigma)| \left[\vec{\nabla} \Phi_i(\boldsymbol{r}, \sigma') \times \langle \sigma | \vec{\sigma} | \sigma' \rangle \right] \,. \tag{2.31}$$

The summations are taken over all occupied single-particle states.

Within these definitions the terms appearing in Eq. (2.27) can be expressed in forms

$$\mathcal{H}_{\text{kin}}(\boldsymbol{r}) = \frac{\hbar^2}{2m} k^2 \,, \tag{2.32}$$

$$
\mathcal{H}_{\text{vol}}(\boldsymbol{r}) = \frac{1}{2}t_0(1 + \frac{1}{2}x_0)\rho^2 - \frac{1}{2}t_0(\frac{1}{2} + x_0)\sum_\tau \rho_\tau^2
$$
$$
+ \frac{1}{12}t_3(1 + \frac{1}{2}x_3)\rho^{\gamma+2} - \frac{1}{12}t_3(\frac{1}{2} + x_3)\rho^\gamma \sum_\tau \rho_\tau^2
$$
$$
+ \frac{1}{4}\left[t_1(1 + \frac{1}{2}x_1) + t_2(1 + \frac{1}{2}x_2)\right]\rho k
$$
$$
- \frac{1}{4}\left[t_1(\frac{1}{2} + x_1) - t_2(\frac{1}{2} + x_2)\right]\sum_\tau \rho_\tau k_\tau \,, \tag{2.33}
$$

$$
\mathcal{H}_{\text{surf}}(\boldsymbol{r}) = - \frac{1}{16}\left[3t_1(1 + \frac{1}{2}x_1) - t_2(1 + \frac{1}{2}x_2)\right]\rho\vec{\nabla}^2\rho
$$
$$
+ \frac{1}{16}\left[3t_1(\frac{1}{2} + x_1) + t_2(\frac{1}{2} + x_2)\right]\sum_\tau \rho_\tau\vec{\nabla}^2\rho_\tau \,, \tag{2.34}
$$

$$
\mathcal{H}_{\text{so}}(\boldsymbol{r}) = -\frac{1}{2}W_0\left(\rho\vec{\nabla}\vec{J} + \sum_\tau \rho_\tau\vec{\nabla}\vec{J}\right) \,. \tag{2.35}
$$

The total densities are defined as $\rho = \rho_n + \rho_p$, $k = k_n + k_p$ (kinetic energy density) and $\vec{J} = \vec{J}_n + \vec{J}_p$ (spin densities), where n, p corresponds to neutrons and protons, respectively.

The Coulomb energy functional consists of two terms, the direct term generated by the proton density ρ_p and the exchange term treated in the Slater approximation [56, 57]:

$$
\mathcal{H}_{\text{Coul}}(\boldsymbol{r}) = \frac{1}{2}\rho_\tau V_{\text{Coul}} - \frac{3e^2}{4}\left(\frac{3}{\pi}\right)^{1/3}\rho_p^{4/3} \,, \tag{2.36}
$$

where e is the electron charge and the Coulomb potential is given by

$$
V_{\text{Coul}}(\boldsymbol{r}) = e^2 \int d\boldsymbol{r}\frac{\rho_p(\boldsymbol{r}')}{|\boldsymbol{r} - \boldsymbol{r}'|} \,. \tag{2.37}
$$

The long-range character of the Coulomb interaction makes the exchange contribution to be only a small fraction of the total Coulomb energy therefore the local approximation for the exchange term, which assures the simplicity of the Skyrme - HF equations, is well satisfied. A comparison with exact calculations shows that the Slater approximation underestimates the Coulomb exchange part by less than 10% [58].

The Hartree-Fock equations for the Skyrme force are obtained by variation of the energy (2.26).

2.3.3 Constrained Hartree-Fock calculations

Unrestricted HF calculations give only one point on the energy surface, namely the local minima. Nevertheless, usually one searches for an energy surface as a function of one or more collective parameters q, *i.e.* quadrupole and hexadecapole

deformations. In these cases we are interested in a wave function $|\Psi_i(q)\rangle$ which minimizes the energy under the constraint that a certain operator has a fixed average value

$$q = \langle\Psi_i|\hat{Q}|\Psi_i\rangle = \langle\hat{Q}\rangle. \tag{2.38}$$

The method for solving this problem is adding an extra term to the Hamiltonian

$$\langle\Psi_i|\hat{H}'|\Psi_i\rangle = \langle\Psi_i|\hat{H}|\Psi_i\rangle + f(\mu, \langle\hat{Q}\rangle), \tag{2.39}$$

where f is a function of μ and $\langle\hat{Q}\rangle$, and minimizing $\langle\Psi_i|\hat{H}'|\Psi_i\rangle$ instead of $\langle\Psi_i|\hat{H}|\Psi_i\rangle$.

In addition to the unconstrained calculations ($f = 0$) one usually considers linear

$$f(\mu, \langle\hat{Q}\rangle) = -\mu\langle\hat{Q}\rangle \tag{2.40}$$

and quadratic

$$f(\mu, \langle\hat{Q}\rangle) = -\frac{C}{2}(\langle\hat{Q}\rangle - \mu)^2 \tag{2.41}$$

forms of constraints.

In the calculations presented in this work the mean value of the mass quadrupole moment

$$\langle\Psi_i|\hat{Q}_{20}|\Psi_i\rangle = \langle\Psi_i|2r^2 P_2(cos\theta)|\Psi_i\rangle \tag{2.42}$$

is considered under constraint. To obtain the required value of the quadrupole moment the quadratic type of constraint (2.41) is applied.

Chapter 3

Experimental signatures of proton-neutron pairing

The strongest evidence of proton-neutron pairing comes so far from measured binding energies– the proton-rich $N \sim Z$ nuclei are much more bound than their neighbours. In phenomenological models of macroscopic-microscopic type [59, 60, 61, 62, 63] as well as in microscopic approaches [64, 65] this additional binding energy needs to be taken into account in the form of the so-called Wigner (or congruence) energy added to the mass formula. Both empirical facts and shell model calculations suggest that the Wigner term can be traced back to the isoscalar part of the nuclear interaction, however it is unclear to what extent it is due to the pairing interaction. The shell model calculations of Ref. [66] have shown that the Wigner term can not be solely explained in terms of correlations between deuteron-like pairs, although their contribution is dominant, and that the mechanism responsible for the extra binding of self-conjugate nuclei is more complex. Interestingly, other shell model calculations done in the same mass region $A \sim 50$ [67] led the authors to the conclusion that the Wigner term can not be at all explained as a pairing effect. Nevertheless, due to the division into particle-hole and particle-particle channel inherent only to mean-field models, some of the shell model definitions of pairing may be not appropriate from the point of view of mean-field calculations [29]. Indeed, the calculations within HFB and BCS frameworks with pn pairs done in Refs. [29, 68] succeeded in reproducing the spike in the isobaric mass parabola for $Z = 24, 38$ isotopic chains.

In the forthcoming sections we will discuss shortly the methods of extracting the informations on the Wigner energy from experimental data [66, 69, 70].

Other facts suggesting the presence of the proton-neutron pairing and the methods proposed to detect the pn pairing experimentally are the following. First, consider the ground states of $N = Z$ odd-odd nuclei. For $A < 40$ these isotopes have a T = 0 ground state that may suggest that the last proton and neutron couple to $T = 0$ rather than to $T = 1$, indicating the nuclear interaction is stronger in the $T = 0$ channel[1]. Most notably, the deuteron is bound with $T = 0$ while dineutron

---

[1]Hereafter we use italic face T to indicate the isospin channels of the two-body interactions. The

(diproton) is not bound. For $A = 42 - 54$ the odd-odd $N = Z$ nuclei have T $= 1$ (except ^{58}Cu). However, it was also argued [25, 26] that the intriguing switch from T $= 0$ to T $= 1$ ground states in odd-odd $N = Z$ nuclei arises from a competition between symmetry energy and full isovector pairing correlations, without any need for the isoscalar pairing. There is unfortunately little experimental data concerning heavier nuclei ($A = 58 - 98$) to be compared with theoretical predictions [71].

It seems that proton-neutron pair transfer reactions could be a proof of the existence of pn pairing correlations: the value of the pair transfer amplitude $\langle A + 2|a_\tau^\dagger a_{\tau'}^\dagger|A\rangle$ depends upon whether the two nucleons form a Cooper pair or not; therefore a proton-neutron transfer amplitude $\langle A + 2|a_p^\dagger a_n^\dagger|A\rangle$ should measure wether or not proton and neutron form a correlated pair and prove pn pairing. At present such data are unavailable.

Let us further consider the Coriolis anti-pairing effect. It is well known that in rotating nuclei $p\bar{p}$ and $n\bar{n}$ pairs are destroyed since the Coriolis force has an opposite effect of each nucleon in the pair. However, for a pn pair the spins of both nucleons may be parallel and rotation alignes both spins along the rotation axis without breaking such a pair and loosing pairing energy. This permits a situation in which the ground state band with $T = 1$ pairing is crossed by a $T = 0$ band at some crossing frequency. Such a scenario was proposed for the ^{74}Rb nucleus and it seems to explain well the experimental evidence [72]. The significance of the so-called delayed alignements in $N = Z$ nuclei are at present investigated both experimentally [73, 74] and theoretically [75, 76, 77].

Another signature of the pn pairing was addressed in Ref. [78], namely the anomalous behaviour of the second moment of inertia in the superdeformed band of ^{60}Zn as compared to its neighbours. This behaviour cannot be explained in a consistent way within standard approaches with $T = 1$ pairing only. The authors of [78] have shown that a correct qualitative reproduction of experimental data can be reached when a $T = 0$ neutron-proton configurations mixing of signature-separated bands is considered.

The proton-neutron pairing is also believed to affect the structure of low-lying collective states [79, 80], $e.g.$ the low energy of the second 0^+ state of ^{98}Mo and its prolate shape are difficult to reproduce by means of existing collective models. An explanation was proposed in Ref. [79] assuming that some features of the collective excitations may be due to the proton-neutron interaction responsible for creation of deuteron-like clusters. The inclusion of the pn pairing within the Interacting Boson Model (IBM-4) improves considerably the agreement of observed and calculated energies and suggest that the competition between isoscalar and isovector modes of pairing vibrations could play a non negligible role in the description of the collective excitations in different regions of nuclei.

Furthermore, the pn pairing is expected to play a significant role in β [81] and double β decay [82, 83, 84, 85], α decay and α correlations and in properties of

---

roman face symbol T would refer to the total nuclear isospin.

low-density nuclear matter.

3.1   Wigner energy

As already said, a sharp increase in the binding energy of $N = Z$ nuclei is observed. In the semi-empirical mass formulae this additional term related to the pn pairing is usually parametrized as

$$B_{pn} = e_{pn}(A)\pi_{pn} - E_W \,, \tag{3.1}$$

where

$$\pi_{pn} = \frac{1}{4}(1 - (-1)^N)(1 - (-1)^Z). \tag{3.2}$$

It is seen that the first contribution to the pn-pairing energy (3.1) is equal to zero for even N, Z, therefore it represents an additional binding due to the residual interaction between the two odd nucleons in an odd-odd nucleus. The second contribution to (3.1) dubbed Wigner energy consists in two parts:

$$E_W = W(A)|N - Z| + d(A)\pi_{pn}\delta_{NZ} \,, \tag{3.3}$$

where the d-term is a correction for odd-odd nuclei. The $|N - Z|$ dependence in Eq. (3.3) was first introduced by Wigner [86] in his analysis of SU(4) spin-isospin symmetry of nuclear forces and then commonly used in literature as it accounts properly for the behaviour of nuclear masses when an isobaric chain crosses the $N = Z$ line.

In Ref. [66] the Wigner energy coefficient W was defined in terms of binding energies (B) of various combinations of nuclei in the quantity $\delta V(N, Z)$, where

$$
\begin{aligned}
\delta V(N, Z) \;=\; & \frac{1}{4}\left[B(N, Z) - B(N - 2, Z)\right. \\
& \left. - \; B(N, Z - 2) + B(N - 2, Z - 2)\right] \sim \frac{\partial^2 B}{\partial N \partial Z}.
\end{aligned} \tag{3.4}
$$

For an even-even nucleus $(N = Z = A/2)$ the Wigner energy strength is given by

$$
\begin{aligned}
W(A) \;=\; & \delta V(\frac{A}{2}, \frac{A}{2}) \\
& - \frac{1}{2}\left[\delta V(\frac{A}{2}, \frac{A}{2} - 2) + \delta V(\frac{A}{2} + 2, \frac{A}{2})\right]
\end{aligned} \tag{3.5}
$$

while for odd-odd nuclei $(N = Z = A/2)$ one has

$$
\begin{aligned}
W(A) \;=\; & \delta V(\frac{A}{2} - 1, \frac{A}{2} - 1) \\
& + \frac{1}{2}\left[\delta V(\frac{A}{2} + 1, \frac{A}{2} + 1) + \delta V(\frac{A}{2} + 1, \frac{A}{2} - 1)\right].
\end{aligned} \tag{3.6}
$$

Figure 3.1: Experimental values of $W(A)$ (filled circles) and $d(A)$ (crosses) of $N = Z$ nuclei extracted from nuclear binding energies according to Eqs. (3.5-3.7). The experimental masses were taken from Ref. [88].

It is seen $W(A)$ for odd-odd nuclei involves only the binding energies B of even-even systems. The term $d(A)$ for odd-odd nuclei is given as

$$
\begin{aligned}
d(A) \quad = \quad & \delta V(\frac{A}{2}, \frac{A}{2} - 2) \\
+ \quad & \frac{1}{2} \left[\delta V(\frac{A}{2} + 2, \frac{A}{2}) - 4\delta V(\frac{A}{2} + 1, \frac{A}{2} - 1) \right] .
\end{aligned} \tag{3.7}
$$

The experimental values of $W(A)$ and $d(A)$ are shown in Fig.3.1. The values of $W(A)$ decrease smoothly with increasing mass number following roughly the dependence $47/A$, showing oscillations around the closed shells. The values of $d(A)$ are more irregular. The estimates of Ref. [87] suggest a constant value of the ratio d/W equal to one.

3.2   Empirical pairing gaps

In order to extract empirical information on the magnitude of pairing correlations one usually implies mass indicators assuming the nuclear mass (binding energy) may be decomposed into a part $\mathcal{M}(Z, N)$ which varies smoothly as a function of N and Z and a fluctuating term. To determine the experimental values of pairing gaps we use the discrete Taylor expansion of the mass in the vicinity of the mass of our interest.

Let us define a smooth variation of the mass surface $\mathcal{M}(Z, N)$ formed by a set of even-even nuclei. In the case of even-even nuclei this value is equal to the measured

mass $M(Z,N)$. The mass of a nucleus with an odd number of nucleons is obtained by adding a pairing gap $D(Z,N)$. We have [89]

$$
\begin{aligned}
M(Z,N)_{\text{even}-\text{even}} &= \mathcal{M}(Z,N)\,, \\
M(Z,N)_{\text{odd}-\text{proton}} &= \mathcal{M}(Z,N) + \Delta_p\,, \\
M(Z,N)_{\text{odd}-\text{neutron}} &= \mathcal{M}(Z,N) + \Delta_n\,, \\
M(Z,N)_{\text{odd}-\text{odd}} &= \mathcal{M}(Z,N) + \Delta_p + \Delta_n - \Delta_{pn}\,,
\end{aligned}
\tag{3.8}
$$

where Δ_p is the proton gap, Δ_n the neutron gap and Δ_{pn} is the attractive residual proton-neutron interaction energy. We represent the mass surface in the vicinity of the mass of interest by the Taylor expansion of $\mathcal{M}(Z,N)$ as a function of the nucleon number. Performing the Taylor expansion as a function of two variables N and Z we obtain

$$
\begin{aligned}
M(Z,N) = &\; \mathcal{M}(Z_0,N_0) + \left[(Z-Z_0)\frac{\partial \mathcal{M}}{\partial Z}(Z_0,N_0) + (N-N_0)\frac{\partial \mathcal{M}}{\partial N}(Z_0,N_0) \right] \\
&+ \frac{1}{2!}\left[(Z-Z_0)^2\frac{\partial^2 \mathcal{M}}{\partial Z^2}(Z_0,N_0) + 2(Z-Z_0)(N-N_0)\frac{\partial^2 \mathcal{M}}{\partial Z \partial N}(Z_0,N_0) \right. \\
&+ \left. (N-N_0)^2\frac{\partial^2 \mathcal{M}}{\partial N^2}(Z_0,N_0) \right] \\
&+ \frac{1}{3!}\left[(Z-Z_0)^3\frac{\partial^3 \mathcal{M}}{\partial Z^3}(Z_0,N_0) + (N-N_0)^3\frac{\partial^3 \mathcal{M}}{\partial N^3}(Z_0,N_0) \right. \\
&+ 3(Z-Z_0)^2(N-N_0)\frac{\partial^3 \mathcal{M}}{\partial^2 Z \partial N}(Z_0,N_0) \\
&+ \left. 3(Z-Z_0)(N-N_0)^2\frac{\partial^3 \mathcal{M}}{\partial Z \partial^2 N}(Z_0,N_0) \right] \\
&+ \cdots + D(Z,N)\,.
\end{aligned}
\tag{3.9}
$$

Taking into account the terms up to the second derivative we obtain the 3-point formula for the pairing gap. For an even-even nucleus one has:
for neutrons

$$
\Delta_n^{(3)} = \frac{1}{2}\left[M(Z,N+1) - 2M(Z,N) + M(Z,N-1) \right]
\tag{3.10}
$$

and for protons

$$
\Delta_p^{(3)} = \frac{1}{2}\left[M(Z+1,N) - 2M(Z,N) + M(Z-1,N) \right]\,.
\tag{3.11}
$$

The same way we may calculate the proton-neutron pairing gap

$$
\begin{aligned}
\Delta_{pn}^{(3)} = &\; \frac{1}{4}\left[M(N+1,Z+1) - M(N-1,Z+1) \right. \\
&- \left. M(N+1,Z-1) + M(N-1,Z-1) \right]\,.
\end{aligned}
\tag{3.12}
$$

Table 3.1: 3 and 5-point pairing indicators (Eqs. 3.10–3.15) determined from experimental masses for $N \sim Z$ Ge $(Z = 32)$ isotopes.

Mass number	$\Delta_n^{(3)}$	$\Delta_p^{(3)}$	$\Delta_{pn}^{(3)}$	$\Delta_n^{(5)}$	$\Delta_p^{(5)}$	$\Delta_{pn}^{(5)}$
62	1.33	1.12	0.63	2.82	1.64	0.49
64	1.48	1.14	1.39	2.14	1.80	1.50
66	1.60	1.21	0.48	1.86	1.58	0.81
68	1.65	1.24	0.52	1.88	1.61	0.63

The 5-point formula for the pairing gap takes into account also the terms of the third order. The expressions for neutron, proton and proton-neutron pairing indicators this time are the following

$$\Delta_n^{(5)} = \frac{1}{8} [M(Z, N + 2) - 4M(Z, N + 1) + 6M(Z, N)$$
$$- \quad 4M(Z, N - 1) + M(Z, N - 2)] \, , \tag{3.13}$$

$$\Delta_p^{(5)} = \frac{1}{8} [M(Z + 2, N) - 4M(Z + 1, N) + 6M(Z, N)$$
$$- \quad 4M(Z - 1, N) + M(Z - 2, N)] \, , \tag{3.14}$$

$$\Delta_{pn}^{(5)} = \frac{1}{4} \{ 2[M(Z, N + 1) + M(Z, N - 1) + M(Z - 1, N)$$
$$+ \quad M(Z + 1, N) - 4M(Z, N)] - [M(Z + 1, N + 1)$$
$$+ \quad M(Z - 1, N + 1) + M(Z + 1, N - 1) + M(Z - 1, N - 1)] \} \, . \tag{3.15}$$

The values of pairing gaps extracted from masses for Ge isotopes of interest in this work are listed in Tab. 3.1. The experimental mass values were taken from Atomic Mass Evaluation (AME2003) of Audi and Wapstra [88].

We have followed the argumentation of Refs. [90, 91] to determine the 3-point gap of an even-even nucleus: the proper measure of pairing correlations of an even system with n nucleons is the average value of the pairing indicators evaluated for its odd neighbours:

$$\Delta_\tau^{(3)}(n = \text{even}) = \frac{1}{2} (\Delta_\tau^{(3)}(n + 1) + \Delta_\tau^{(3)}(n - 1)) \, . \tag{3.16}$$

In cases where the experimental data was not sufficient to calculate the average value of two pairing gaps, we have adopted the gap of one odd neighbour to be the 3-point gap of the even nucleus. In addition to empirical values extracted from masses, in Table 3.2 we give the values of two average models for pairing gaps: the traditional

Table 3.2: Average pairing gaps (see Eq.(3.17)) for $N \sim Z$ Ge ($Z = 32$) isotopes.

Mass number	Traditional model		Vogel *et al.*	
	$\bar{\Delta}_{n,p}$	$\bar{\Delta}_{pn}$	$\bar{\Delta}_{n,p}$	$\bar{\Delta}_{pn}$
62	1.52	0.32	1.80	0.50
64	1.50	0.31	1.80	0.48
66	1.47	0.30	1.77	0.47
68	1.45	0.29	1.72	0.45

model [92] and the model developed by Vogel *et al.* [93]. The parametrizations of pairing gaps in these two models are specified as:

$$\bar{\Delta}_{\tau} = 12 \text{MeV}/\sqrt{A}\,, \qquad\qquad \bar{\Delta}_{pn} = 20 \text{MeV}/A \qquad (\text{traditional model})$$

$$\bar{\Delta}_{\tau} = \left(7.2 - 44(\frac{N-Z}{A})^2\right) \text{MeV}/A^{1/3}\,, \qquad \bar{\Delta}_{pn} = 31 \text{MeV}/A \qquad (\text{Vogel}\,\textit{et al.})$$

$$(3.17)$$

It is seen that the traditional model values are closer to those of 3-point gaps while the model of Vogel reproduces better 5-point gaps. It should be noticed that in any of the models the values of proton-neutron gaps are not negligible thus the proton-neutron interaction is expected to play a significant role in the construction of the quasiparticle field in these nuclei. On the other hand, one should bear in mind that since pair-correlation indicators are given by finite differences, the physical interpretation of exctracted quantities is disturbed near the $N = Z$ line. Another remark, concerning as well the values derived in Sec. 3.1, is that with the present set of experimental mass data near the $N = Z$ line the uncertainties for extracted quantities may be consequential.

Chapter 4

Proton-neutron pairing in BCS-type approaches

The initial theory of nucleon pair correlations included Cooper pairs which contain two protons or two neutrons [1, 2]. In this theory, known as the BCS approximation, quasiparticle operators are defined by a 2×2 unitary transformation of particle operators. In $N \sim Z$ nuclei, valence neutrons and protons fill similar shell model orbitals and interact through the stronger $T = 0$ force as well as the $T = 1$ force. One may therefore expect the appearance of a static pn pair condensate, especially in heavier $N \sim Z$ nuclei where the large valence space allows for creation of many pn pairs. In the early 1960's it was recognized that the pairing theory was incomplete and that for $N \sim Z$ nuclei it should be generalized to include as well proton-neutron Cooper pairs [4]. In the forthcoming years (1964-1972) this generalization was done in several steps. First, Goswami and others [5, 6, 8] have generalized a special quasiparticle transformation to include $p\bar{p}$, $n\bar{n}$ and $p\bar{n}$ pairs, where the bar indicates that the second particle occupies a time-reversed orbital. In these pioneering articles the two particles were coupled to $T = 1$ isospin. Then a BCS theory for $p\bar{n}$ pairs coupled to $T = 0$ was presented in Ref. [7]. A synthesized formalism to deal with $T = 1$ and $T = 0$ Cooper pairs of the $p\bar{p}$, $n\bar{n}$ and $p\bar{n}$ type was developed in Refs. [9, 10]. In such a theory quasiparticles are defined by a 4×4 unitary transformation of particle operators.

Since neutrons and protons are not hindered by the Pauli exclusion principle to occupy the same spatial orbitals, they can form correlated pairs of the pn type. A completely isospin generalized BCS theory which includes pn (and $\bar{p}\bar{n}$) pairs, as well as $p\bar{p}$, $n\bar{n}$ and $p\bar{n}$ Cooper pairs was derived by Goodman in Ref. [11]. This time the quasiparticles are given by 8×8 unitary transformation of particle operators.

The starting point of our considerations are the eigenstates of an axially-deformed Hamiltonian (see Appendix A). The basis consists in two groups of states with respect to the time-reversal symmetry. Since the $p\bar{n}$ mode tends to restore axial symmetry while the pn mode introduces nonaxial deformations [94], we restrict our-

selves here to include the nucleonic pairs in time-reversed orbits which we will refer to as *pp*, *nn* and *pn* pairing.

4.1   Pairing Hamiltonian

In the following we propose a generalized pairing Hamiltonian which contains all possible kinds of pairs of nucleons moving in time-reversed orbitals interacting via a two-body force represented by its antisymmetrized matrix elements $g_{kl,\tau\tau'}^T$:

$$
\begin{aligned}
\hat{H}_{\text{pair}} = \ & - \ \sum_{k,l} g_{kl,pp}^{T=1} \mathcal{P}_{kpp}^{T=1\dagger} \mathcal{P}_{lpp}^{T=1} \\
& - \ \sum_{k,l} g_{kl,nn}^{T=1} \mathcal{P}_{knn}^{T=1\dagger} \mathcal{P}_{lnn}^{T=1} \\
& - \ \sum_{k,l} g_{kl,pn}^{T=1} \mathcal{P}_{kpn}^{T=1\dagger} \mathcal{P}_{lpn}^{T=1} \\
& - \ \sum_{k,l} g_{kl,pn}^{T=0} \mathcal{P}_{kpn}^{T=0\dagger} \mathcal{P}_{lpn}^{T=0} \, ,
\end{aligned}
\tag{4.1}
$$

where the operators $\mathcal{P}^{T=1\dagger}$ and $\mathcal{P}^{T=0\dagger}$ accounting for different isospin pairs of particles read

$$
\mathcal{P}_{kpp}^{T=1\dagger} \ = \ a_{kp}^\dagger a_{\bar{k}p}^\dagger \, ,
\tag{4.2}
$$

$$
\mathcal{P}_{knn}^{T=1\dagger} \ = \ a_{kn}^\dagger a_{\bar{k}n}^\dagger \, ,
\tag{4.3}
$$

$$
\mathcal{P}_{kpn}^{T=1\dagger} \ = \ \frac{1}{\sqrt{2}} \left(a_{kp}^\dagger a_{\bar{k}n}^\dagger + a_{kn}^\dagger a_{\bar{k}p}^\dagger \right) \, ,
\tag{4.4}
$$

$$
\mathcal{P}_{kpn}^{T=0\dagger} \ = \ \frac{1}{\sqrt{2}} \left(a_{kp}^\dagger a_{\bar{k}n}^\dagger - a_{kn}^\dagger a_{\bar{k}p}^\dagger \right) \, ,
\tag{4.5}
$$

and where $a_{k\tau}^\dagger$ is either a particle creation operator of a neutron ($\tau = 1$ or n) or of a proton ($\tau = -1$ or p).

The antisymmetrized matrix elements $g_{kl,\tau\tau'}$ are given by

$$
g_{kl,\tau\tau'}^T = \langle k\tau, \bar{k}\tau' | \hat{v}_{\text{pair}}^T | \widetilde{l\tau, \bar{l}\tau'} \rangle \, .
\tag{4.6}
$$

Here $\bar{k}$ is the time-reversal partner of the state k. The choice of the pairing force is rather arbitrary but may influence further results. The simplest way to treat pairing correlations is to assume a constant value of matrix elements (4.6)

$$
G = \langle i\bar{i} | \hat{v}_{\text{pair}}^T | j\bar{j} \rangle = \text{const} \, ,
\tag{4.7}
$$

where G is the overall strength of the interaction. This approach is known as monopole pairing or seniority pairing and has been applied in different calculations

for many years. It should be pointed out that the majority of calculations with the *pn* pairing in HFB-type approaches were done using these schematic pairing forces with constant matrix elements (see *e.g.* [11, 28, 29]).

More realistic pairing interactions are those with state-dependent matrix elements: Gogny and δ forces. The Gogny force was originally introduced within the conventional Hartree-Fock-Bogoliubov method as it is suitable to reproduce data in both, particle-particle and particle-hole channels [95]. This is so because the Gogny force has been chosen of finite range in the singlet even channel which describes like-particle pairings [96].

The δ force has been used to simulate pairing interaction in different nuclear calculations for over fourty years. Green and Moszkowski [97] have used a δ force to describe the pairing correlations understood as a surface phenomenon in the surface delta interaction (SDI). A modification of this interaction that contained a density dependence was first proposed by Chasman in Ref. [98]. However, the most popular is a simple, density independent δ interaction. One of the first calculations with such a volume δ force was done in Refs. [99, 100, 101, 102].

Contrary to the finite range of the Gogny force the δ is the zero-range force. The zero-range nature of pairing interaction tends to overestimate the coupling to continuum states. This defect does not occur in the case of finite range forces but can be easily cured by introducing an energy cut-off which plays the role of an additional parameter (similarly, a cut-off is necessary when using the monopole pairing interaction). Any change of the dimension of the single-particle space requires a readjustment of the pairing strength, thus the definition of the pairing interaction is complete for the cut-off and pairing strength given together.

These seemingly different types of pairing interactions should in fact produce similar results– the coherence length (the size of a Cooper pair) is of the order of the size of a nucleus, thence its structure should not be sensitive to the details of the interaction in the particle-particle channel [103]. In Ref. [104] we have shown that at least in proton-proton and neutron-neutron channels both Gogny and δ forces after a proper renormalization lead to the pairing matrix elements of similar magnitudes.

Since the Gogny force is more difficult to handle numerically we choose the volume δ force to evaluate the matrix elements of the pairing interaction in *pp*, *nn* and *pn* channels. Nevertheless, due to the fact that such an interaction is active only in $L = 0$ channel, the space-spin-isospin possibilities are limited: since the two-particle function needs to be antisymmetric we have only $L = 0$, $S = 0$ in the $T = 1$ channel and $L = 0$, $S = 1$ for the $T = 0$ channel. The latter component becomes strongly quenched due to the destructive influence of the spin-orbit interaction when entering *pf* nuclei [67]. A relatively simple way to enrich the δ interaction to have all spin-isospin channels like in the case of the Gogny force, is to add a Skyrme, t_2-like component (cf. Eq. (2.24)) to the δ force. The extended, Skyrme-like form of the pairing interaction is given as

$$\hat{V}_{\text{pair}} \;\; = \;\; \hat{V}_{\delta} + \hat{V}_{\boldsymbol{k}'\delta\boldsymbol{k}}$$

$$= \sum_T V_{0\tau}^T [\delta(\vec{r}_{12}) + \text{x} \boldsymbol{k}'\delta(\vec{r}_{12})\boldsymbol{k}]\Pi^S \Pi^T, \tag{4.8}$$

where

$$\boldsymbol{k}'\delta(\vec{r}_{12})\boldsymbol{k} = \frac{-1}{2i}(\overleftarrow{\nabla}_1 - \overleftarrow{\nabla}_2)\delta(\vec{r}_1 - \vec{r}_2)\frac{1}{2i}(\overrightarrow{\nabla}_1 - \overrightarrow{\nabla}_2), \tag{4.9}$$

$V_{0\tau}^T$, x determine the strength of the interaction and Π^S, Π^T are the operators projecting onto spin-isospin subspaces:

$$\hat{\Pi}^S = \frac{1}{2}\left(1 - (-1)^S P^\sigma\right), \tag{4.10}$$

$$\hat{\Pi}^T = \frac{1}{2}\left(1 - (-1)^T P^\tau\right), \tag{4.11}$$

where $P^\sigma = 1/2(1 + \vec{\sigma}_1 \cdot \vec{\sigma}_2)$, $P^\tau = 1/2(1 + \vec{\tau}_1 \cdot \vec{\tau}_2)$ are the standard spin and isospin exchange operators. The second term of (4.8) is antisymmetric in its spatial part ($L = 1$), therefore active in $S = 1$, $T = 1$ and $S = 0$, $T = 0$ channels. However, it is not clear what the ratio of $L = 0/L = 1$ components in the particle-particle channel should be thus the x parameter needs to be fitted by comparison to available data. The integral formulae for pairing matrix elements of the interaction (4.8) derived in the axially symmetric harmonic oscillator basis are given in Appendix B.3. It should be added that the matrix elements can be as well evaluated using the properties of the asymptotic basis, as was proposed in Ref. [105]. Such a calculation is highly time-consuming as compared to the integral method but may serve as a test, therefore in Appendix B.2 we remind the formulae necessary to calculate the two-body matrix elements of the interaction (4.8) in the asymptotic basis.

Examples of the matrix elements of the interaction (4.8) and a discussion of the results obtained with such an extended interaction are given in Sec. 4.4.2.

4.2 Generalized BCS theory

4.2.1 Quasiparticle transformation

The conventional BCS theory which omits the proton-neutron interaction defines the quasiparticle operators $\alpha^\dagger$ by a two-dimensional transformation of the particle operators $a^\dagger$

$$\begin{pmatrix} \alpha_k^\dagger \\ \alpha_{\bar{k}} \end{pmatrix} = \begin{pmatrix} u_k & -v_k \\ v_k & u_k \end{pmatrix} \begin{pmatrix} a_k^\dagger \\ a_{\bar{k}} \end{pmatrix}, \tag{4.12}$$

where k is a single-particle (HF) orbital. The isospin generalized BCS theory replaces Eq. (4.12) with the eight-dimensional transformation

$$\begin{pmatrix} \boldsymbol{\alpha}^\dagger(k) \\ \boldsymbol{\alpha}(k) \end{pmatrix} = \begin{pmatrix} U(k) & -V(k) \\ -V^\star(k) & U^\star(k) \end{pmatrix} \begin{pmatrix} \boldsymbol{a}^\dagger(k) \\ \boldsymbol{a}(k) \end{pmatrix}, \tag{4.13}$$

where $\boldsymbol{\alpha}^\dagger(k)$ and $\boldsymbol{a}^\dagger(k)$ are the four-component vectors

$$\boldsymbol{\alpha}^\dagger(k) = \begin{pmatrix} \alpha^\dagger_{k1} \\ \alpha^\dagger_{k2} \\ \alpha^\dagger_{\bar{k}1} \\ \alpha^\dagger_{\bar{k}2} \end{pmatrix}, \qquad \boldsymbol{a}^\dagger(k) = \begin{pmatrix} a^\dagger_{kp} \\ a^\dagger_{kn} \\ a^\dagger_{\bar{k}p} \\ a^\dagger_{\bar{k}n} \end{pmatrix}, \tag{4.14}$$

$U(k)$ and $V(k)$ are four-dimensional complex matrices. Since we consider here only the $k\bar{k}$ pairing, the transformation (4.13) splits into two 4×4 transformations, the following one [28]

$$\begin{pmatrix} \alpha^\dagger_{k1} \\ \alpha^\dagger_{k2} \\ \alpha_{\bar{k}1} \\ \alpha_{\bar{k}2} \end{pmatrix} = \begin{pmatrix} u_{k1p} & u^\star_{k1n} & v_{k1p} & v^\star_{k1n} \\ u^\star_{k2p} & u_{k2n} & v^\star_{k2p} & v_{k2n} \\ -v_{k1p} & -v^\star_{k1n} & u_{k1p} & u^\star_{k1n} \\ -v^\star_{k2p} & -v_{k2n} & u^\star_{k2p} & u_{k2n} \end{pmatrix} \begin{pmatrix} a^\dagger_{kp} \\ a^\dagger_{kn} \\ a_{\bar{k}p} \\ a_{\bar{k}n} \end{pmatrix} \tag{4.15}$$

and its Hermite conjugate. The matrices $V(k)$, $U(k)$ of Eq.(4.13) have now the form

$$V(k) = \begin{pmatrix} 0 & 0 & -v_{k1p} & -v^\star_{k1n} \\ 0 & 0 & -v^\star_{k2p} & -v_{k2n} \\ v_{k1p} & v_{k1n} & 0 & 0 \\ v_{k2p} & v_{k2n} & 0 & 0 \end{pmatrix}, \tag{4.16}$$

$$U(k) = \begin{pmatrix} u_{k1p} & u^\star_{k1n} & 0 & 0 \\ u^\star_{k2p} & u_{k2n} & 0 & 0 \\ 0 & 0 & u_{k1p} & u_{k1n} \\ 0 & 0 & u_{k2p} & u_{k2n} \end{pmatrix}. \tag{4.17}$$

The occupation amplitudes u_{k1p}, u_{k2n}, v_{k1p} and v_{k2n} are real numbers while u_{k1n}, u_{k2p}, v_{k1n} and v_{k2p} are complex.

The Bogoliubov transformation needs to be unitary and preserve the Fermi anticommutation relations

$$\{\alpha_{kq}, \alpha^\dagger_{lq'}\} = \delta_{kl}\delta_{qq'}, \qquad \{\alpha_{kq}, \alpha_{lq'}\} = \{\alpha^\dagger_{kq}, \alpha^\dagger_{lq'}\} = 0, \qquad q, q' = 1, 2 \tag{4.18}$$

what requires the standard normalization conditions for u and v amplitudes

$$\sum_{\tau=p,n} \left(|u_{kq\tau}|^2 + |v_{kq\tau}|^2 \right) = 1. \tag{4.19}$$

In the limit where there is no proton-neutron pairing $u_{k1n} = u_{k2p} = v_{k1n} = v_{k2p} = 0$ and the isospin generalized transformation (4.15) reduces to two conventional 2×2 BCS transformations (4.12), first for protons ($u_{k1p} \equiv u_{kp}, v_{k1p} \equiv v_{kp}$) and the second one for neutrons ($u_{k2n} \equiv u_{kn}, v_{k2n} \equiv v_{kn}$).

To obtain the BCS equations it is also indispensable to know the inverse transformation of (4.15) which reads

$$\begin{pmatrix} a^\dagger_{kp} \\ a^\dagger_{kn} \\ a_{\bar{k}p} \\ a_{\bar{k}n} \end{pmatrix} = \begin{pmatrix} u_{k1p} & u_{k2p} & -v_{k1p} & -v_{k2p} \\ u_{k1n} & u_{k2n} & -v_{k1n} & -v_{k2n} \\ v_{k1p} & v_{k2p} & u_{k1p} & u_{k2p} \\ v_{k1n} & v_{k2n} & u_{k1n} & u_{k2n} \end{pmatrix} \begin{pmatrix} \alpha^\dagger_{k1} \\ \alpha^\dagger_{k2} \\ \alpha_{\bar{k}1} \\ \alpha_{\bar{k}2} \end{pmatrix}. \tag{4.20}$$

Let us define the density matrix and the pairing tensor given by their matrix elements as

$$\rho_{kl} = \langle a_l^\dagger a_k \rangle , \tag{4.21}$$

$$\kappa_{kl} = \langle a_l a_k \rangle . \tag{4.22}$$

In matrix notation one has

$$\rho = V^\dagger V , \tag{4.23}$$

$$\kappa = V^\dagger U . \tag{4.24}$$

The structures of (4.23) and (4.24) are found by substituting Eqs. (4.16) and (4.17) into Eqs. (4.21) and (4.22):

$$\rho = \begin{pmatrix} \rho_{kk}^{pp} & \rho_{kk}^{pn} & 0 & 0 \\ \rho_{kk}^{pn\star} & \rho_{kk}^{nn} & 0 & 0 \\ 0 & 0 & \rho_{kk}^{pp} & \rho_{kk}^{pn\star} \\ 0 & 0 & \rho_{kk}^{pn} & \rho_{kk}^{nn} \end{pmatrix} , \tag{4.25}$$

$$\kappa = \begin{pmatrix} 0 & 0 & \kappa_{k\bar{k}}^{pp} & \kappa_{k\bar{k}}^{pn} \\ 0 & 0 & \kappa_{k\bar{k}}^{np} & \kappa_{k\bar{k}}^{nn} \\ -\kappa_{k\bar{k}}^{pp\star} & -\kappa_{k\bar{k}}^{pn\star} & 0 & 0 \\ -\kappa_{k\bar{k}}^{np\star} & -\kappa_{k\bar{k}}^{nn\star} & 0 & 0 \end{pmatrix} , \tag{4.26}$$

with the components listed below

$$\rho_{kk}^{pp} = v_{k1p}^2 + |v_{k2p}|^2 , \tag{4.27}$$

$$\rho_{kk}^{nn} = |v_{k1n}|^2 + v_{k2n}^2 , \tag{4.28}$$

$$\rho_{kk}^{pn} = v_{k1p}v_{k1n} + v_{k2p}v_{k2n}^\star , \tag{4.29}$$

$$\kappa_{k\bar{k}}^{nn} = v_{k1n}^\star u_{k1n} + v_{k2n}u_{k2n} , \tag{4.30}$$

$$\kappa_{k\bar{k}}^{pp} = v_{k1p}u_{k1p} + v_{k2p}^\star u_{k2p} , \tag{4.31}$$

$$\kappa_{k\bar{k}}^{pn} = v_{k1p}u_{k1n} + v_{k2p}^\star u_{k2n} , \tag{4.32}$$

$$\kappa_{k\bar{k}}^{np} = v_{k1n}^\star u_{k1p} + v_{k2n}u_{k2p} . \tag{4.33}$$

Due to the conservation of the time-reversal symmetry (see Sec. 4.2.4) the ρ density does not connect the states k with $\bar{k}$ while the pairing tensor has non-zero elements only between k and $\bar{k}$ states.

The ρ_{kk}^{nn}, ρ_{kk}^{pp}, $\kappa_{k\bar{k}}^{nn}$ and $\kappa_{k\bar{k}}^{pp}$ tensors are real while in the complex proton-neutron part the consequent relations are fulfilled

$$\rho_{kk}^{pn} = \rho_{kk}^{np\star} , \tag{4.34}$$

$$\kappa_{k\bar{k}}^{pn} = \kappa_{k\bar{k}}^{np\star} . \tag{4.35}$$

4.2.2 Quasiparticle vacuum

Consider any Bogoliubov transformation of the form (cf. Appendix C.2)

$$\alpha_i^\dagger = \sum_k \left(A_{ki} a_k^\dagger + B_{ki} a_k \right) ,$$
$$\alpha_i = \sum_k \left(A_{ki}^\star a_k + B_{ki}^\star a_k^\dagger \right) . \tag{4.36}$$

The Thouless theorem [39] states that any product wave function which is not orthogonal to the vacuum $|0\rangle$ may be expressed in the form

$$|\Phi\rangle = \mathcal{N} \exp \left(-\frac{1}{2} \sum_{\mu\nu} Z_{\mu\nu}^\dagger a_\mu^\dagger a_\nu^\dagger \right) |0\rangle , \tag{4.37}$$

where the normalization factor $\mathcal{N} = \det^{1/2} A^\dagger$ and $Z = BA^{-1}$. With the use of the Thouless theorem we may now construct the quasiparticle vacuum for the transformation (4.13). We have

$$Z = BA^{-1} = -\tilde{V}(\tilde{U})^{-1} , \tag{4.38}$$

where tilde means a transposed matrix. Using the antisymmetry properties of the Z matrix after strigthforward calculation we obtain from Eq. (4.37)

$$
\begin{aligned}
|\text{vacuum}\rangle = \prod_k [& u_{k1p} u_{k2n} - u_{k2p} u_{k1n} \\
& + (v_{k1p} u_{k2n} - v_{k2p}^\star u_{k1n}) a_{kp}^\dagger a_{\bar{k}p}^\dagger \\
& + (v_{k2n} u_{k1p} - v_{k1n}^\star u_{k2p}) a_{kn}^\dagger a_{\bar{k}n}^\dagger \\
& + (v_{k2p}^\star u_{k1p} - v_{k1p} u_{k2p}) a_{kp}^\dagger a_{\bar{k}n}^\dagger \\
& + (v_{k1n}^\star u_{k2n} - v_{k2n} u_{k1n}) a_{\bar{k}p}^\dagger a_{kn}^\dagger \\
& + (v_{k1p} v_{k2n} - v_{k1n}^\star v_{k2p}^\star) a_{kp}^\dagger a_{kn}^\dagger a_{\bar{k}p}^\dagger a_{\bar{k}n}^\dagger] |0\rangle .
\end{aligned}
\tag{4.39}
$$

In the case of the usual BCS theory which omits the proton-neutron coupling we have $u_{k1n} = u_{k2p} = v_{k1n} = v_{k2p} = 0$ and the vacuum state (4.39) reduces to the well known form of the BCS wave function

$$|\text{vacuum}\rangle = \prod_k [u_{kp} + v_{kp} a_{kp}^\dagger a_{\bar{k}p}^\dagger] \times [u_{kn} + v_{kn} a_{kn}^\dagger a_{\bar{k}n}^\dagger] |0\rangle . \tag{4.40}$$

4.2.3 Isospin generalized gap equations

Having defined the quasiparticle transformation Eq. (4.15) one can decompose the Hamiltonian of the system

$$\hat{H} = \hat{H}_{\text{sp}}^n + \hat{H}_{\text{sp}}^p + \hat{H}_{\text{pair}} \tag{4.41}$$

with $\hat{H}_{\text{pair}}$ given by Eq. (4.1) in terms of quasiparticle operators

$$\hat{H} = \hat{H}_{00} + \hat{H}_{11} + \hat{H}_{20} + \hat{H}_{02} + \hat{H}_{22} + \hat{H}_{31} + \hat{H}_{13} + \hat{H}_{40} + \hat{H}_{04} , \tag{4.42}$$

where the indices denote the numbers of creation and annihilation quasiparticle operators, *e.g.*,

$$\hat{H}_{22} = \sum_{ab;cd} H_{ab;cd} \alpha_a^\dagger \alpha_b^\dagger \alpha_c \alpha_d \,, \qquad (4.43)$$

and $H_{ab;cd}$ are expansion coefficients. The terms $\hat{H}_{22}$, $\hat{H}_{31}, \hat{H}_{13}, \hat{H}_{40}$ and $\hat{H}_{04}$ which describe the residual interaction between quasiparticles are neglected in this formalism. The standard BCS condition

$$\hat{H}_{20} + \hat{H}_{02} = 0 \qquad (4.44)$$

leads to the generalized set of equations which allow to treat protons and neutrons as non-separable systems

$$\begin{pmatrix} \tilde{\epsilon}_{kp} & 0 & \Delta_k^{pp} & \Delta_k^{pn} \\ 0 & \tilde{\epsilon}_{kn} & \Delta_k^{pn\star} & \Delta_k^{nn} \\ \Delta_k^{pp} & \Delta_k^{pn} & -\tilde{\epsilon}_{kp} & 0 \\ \Delta_k^{pn\star} & \Delta_k^{nn} & 0 & -\tilde{\epsilon}_{kn} \end{pmatrix} \begin{pmatrix} u_{kqp} \\ u_{kqn} \\ v_{kqp} \\ v_{kqn} \end{pmatrix} = E_{kq} \begin{pmatrix} u_{kqp} \\ u_{kqn} \\ v_{kqp} \\ v_{kqn} \end{pmatrix} \,, \qquad (4.45)$$

where $\tilde{\epsilon}_{k\tau} = e_{k\tau} - \lambda_\tau$. The diagonalization of the matrix (4.45) for each state k yields quasiparticle energies E_{kq} and occupation amplitudes u, v. The state-dependent pairing gaps appearing in Eq. (4.45) are given by

$$\begin{aligned} \Delta_m^{\tau\tau} &= \sum_{k,q} g_{mk,\tau\tau}^{T=1} v_{kq\tau} u_{kq\tau}^\star, \\ \Delta_m^{pn} &= \Delta_m^{1pn} + i\Delta_m^{0pn}, \\ \Delta_m^{1pn} &= \sum_{k,q} g_{mk,pn}^{T=1} \Re e \left(v_{kqp} u_{kqn}^\star \right), \\ \Delta_m^{0pn} &= \sum_{k,q} g_{mk,pn}^{T=0} \Im m \left(v_{kqp} u_{kqn}^\star \right) . \end{aligned} \qquad (4.46)$$

It is seen that the proton-neutron pairing gap in this formalism is a complex quantity with the real part associated to the $T = 1$ pairing mode and the imaginary part containing $T = 0$ pairs.

The Fermi levels λ_τ for protons and neutrons are adjusted as usually so that the particle number conservation relations for neutrons and protons

$$N = 2 \sum_{kq} v_{kqn} v_{kqn}^\star \,, \qquad Z = 2 \sum_{kq} v_{kqp} v_{kqp}^\star \qquad (4.47)$$

are satisfied. The pairing energy, calculated as the mean value of the Hamiltonian (4.1) in the BCS state, has the form

$$E_{\text{pair}} = - \sum_{kl,\tau\tau',T} g_{kl,\tau\tau'}^T \kappa_{k\bar{k}}^{\tau\tau'} \kappa_{l\bar{l}}^{\tau\tau'\star} . \qquad (4.48)$$

In practice the equations (4.45-4.47) are solved iteratively until the acquired accuracy for pairing gaps (or pairing energy, equivalently) and the particle number is achieved.

4.2.4 Time-reversal invariance and isospin symmetry breaking

It was shown by Goodman [11] that the time-reversal invariance and other symmetries limit considerably possible solutions of the generalized BCS theory. In this section we study the consequences of imposing time-reversal invariance and axiality in isospace on the possible BCS solutions in the case of Bogoliubov transformation (4.15) adopted in our calculations.

First, the time-reversal invariance condition:

$$\begin{pmatrix} \alpha_{\bar{k}1}^{\dagger} \\ \alpha_{\bar{k}2}^{\dagger} \end{pmatrix} = \hat{T} \begin{pmatrix} \alpha_{k1}^{\dagger} \\ \alpha_{k2}^{\dagger} \end{pmatrix} \hat{T}^{-1} , \tag{4.49}$$

where $\hat{T}$ is the time-reversal operator, implies the following relations:

- for hermitian density matrix:

$$\rho_{kk}^{\tau\tau} = \rho_{\bar{k}\bar{k}}^{\tau\tau\star} , \tag{4.50}$$

$$\rho_{kk}^{\tau\tau'} = \rho_{\bar{k}\bar{k}}^{\tau\tau'\star} , \tag{4.51}$$

$$\rho_{k\bar{k}}^{\tau\tau} = 0 , \tag{4.52}$$

$$\rho_{k\bar{k}}^{\tau\tau'} = 0 , \tag{4.53}$$

- and for antisymmetric pairing tensor:

$$\kappa_{k\bar{k}}^{\tau\tau} = \kappa_{\bar{k}k}^{\tau\tau\star} , \tag{4.54}$$

$$\kappa_{kk}^{\tau\tau'} = 0 , \tag{4.55}$$

$$\kappa_{kk}^{\tau\tau} = 0 , \tag{4.56}$$

$$\kappa_{k\bar{k}}^{\tau\tau'} = -\kappa_{\bar{k}k}^{\tau\tau'\star} , \tag{4.57}$$

where τ is p or n. The components $\rho_{kk}^{\tau\tau}$ and $\kappa_{k\bar{k}}^{\tau\tau}$ are real.

Next, consider the generalized density matrix R:

$$R = \begin{pmatrix} \rho & \kappa \\ \kappa^{\dagger} & 1 - \tilde{\rho} \end{pmatrix} , \tag{4.58}$$

where $\tilde{\rho}$ is the transposed ρ matrix. From the idempotency condition $R^2 = R$ (which implies $\rho^2 - \rho = \kappa^{\dagger}\kappa, \rho\kappa = \kappa\tilde{\rho}$), one obtains

$$\kappa_{k\bar{k}}^{pn}(\rho_{kk}^{pp} - \rho_{kk}^{nn}) = \rho_{kk}^{pn}(\kappa_{k\bar{k}}^{pp} - \kappa_{k\bar{k}}^{nn}) ,$$

$$\kappa_{k\bar{k}}^{pp2} + |\kappa_{k\bar{k}}^{pn}|^2 = \rho_{kk}^{pp2} - \rho_{kk}^{pp} + |\rho_{kk}^{pn}|^2 ,$$

$$\kappa_{k\bar{k}}^{nn2} + |\kappa_{k\bar{k}}^{pn}|^2 = \rho_{kk}^{nn2} - \rho_{kk}^{nn} + |\rho_{kk}^{pn}|^2 ,$$

$$\kappa_{k\bar{k}}^{pn}(\kappa_{k\bar{k}}^{pp} + \kappa_{k\bar{k}}^{nn}) = \rho_{kk}^{pn}(\rho_{kk}^{pp} + \rho_{kk}^{nn} - 1) . \tag{4.59}$$

The condition of the isospin conservation vector is given by

$$\langle \hat{T} \rangle = 0 , \tag{4.60}$$

and is analogous to the more familiar constraint $\langle \hat{J} \rangle = 0$. Deformed HF intrinsic states do not have angular momentum as a good quantum number, nevertheless one may insist that the average of $\hat{J}$ vanishes in the ground state. Similarily, the HFB (BCS) states can be deformed in the isospin space, so that T is not a good quantum number. Still one can require that the average of $\hat{T}$ vanish in the ground state. For a $N = Z$ nucleus it means sphericity in isospace $\langle \hat{T}_x \rangle = \langle \hat{T}_y \rangle = \langle \hat{T}_z \rangle = 0$. In a $N \neq Z$ nucleus $T_z = (N - Z)/2$ is not equal to zero so the imposed symmetry is this time the axiality in isospace. The condition (4.60) requires that (see Appendix E)

$$\langle \hat{T}_x \rangle = \Re e \sum_k \rho_{kk}^{pn} = 0 \tag{4.61}$$

and

$$\langle \hat{T}_y \rangle = \Im m \sum_k \rho_{kk}^{pn} = 0 \,. \tag{4.62}$$

The last two relations are fulfilled if ρ_{kk}^{pn} is equal to zero. It is seen from conditions (4.59) that then the non-trivial pn solutions are possible if $\rho_{kk}^{nn} = \rho_{kk}^{pp}$ and $\kappa_{k\bar{k}}^{pp} = -\kappa_{k\bar{k}}^{nn}$ which is fulfilled for $N = Z$ only. This is the solution found by Goodman [11]. In $N \neq Z$ nuclei neither $\rho_{kk}^{nn} = \rho_{kk}^{pp}$ nor $\kappa_{k\bar{k}}^{pp} = -\kappa_{k\bar{k}}^{nn}$ so the generalized BCS theory does not allow for a coherent pn paired solution. In conclusion, the pn pairing is ruled out due to the imposed symmetries: time-reversal invariance and axiality in isospace.

For Bogoliubov transformations which yield purely imaginary off-diagonal elements of the density matrix (as the transformation (4.15) does) the condition $\langle \hat{T}_x \rangle = 0$ is automatically fulfilled. For $N = Z$ nuclei we obtain in our model a class of solutions in which the condition (4.60) is satisfied.[1] For $N \neq Z$ the presented solutions are triaxial in isospace, *i.e.*, $\langle \hat{T}_z \rangle \neq 0$ and $\langle \hat{T}_y \rangle \neq 0$. Hence, the appearance of the pn paired field can be viewed as the spontaneous isospin symmetry breaking.

The non-conservation of the isospin is a drawback of the BCS theory and a deficiency of our model. The methods proposed to restore isospin symmetry include *e.g.*, Random Phase Approximation [106, 107], exact projection [108], cranking in isospace [75, 109, 110]. It is beyond the scope of the present study to apply the isospin symmetry conservation techniques in the case of the BCS approach. In the next section we focus on another problem related to the BCS approach, that is on the non-conservation of the particle number.

4.3   Generalized Lipkin-Nogami approach

A strightforward application of the BCS theory to finite systems has two main drawbacks. First, the BCS function is not an eigenstate of the particle number operator,

---

[1]In actual calculations the isospin symmetry is already broken on the mean-field level. Thus even for the $N = Z$ nucleus the symmetry conditions are not fulfilled.

so the number fluctuation is an issue for small systems like nuclei. Second, there is some critical value of the pairing strength below which no non-trivial solution can be found. Several methods were proposed to cure this problem: Random Phase Approximation (RPA) calculations in addition to BCS [111], particle number projection after variation (PAV) [112] which is valid only for pairing strengths above the critical value, similarly as the approach based on the Generator Coordinate Method (GCM) within the Gaussian Overlap Approximation [113, 114, 115]. Projecting the wave functions before variation (VAP) in principle works well for all pairing strengths [116]. It should be, however, mentioned that solving the VAP equations is not easy and numerical calculations of that type are highly time consuming. Additionally, the full projection of the BCS functions in the case of the *pn* pairing taken into account becomes quite complicated already on the formal level. A simplified prescription for the last technique is an approach proposed by Lipkin [117] and applied by Nogami [118] which has been quite successful in overcoming some of the problems related to applications of the BCS to nuclei (for early applications see *e.g.* [119, 120]).

In the forthcoming we describe the generalized Lipkin-Nogami method suitable to treat as well *pn* pairing correlations. We follow here the considerations of Refs. [121, 122] done in the case of rotating nuclei with *nn* and *pp* monopole pairing. It should be added that the Lipkin-Nogami formalism extended to the case of $T = 1$ and $T = 0$ monopole pairing was already presented and applied in Refs. [29, 109].

4.3.1 Outline of the method

Let $|\psi_{NZ}\rangle$ be a quasiparticle vacuum state of the system consisting of neutrons and protons

$$\alpha_K|\psi_{NZ}\rangle = 0\,, \tag{4.63}$$

where the subscripts NZ denote the average numbers of particles, both neutrons N and protons Z. The usual conditions of particle number conservation are

$$\langle\psi_{NZ}|\hat{N}_\tau|\psi_{NZ}\rangle = \left\{ \begin{array}{ll} N, & \tau = n, \\ Z, & \tau = p \end{array} \right. \tag{4.64}$$

and $\hat{N}_\tau = \sum_k a^\dagger_{k\tau}a_{k\tau}$ is the corresponding particle number operator.

The particle number operators $\hat{N}_\tau$ commute with the Hamiltonian (4.41): $[H, \hat{N}_\tau] = 0$ and the set of operators $\{\hat{N}, \hat{Z}, \hat{H}\}$ has common eigenfunctions which we denote by $|\phi_{N_0Z_0}\rangle$:

$$\hat{N}_\tau|\phi_{N_0Z_0}\rangle = N_{0\tau}|\phi_{N_0Z_0}\rangle\,, \tag{4.65}$$
$$\hat{H}|\phi_{N_0Z_0}\rangle = E_{N_0Z_0}|\phi_{N_0Z_0}\rangle\,. \tag{4.66}$$

This allows to write the quasiparticle vacuum state (4.63) in terms of the eigenstates of $\hat{N}_\tau$ and $\hat{H}$:

$$|\psi_{NZ}\rangle = \sum_{N_0Z_0} c_{NZ,N_0Z_0}|\phi_{N_0Z_0}\rangle\,. \tag{4.67}$$

From Eq. (4.65) it follows

$$\langle\psi_{NZ}|\hat{N}^K\hat{Z}^L|\psi_{NZ}\rangle = \sum_{N_0Z_0}|c_{NN_0,ZZ_0}|^2 N_0^K Z_0^L\,, \tag{4.68}$$

for $K, L = 0, 1, \ldots$.

Suppose that the eigenvalue E_{NZ} can be expanded in particle-projected state (limiting this expansion to terms of the second order in N and Z) as

$$E_{NZ} = \langle\phi_{NZ}|\hat{H}|\phi_{NZ}\rangle = \lambda_0 + \sum_\tau \lambda_\tau N_\tau + \sum_{\tau\tau'}\lambda_{\tau\tau'}N_\tau N_{\tau'}\,. \tag{4.69}$$

The expectation value of the operator

$$\mathcal{H} = \hat{H} - \sum_\tau \lambda_\tau\hat{N}_\tau - \sum_{\tau\tau'}\lambda_{\tau\tau'}\hat{N}_\tau\hat{N}_{\tau'} \tag{4.70}$$

in the $|\Psi_{NZ}\rangle$ state equals

$$\langle\Psi_{NZ}|\mathcal{H}|\Psi_{NZ}\rangle = \sum_{N_0Z_0}|c_{NN_0,ZZ_0}|^2\langle\phi_{N_0Z_0}|\mathcal{H}|\phi_{N_0Z_0}\rangle = \lambda_0\,. \tag{4.71}$$

Consequently, substituting (4.71) into (4.69) one obtains

$$\begin{aligned}
\langle\phi_{N_0Z_0}|\hat{H}|\phi_{N_0Z_0}\rangle &= \langle\psi_{NZ}|\hat{H}|\psi_{NZ}\rangle \\
&- \sum_\tau \lambda_\tau\langle\psi_{NZ}|\hat{N}_\tau - N_\tau|\psi_{NZ}\rangle \\
&- \sum_{\tau\tau'}\lambda_{\tau\tau'}\langle\psi_{NZ}|(\hat{N}_\tau\hat{N}_{\tau'} - N_\tau N_{\tau'})|\psi_{NZ}\rangle\,.
\end{aligned} \tag{4.72}$$

The last equation shows that the minimization of the energy $E_{N_0Z_0} = \langle\phi_{N_0Z_0}|\hat{H}|\phi_{N_0Z_0}\rangle$ in the projected state $|\phi_{N_0Z_0}\rangle$ is equivalent to the minimization of the right hand side of this equation which depends on the displayed expectation values calculated in the quasiparticle vacuum state $|\psi_{NZ}\rangle$.

The set of constants $\{\lambda\}$ entering the equation (4.72) has to be determined. To do this let us calculate the average value of the operator

$$\mathcal{H}(\lambda)\hat{N}^K\hat{Z}^L\,, \tag{4.73}$$

where $\mathcal{H}(\lambda)$ is given by Eq. (4.70) and $K, L = 0, 1, \ldots$, in the quasiparticle vacuum state $|\psi_{nz}\rangle$. After using the expansions (4.67) and (4.69) as well as the formula (4.68) one obtains

$$\langle\psi_{NZ}|\mathcal{H}(\lambda)\hat{N}^K\hat{Z}^L|\psi_{NZ}\rangle = \langle\psi_{NZ}|\mathcal{H}(\lambda)|\psi_{NZ}\rangle\langle\psi_{NZ}|\hat{N}^K\hat{Z}^L(\lambda)|\psi_{NZ}\rangle\,. \tag{4.74}$$

In the given second order approximation in λ's the equations (4.74) for λ_τ and $\lambda_{\tau\tau'}$ are specified by taking $K, L = 0, 1, 2$:

$$\begin{aligned}
\langle\psi_{NZ}|\mathcal{H}(\lambda)\hat{N}_\tau|\psi_{NZ}\rangle &= \langle\psi_{NZ}|\mathcal{H}(\lambda)|\psi_{NZ}\rangle\langle\psi_{NZ}|\hat{N}_\tau|\psi_{NZ}\rangle \tag{4.75} \\
\langle\psi_{NZ}|\mathcal{H}(\lambda)\hat{N}_\tau\hat{N}_{\tau'}|\psi_{NZ}\rangle &= \langle\psi_{NZ}|\mathcal{H}(\lambda)|\psi_{NZ}\rangle\langle\psi_{NZ}|\hat{N}_\tau\hat{N}_{\tau'}|\psi_{NZ}\rangle\,. \tag{4.76}
\end{aligned}$$

The variation of $\langle \psi_{NZ} | \mathcal{H}(\lambda) | \psi_{NZ} \rangle$ at constant λ_τ and under the constraints (4.64) leads to the expression for λ_τ satisfying automatically equations (4.75). The last four equations (4.76) have to be solved separately.

In the model of non-interacting quasiparticles one assumes the terms of $\hat{H}_{31} + \hat{H}_{13}$ and of higher order in the Hamiltonian of Eq. (4.42) vanish. The variation of the energy is equivalent to the BCS condition (4.44). Therefore, in this approximation the equations (4.76) take the form

$$\sum_{\{\tilde{4}\}} \langle \tilde{0} | \mathcal{H}(\lambda)_{04} | \tilde{4} \rangle \langle \tilde{4} | (\hat{N}_\tau \hat{N}_{\tau'})_{40} | \tilde{0} \rangle = 0 \,, \tag{4.77}$$

where $|\tilde{4}\rangle\langle\tilde{4}|$ projects onto the subspace of all 4-quasiparticle states. From the above conditions one determines the values of $\lambda_{\tau\tau'}$.

The term $(\mathcal{H}(\lambda))_{04}$ in Eq. (4.77) consists of the two following terms (up to second order in λ)

$$\mathcal{H}(\lambda)_{04} = -\sum_{\rho\rho'} (G^{\rho\rho'})_{04} - \sum_{\rho\rho'} \lambda_{\rho\rho'} (N_\rho N_{\rho'})_{04} \,, \tag{4.78}$$

where the operator $G^{\rho\rho'}$ is the two-body part of the Hamiltonian (4.41) and $\rho, \rho' = p, n$. The other parts of the full Hamiltonian of the system do not contribute to the (04) part of this decomposition. We can rewrite Eqs. (4.77) in the form

$$\mathcal{G}^{\tau\tau'} + \sum_{\rho\rho'} \lambda_{\rho\rho'} \mathcal{N}^{\tau\tau'}_{\rho\rho'} = 0 \,, \tag{4.79}$$

where

$$\mathcal{G}^{\tau\tau'} = \sum_{\rho\rho',\{\tilde{4}\}} \langle \tilde{0} | (G^{\rho\rho'})_{40} | \tilde{4} \rangle \langle \tilde{4} | (\hat{N}_\tau \hat{N}_{\tau'})_{04} | \tilde{0} \rangle \,, \tag{4.80}$$

and

$$\mathcal{N}^{\tau\tau'}_{\rho\rho'} = \sum_{\{\tilde{4}\}} \langle \tilde{0} | (\hat{N}_\rho \hat{N}_{\rho'})_{40} | \tilde{4} \rangle \langle \tilde{4} | (\hat{N}_\tau \hat{N}_{\tau'})_{04} | \tilde{0} \rangle \,. \tag{4.81}$$

The Eq. (4.79) is in fact the set of three linear equations, as $\lambda_{pn} = \lambda_{np}$. The exact expressions for $\mathcal{G}^{\tau\tau'}$ and $\mathcal{N}^{\tau\tau'}_{\rho\rho'}$ as well as special cases of solutions are given in Appendix D.

4.3.2   Isospin generalized Lipkin-Nogami equations

As already said, the Lipkin-Nogami method aims at minimizing the expectation value of the operator (4.70). The coefficients $\lambda_{\tau\tau'}$ contrary to λ_τ are not Lagrange multipliers. Their values are obtained from subsidiary conditions (4.76) which lead to the set of linear equations (4.79). Having calculated the values of $\lambda_{\tau\tau'}$ one can obtain the Lipkin-Nogami equations which take the form of BCS equations with single-particle energies and pairing gaps renormalized as follows

$$\tilde{\epsilon}^{(\text{LN})}_{k\tau} = \tilde{\epsilon}_{k\tau} + 2\lambda_{\tau\tau} \rho^{\tau\tau}_{kk} \,,$$
$$\Delta^{\tau\tau'(\text{LN})}_k = \Delta^{\tau\tau'}_k - 2\lambda_{\tau\tau} \kappa^{\tau\tau'}_{k\bar{k}} \,, \tag{4.82}$$

with particle desities ρ and pairing tensor κ defined as before (Eqs. (4.21,4.22)). The pairing energy in the Lipkin-Nogami approximation is given by

$$E_{\text{LN}} = E_{\text{pair}} - 2 \sum_{k,\tau\tau'} \lambda_{\tau\tau'} \kappa_{k\bar{k}}^{\tau\tau'} \kappa_{k\bar{k}}^{\tau\tau'\star} . \tag{4.83}$$

Solving the LN problem is therefore equivalent to the diagonalization of the matrix

$$\begin{pmatrix} \tilde{\epsilon}_{kp}^{(\text{LN})} & 0 & \Delta_k^{pp(\text{LN})} & \Delta_k^{pn(\text{LN})} \\ 0 & \tilde{\epsilon}_{kn}^{(\text{LN})} & \Delta_k^{pn(\text{LN})\star} & \Delta_k^{nn(\text{LN})} \\ \Delta_k^{pp(\text{LN})} & \Delta_k^{pn(\text{LN})} & -\tilde{\epsilon}_{kp}^{(\text{LN})} & 0 \\ \Delta_k^{pn(\text{LN})\star} & \Delta_k^{nn(\text{LN})} & 0 & -\tilde{\epsilon}_{kn}^{(\text{LN})} \end{pmatrix} \begin{pmatrix} u_{kqp} \\ u_{kqn} \\ v_{kqp} \\ v_{kqn} \end{pmatrix} = E_{kq}^{(\text{LN})} \begin{pmatrix} u_{kqp} \\ u_{kqn} \\ v_{kqp} \\ v_{kqn} \end{pmatrix} \tag{4.84}$$

for each single-particle state which provides new amplitudes u and v necessary to calculate $\lambda_{\tau\tau'}$ coefficients, pairing gaps and particle numbers. Proceeding like in the BCS case we obtain the Lipkin-Nogami equations solutions in an iterative procedure when the required accuracy is reached.

4.4   Results

4.4.1   Potential energy curves of N∼Z Ge nuclei

In the present section we describe the results of our investigation of potential energy curves of the ^{64}Ge ($N = Z$) nucleus and the neighbouring isotopes ($N = 28 - 36$) obtained in the Skyrme-HF model with two variants of the residual interaction employed in pp and nn channels. The self-consistent fields obtained here in the minima of deformation will serve as a departure point for further calculations in the BCS(LN) approaches and in the HTDA method (Chap. 5).

The ^{64}Ge nucleus has already been a subject of many theoretical investigations. The ground state shape of this nucleus is very sensitive to the model used in calculations. The HF and HFB approaches with central Yukawa potential [123, 124] predicted ^{64}Ge to be deformed with an oblate shape. In Strutinsky-like calculations with folded Yukawa single-particle potential [125] the ground-state minimum was found to be prolate with ϵ_2=0.2 deformation. The calculations based on a non-axial WS potential predicted a triaxial ground state minimum with β_2=0.2 [126]. The Skyrme-HF model, with SIII force and constant pairing gap approximation suggest a prolate minimum, however with a small prolate-oblate difference [127].

The Ge isotopes ^{66}Ge and ^{68}Ge have been also a subject of a great interest in both experimental [128, 129, 130, 131, 132] and theoretical studies [133, 134, 135, 136] for many years. Due to large gaps between single-particle spectra at prolate and oblate minima of $N, Z = 34 - 36$ nuclei, shape coexistence is a typical phenomenon in this region. The prolate-oblate shape transition and possible γ-softness in these germanium isotopes were suggested by many authors, however different models do not necessarily provide the same picture of ground state deformations.

To find the dependence of the total energy of a nucleus on the quadrupole deformation we have performed constrained HF+BCS calculations assuming the axial symmetry of the nucleus. The calculations were done with the SIII parametrization of the Skyrme force which was shown to be a very good interaction as far as spectroscopic (single-particle or collective) properties of nuclei are concerned. All the results were obtained with an axially deformed harmonic oscillator basis with N_0=16 shells. The parameters $q = \omega_\perp/\omega_z$ and $b = \sqrt{m\omega_0/\hbar}$ (with $\omega_0 = (\omega_\perp^2 \omega_z)^{1/3}$), characterizing the oscillator basis, were optimized all along the energy curve, as described *e.g.* in Ref. [137]. To obtain the needed deformation we use a quadratic constraint on the quadrupole mass moment with an approach which adjusts iteratively the Lagrange multipliers to provide the requested expectation value of the constraint operator [138].

Pairing correlations were treated in two approaches: the usual BCS formalism with a seniority force (G force) and the state-dependent one based on the surface-independent (volume) δ interaction. In both cases the BCS equations were solved in a truncated space of single-particle levels, taking into account states with energies less or equal to e_F+8 MeV, e_F being the Fermi level energy. The constant matrix elements of the G force are given by

$$G_\tau = \frac{g_\tau}{11 + N_\tau} \,, \tag{4.85}$$

where N_τ is the number of particles with isospin τ (neutrons or protons) and

$$g_n = 17.1 \,\text{MeV}, \quad g_p = 15.6 \,\text{MeV}. \tag{4.86}$$

This parametrization was found for four germanium nuclei ($A = 62-68$) by comparing the calculated minimal quasiparticle energies with those obtained from nuclear binding energies by 3-point formula. The fit was done in the minima of the potential energy. In Fig. 4.1 theoretical and experimental pairing gaps for protons and neutrons are shown for considered nuclei. The zero-range δ interaction acting in the isovector ($|T_z| = 1$) channel is of the form[2]

$$\hat{V}_\delta(\vec{r}_{12}) = V_{0\tau} \frac{1 - \vec{\sigma}_1 \cdot \vec{\sigma}_2}{4} \delta(\vec{r}_1 - \vec{r}_2) \,, \tag{4.87}$$

where $V_{0\tau}$ is the coupling constant for particles of a given τ. Since the level densities of neutrons and protons are a priori different, the numbers of neutron and proton levels contained in the window of the same size $e_F + X$ MeV may differ considerably, and thus similarly the adjusted V_{0n}, V_{0p} values. Nevertheless, this is no longer the case of $N \sim Z$ nuclei where assuming that $V_{0n} = V_{0p}$ is well justified.

To make a reasonable comparison of the results obtained with G and δ- forces, the intensities of the latter have to be adjusted properly. We determine $V_{0\tau}$ from the condition that the traces of the pairing tensors are the same as in the G force

---

[2]Indices T, τ in $V_{0\tau}^T$ will be dropped in cases where it will not lead to a misunderstanding.
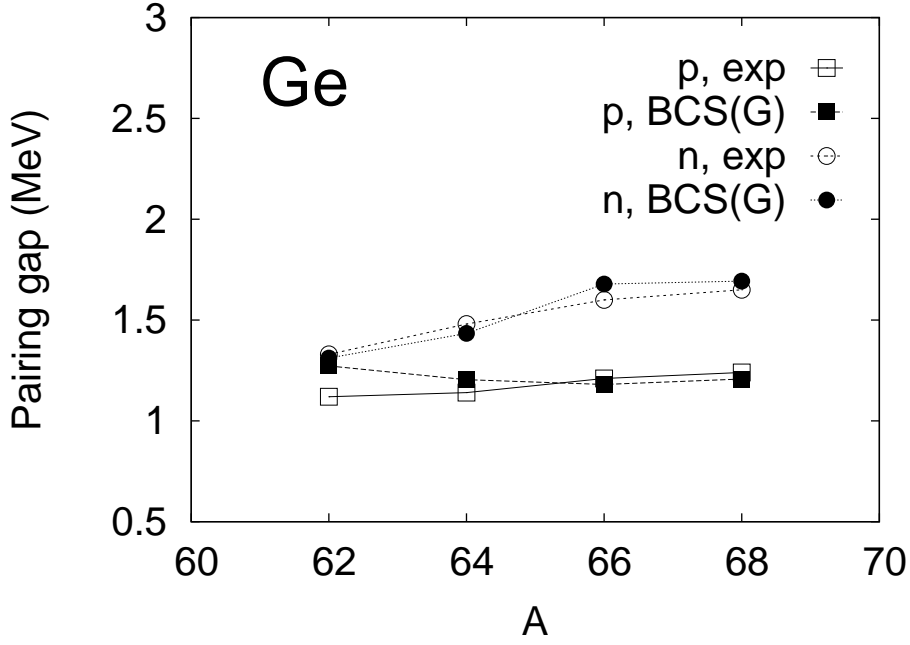
Figure 4.1: Neutron (circles) and proton (squares) pairing gaps calculated with G force in comparison to $\Delta^{(3)}$ pairing indicators.
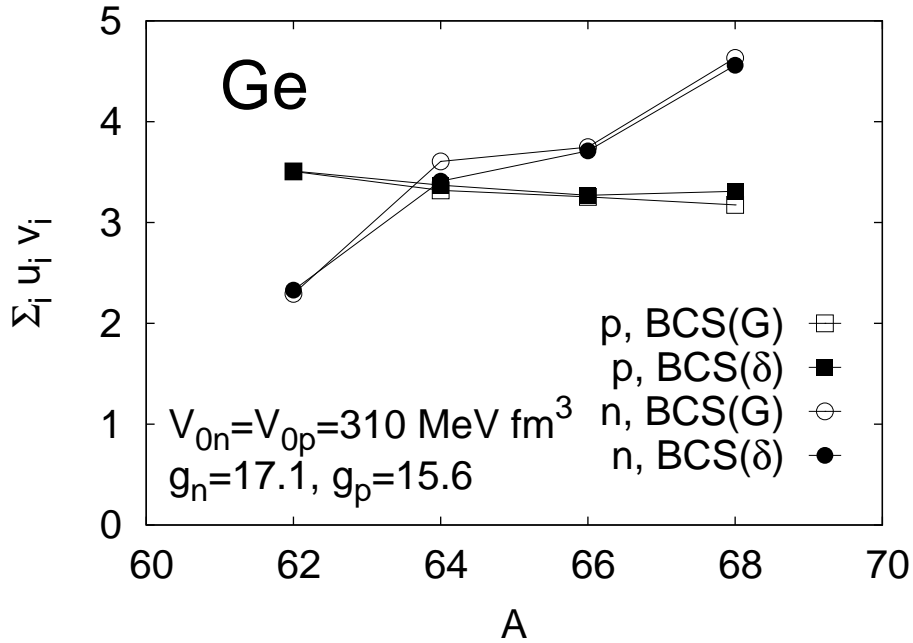
Figure 4.2: Traces of the pairing tensor $\sum_{i>0} u_i v_i$ calculated with seniority and δ forces for neutrons (circles) and protons (squares).
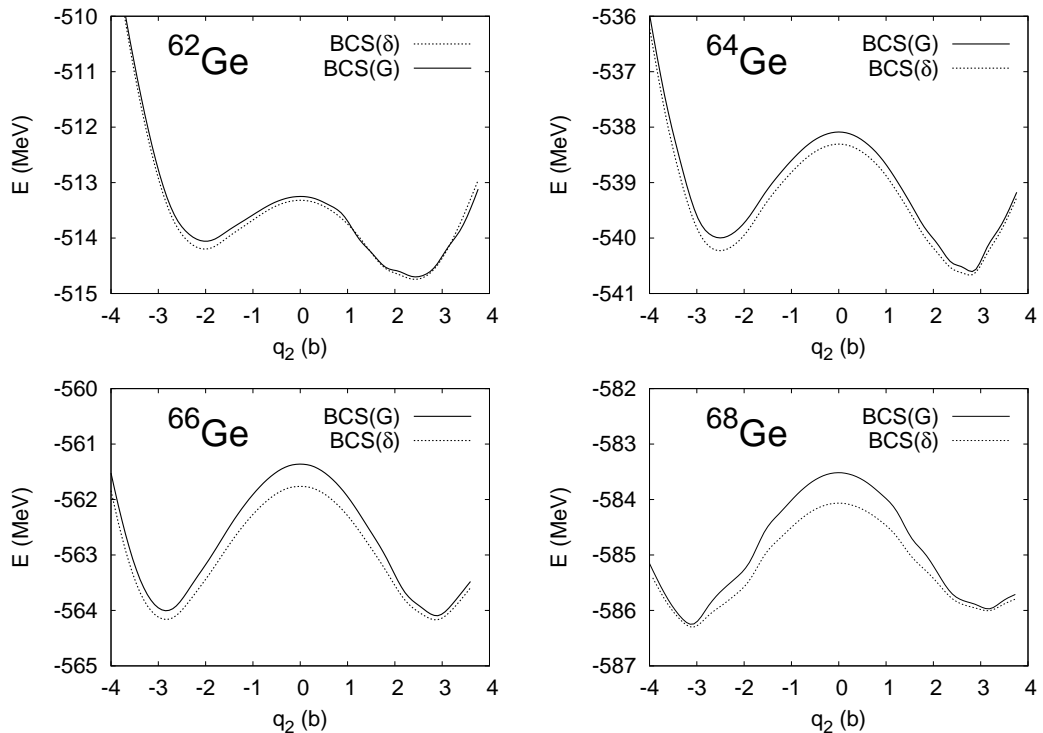
Figure 4.3: The potential energy E (MeV) as a function of the mass quadrupole moment $q_2 = \langle \hat{Q}_{20} \rangle$ (in barns) for germanium ($Z = 32$) nuclei with mass numbers $A = 62 - 68$. The results of two calculations are presented: BCS calculations with constant matrix elements (solid line) and with the δ force (dashed line).

case. This way we obtain the δ force strengths for both charge states and for all considered nuclei equal to

$$V_{0n} = V_{0p} = 310 \, \text{MeV} \, \text{fm}^3 \,. \tag{4.88}$$

The traces $\sum_{i>0} u_i v_i$ of pairing tensors κ evaluated with both pairing forces with parametrizations described above are shown in Fig. 4.2.

The potential energy as a function of the mean value of the mass quadrupole moment (Eq. (2.42))

$$q_2 = \langle \hat{Q}_{20} \rangle \tag{4.89}$$

for studied Ge isotopes is depicted in Fig. 4.3. The results of two calculations are reported: with seniority and δ forces. Although the energy curves depend on the pairing type, the general conclusions concerning the shape of the nuclei under consideration remain the same. Namely, ^{62}Ge is predicted to be prolate however the energy difference between both deformed minima is only about 700 keV. ^{64}Ge, as said previously, is predicted to be prolate in its ground state, with the oblate minimum being higher on about 0.5 MeV. ^{66}Ge appears to be a transitional system with two almost degenerate minima, the prolate one laying about 20 keV lower in

Table 4.1: Oblate $\langle \hat{Q}_{20} \rangle_{\mathrm{o}}$ and prolate $\langle \hat{Q}_{20} \rangle_{\mathrm{p}}$ deformations (in barn) and corresponding energy values E (in MeV) for studied nuclei. The results concerns the calculations with the G force.

nucleus	$\langle \hat{Q}_{20} \rangle_{\mathrm{o}}$ (b)	E (MeV)	$\langle \hat{Q}_{20} \rangle_{\mathrm{p}}$ (b)	E (MeV)
^{62}Ge	-2.1	-514.0	2.4	-514.7
^{64}Ge	-2.4	-540.0	2.6	-540.5
^{66}Ge	-2.6	-563.9	2.8	-564.1
^{68}Ge	-3.0	-586.2	2.9	-585.8

Table 4.2: Same as in Table 4.2 but for the δ force.

nucleus	$\langle \hat{Q}_{20} \rangle_{\mathrm{o}}$ (b)	E (MeV)	$\langle \hat{Q}_{20} \rangle_{\mathrm{p}}$ (b)	E (MeV)
^{62}Ge	-2.1	-514.1	2.3	-514.7
^{64}Ge	-2.4	-540.2	2.6	-540.6
^{66}Ge	-2.7	-564.1	2.9	-564.1
^{68}Ge	-3.0	-586.3	2.9	-585.9

the case of the G force. A similar case is ^{68}Ge nucleus, this time the oblate minimum being energetically favoured. The detailed values of equilibrium deformations and corresponding total energies resulting our calculations are listed in Tables 4.1 (the seniority force case) and 4.2 (for the δ force).

The effects of including proton-neutron pairing and applying different methods to solve the pairing problem presented in the forthcoming sections are studied with the spectra generated as described here in the ground states of considered germanium isotopes.

4.4.2   Skyrme force-like extension of nuclear pairing interaction

In Sec. 4.1 we have introduced the pairing interaction Eq. (4.8) in the form which allows to study all possible space-spin-isospin components and is relatively simple for numerical calculations. First, consider the matrix elements of such an interac-
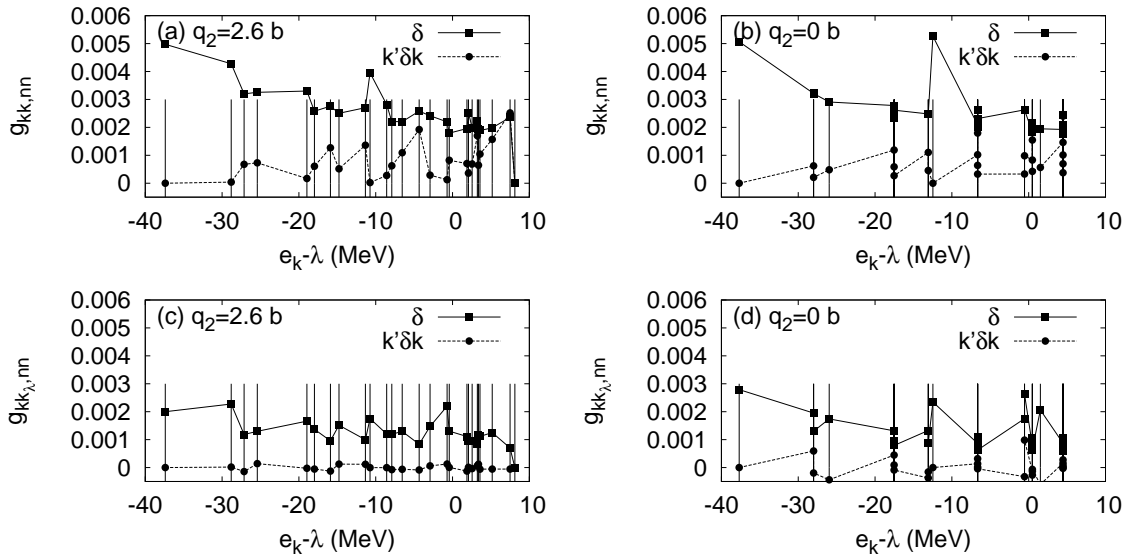
Figure 4.4: Neutron-neutron pairing matrix elements vs single-particle energies normalized to the energy of Fermi level for ^{64}Ge nucleus. The upper panels show diagonal matrix elements in the equilibrium deformation (a) and in the spherical point (b). Panels (c) and (d) shows off-diagonal matrix elements for levels k with the k_λ corresponding to the Fermi energy. Squares corresponds to the δ force antisymmetrized matrix elements, filled circles to the $\boldsymbol{k}'\delta\boldsymbol{k}$ case. Vertical lines represent single-particle spectrum.

tion in the like-particle case. In Figs. 4.4, 4.5 we show an excerpt of bare (*i.e.*, $V_{0\tau}^T = 1, \mathrm{x} = 1$) antisymmetrized pairing matrix elements of $\hat{V}_\delta$ (squares) and $\hat{V}_{\boldsymbol{k}'\delta\boldsymbol{k}}$ (filled circles) interactions (see Eq. (4.8)) calculated for the ^{64}Ge nucleus in its equilibrium deformation and in the spherical point as functions of the single-particle levels relative to the Fermi energy. It is seen that the bare pairing matrix elements of the δ force are larger than those of $\boldsymbol{k}'\delta\boldsymbol{k}$ and that they are not correlated. The non-diagonal matrix elements of the $\boldsymbol{k}'\delta\boldsymbol{k}$ force are nearly equal to zero or negative suggesting a locally repulsive character of the interaction in $T = 1$, $L = 1$, $S = 1$ channel. The behaviour shown in Figs. 4.4 and 4.5 is common for all studied nuclei.

Similarily, in Figs. 4.6, 4.7 we show an excerpt of antisymmetrized proton-neutron matrix elements of δ (squares) and $\boldsymbol{k}'\delta\boldsymbol{k}$ (filled circles) forces calculated for ^{64}Ge in its equilibrium deformation and in the spherical point as functions of single-particle levels normalized to the Fermi level energy. We chose the proton spectrum as the reference one. It is seen that the *pn* pairing matrix elements in the $T = 1$ channel (Fig. 4.6) have a similar behaviour as those of *pp* and *nn* pairing interactions shown in the preceding, however they are on about two times smaller. The diagonal *pn* pairing matrix elements in $T = 1$ and $T = 0$ channels are pretty equal for both kinds of interactions, while the off-diagonal ones have somewhat different behaviour. As in the case of the like-particle pairing, the $\boldsymbol{k}'\delta\boldsymbol{k}$ elements are much smaller than
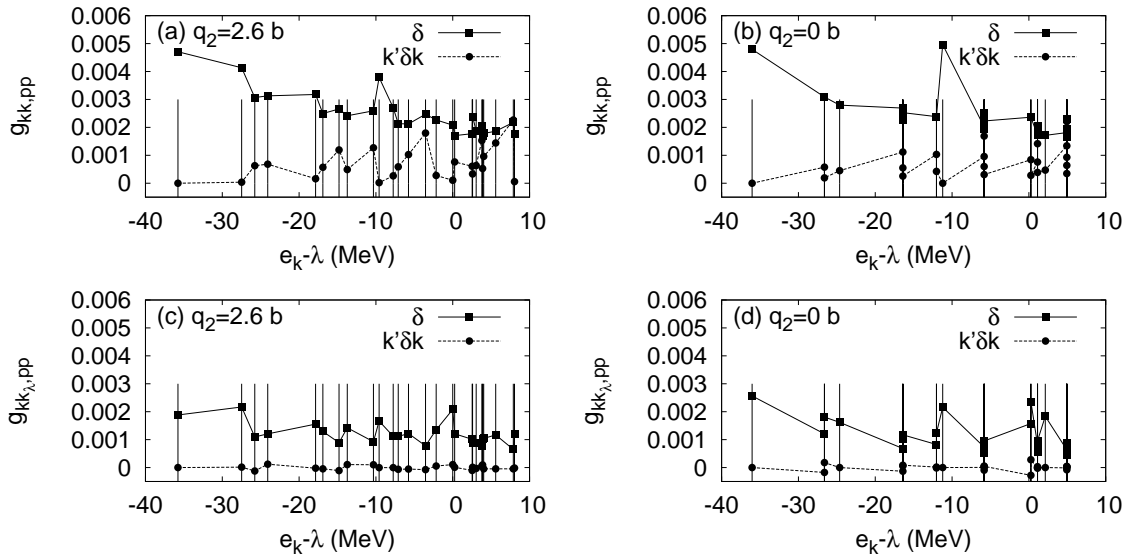
Figure 4.5: Same as in Fig. 4.4 but for proton-proton pairing interaction.

those of the δ force in all cases.

In Fig. 4.8 the pairing gap deviation as a function of the strengths of the pairing interaction in $L = 0$ and $L = 1$ channels is displayed. The gap deviation is defined as

$$\sigma_\Delta = \sqrt{\frac{1}{2} \sum_{\tau = p,n} (\Delta_\tau^{\text{th}} - \Delta_\tau^{\text{exp}})^2} \, , \tag{4.90}$$

where the lowest quasiparticle energy is adopted as a theoretical pairing gap and the experimental one is the 3-point pairing indicator. As seen, for all considered cases there exists a valley of equivalent minima, no x value being conspicuously favoured. In Ref. [139] we have shown that an analogous situation is found when the proton-neutron pairing is taken into account and that the inclusion of the $\hat{V}_{\boldsymbol{k}'\delta\boldsymbol{k}}$ term does not influence much the obtained results as far as the behaviour of the BCS solutions and the Wigner energy are concerned. Hence, in the forthcoming sections we will use only the δ force to perform the BCS(LN) calulations with the pn pairing.
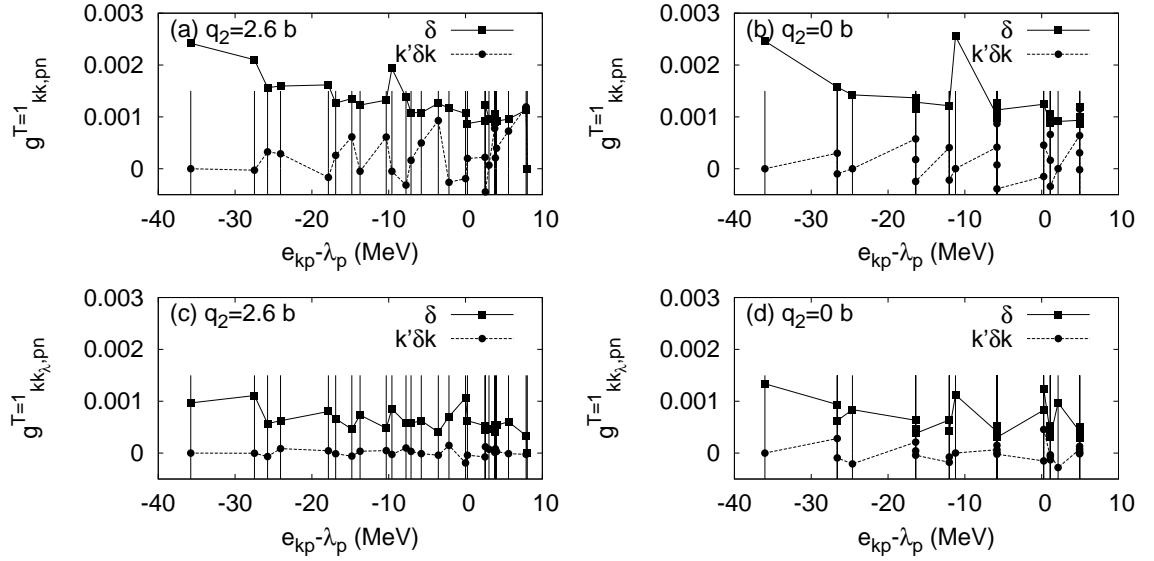
Figure 4.6: Proton-neutron pairing interaction matrix elements in the $T = 1$ channel vs proton single-particle energies normalized to the Fermi level energy for ^{64}Ge nucleus. The upper panels shows diagonal matrix elements in the equilibrium deformation (a) and in the spherical point (b). Panels (c) and (d) shows off-diagonal matrix elements for the level λ corresponding to the Fermi energy. Squares correspond to the δ force antisymmetrized matrix elements, filled circles to the $\boldsymbol{k'}\delta\boldsymbol{k}$ case. Vertical lines represent single-particle spectrum.
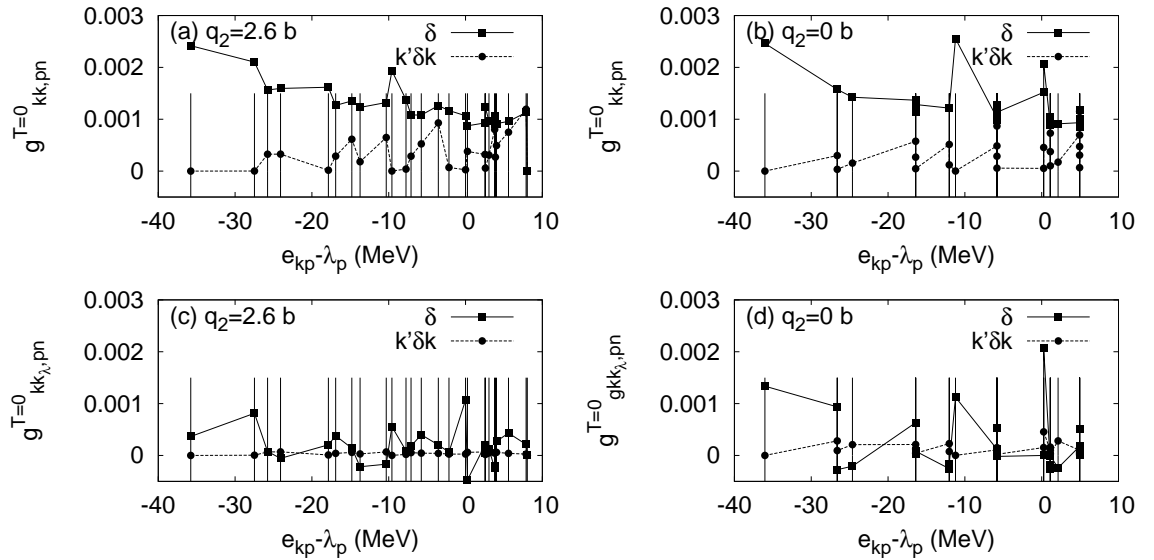
Figure 4.7: Same as in Fig. 4.4 but for proton-neutron $T = 0$ pairing interaction.
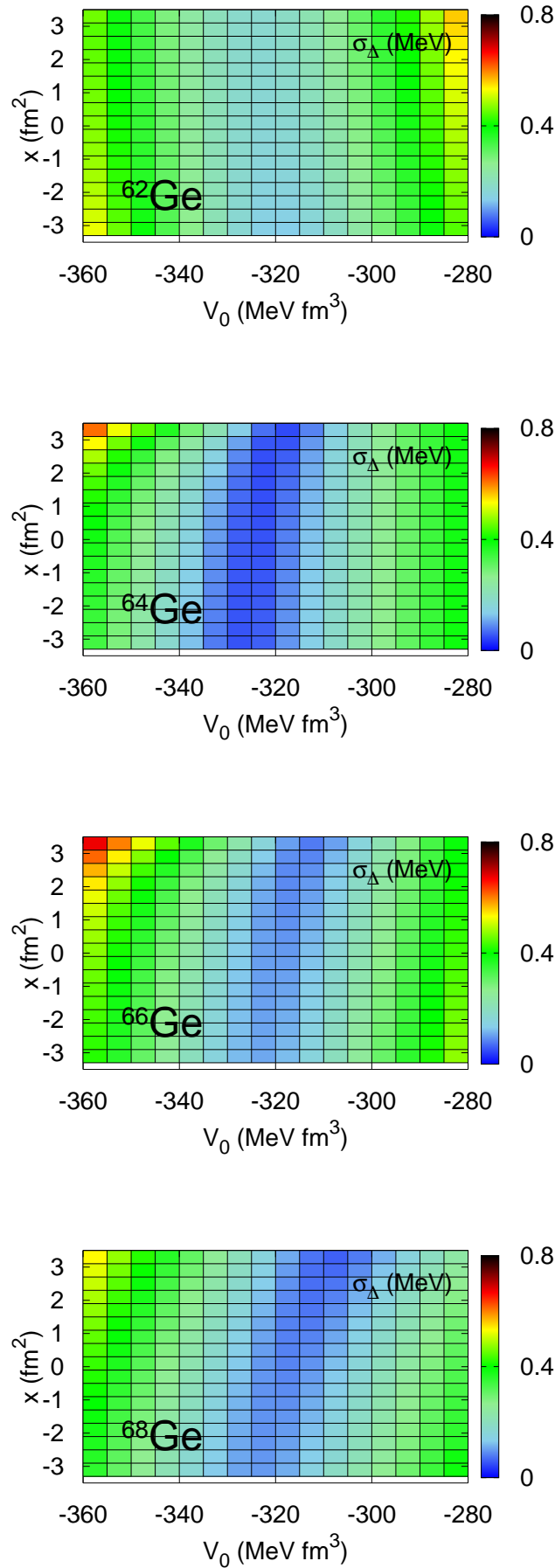
Figure 4.8: Pairing gap deviation (σ_Δ) as a function of the δ interaction strength V_0 and of the ratio x of the strengths of $\boldsymbol{k}'\delta\boldsymbol{k}$ and δ forces.

4.4.3   Generalized BCS results

The results discussed in here are obtained in the minima of the energy of Ge isotopes calculated as decribed in Sec 4.4.1. We will use the variant with the δ force since this is the main interaction we will consider in generalized BCS(LN) calculations. We adopt the same value of the interaction strength $V_0^{T=1} = 310$MeV fm^3 for pp, nn and pn pairing in the $T = 1$ channel basing ourselves on isospin invariance arguments. It has been proposed that the pn collectivity can be also accounted for in an isospin broken model with $V_{0pn}^{T=1} > V_{0n,p}^{T=1}$, see *e.g.* [140, 141, 142]. Nonetheless, we do not see any argument supporting such an approach.

While fitting the strengths in like-particle channels basing on experimental data is well established, for the $T = 0$ channel very little is known on the subject. Since $T = 0$ pairing correlations are believed to be responsible for the occurence of the Wigner term the pairing strength might be then adjusted to reproduce this quantity. On the other hand, one may try to fit the pn pairing gap extracted from masses but, as already mentionned, the meaning of this gap for $N \sim Z$ nuclei is not clear. However, it is not our aim here to reproduce the experimental data but to study the basic features of the pn pairing in our model. Hence, in the following we discuss most of the results of BCS and LN calculations as functions of the ratio of the pairing strengths in $T = 0$ and $T = 1$ channels

$$x = V_0^{T=0}/V_0^{T=1} \; . \tag{4.91}$$

The pn pairing is supposed to play a significant role mostly in self-conjugate nuclei. Increasing the number of neutron pairs increases the collectivity of the neutron condensate, making fewer neutrons available to pair with protons and the binding of pn condensate dropping dramatically. The situation can be viewed as a blocking phenomenon where the role of an odd particle is played by the additional neutrons (or protons) outside the $N = Z$ core [29].

A general feature of most calculations with the pn pairing [29, 66, 143, 144] is quenching of the pn pairing in the ground state of $|N - Z| = 4$ nuclei. Surprisingly, the authors of Ref. [28] have obtained the pn superfluid solutions even for the $N - Z = 8$ nucleus (^{78}Ge) in a BCS approach with the Bogoliubov transformation (4.15) in the calculations with monopole pairing forces and the single-particle levels of an axially deformed Woods-Saxon potential. Our previous calculations of this type [139, 145] are in agreement with those of Ref. [29], *i.e.* no collective pn pairing was observed for T$_z > 2$. In the present study, in both BCS and LN schemes, in T$_z = -1$ and T$_z = 2$ Ge nuclei only trivial pn solutions are found in the studied range of parameters thus the majority of the results is discussed only for the cases of ^{64}Ge and ^{66}Ge.

Pairing gaps

Since we deal here with the state-dependent pairing, *i.e.* for each single-particle level there exist a BCS pairing gap parameter, it is convenient to present the results

for the so-called spectral pairing gap which we consider to be a reasonable measure of pairing correlations. This quantity in the case of the usual BCS treatment is defined as

$$\Delta = \frac{\sum_{i>0} \Delta_i u_i v_i}{\sum_{i>0} u_i v_i} \; . \tag{4.92}$$

In our particular case with the Bogoliubov transformation (4.15) this definition leads to the subsequent expressions for nn, pp and pn spectral gaps

$$\Delta^{nn} = \frac{\sum_{i>0} \Delta_i^{nn}(v_{i1n}u_{i1n}^{\star} + u_{i2n}v_{i2n})}{\sum_{i>0}(v_{i1n}u_{i1n}^{\star} + u_{i2n}v_{i2n})} \; , \qquad \Delta^{pp} = \frac{\sum_{i>0} \Delta_i^{pp}(v_{i2p}u_{i2p}^{\star} + u_{i1p}v_{i1p})}{\sum_{i>0}(v_{i2p}u_{i2p}^{\star} + u_{i1p}v_{i1p})} \; ,$$

$$\Delta^{pn} = \frac{\sum_{i>0}(\Delta_i^{pn,T=1}\Re e(v_{i1p}u_{i1n}^{\star} + v_{i2p}u_{i2n}) + \Delta_i^{pn,T=0}\Im m(v_{i1p}u_{i1n}^{\star} + v_{i2p}u_{i2n}))}{\sum_i(v_{i1p}u_{i1n}^{\star} + v_{i2p}u_{i2n})} \; .$$

In Fig. 4.9 the dependence of the pp, nn and pn spectral pairing gaps as functions of the x parameter is shown for ^{64}Ge and ^{66}Ge nuclei for BCS and Lipkin-Nogami calculations. The pn pairing gap is a priori a sum of the solutions in $T = 0$ and $T = 1$ channels (see Eq. (4.46)). However, in fact, the $T = 1$ pn pairing gap is constantly equal to zero (cf. Fig. 4.10). It is found that in the BCS scheme in the $N = Z$ nucleus above some critical value of the x parameter ($x_{\mathrm{crit}} \sim 2.03$) the pn solution arises, at the same time the like-particle gaps being decreased. There is a narrow region of x in which all the three gaps do coexist. In the calculations with schematic pairing forces there was rather a sharp transition from $T = 1$ to $T = 0$ pairing at the critical point (see e.g. [28, 29]). Let us mention that in the calculations with the seniority pairing a simple relation is fulfilled: a non-trivial $T = 0$ solution emerges for $G_{np}^{T=0} > G_{np}^{T=1}$, so that the critical value is close to 1. The fact that the critical value found here is two times larger should be attributed to the magnitudes of the matrix elements of the δ force dependent on the channel.

A situation different from that observed in the $N = Z$ case is realised in ^{66}Ge nucleus, where the mixing of the $T = 1$ and $T = 0$ phases is allowed for all $x > x_{\mathrm{crit}} \sim 2$.

In the approximately particle conserving LN scheme the scenario changes in the $N = Z$ nucleus: the pn mode shows up at a larger value of x parameters ($x_{\mathrm{crit}} \sim 2.06$) but coexists with like-particle coherent field, similarily like in the $N \neq Z$ nucleus. The situation in ^{66}Ge is qualitatively the same in LN and BCS cases, the only differences being the magnitudes of pairing gaps at a given x value and the increase of x_{crit} in LN approach.

It is worth noting that in the Lipkin-Nogami case the gaps are considerably enhanced in the absence of the proton-neutron pairing in both ^{64}Ge (on average 0.5 MeV) and ^{66}Ge (0.25 MeV) nuclei as compared to the corresponding BCS solutions. For comparison, in the neighbouring ^{62}Ge and ^{68}Ge nuclei the change of the pairing gap in the particle-conserving approach is less than 0.15 MeV.

In Fig. 4.10 we show the pairing gap parameters $\Delta_i^{\tau\tau'}$ plotted on the sp spectra (as previously, proton spectra is chosen) normalized to the Fermi level energy in the
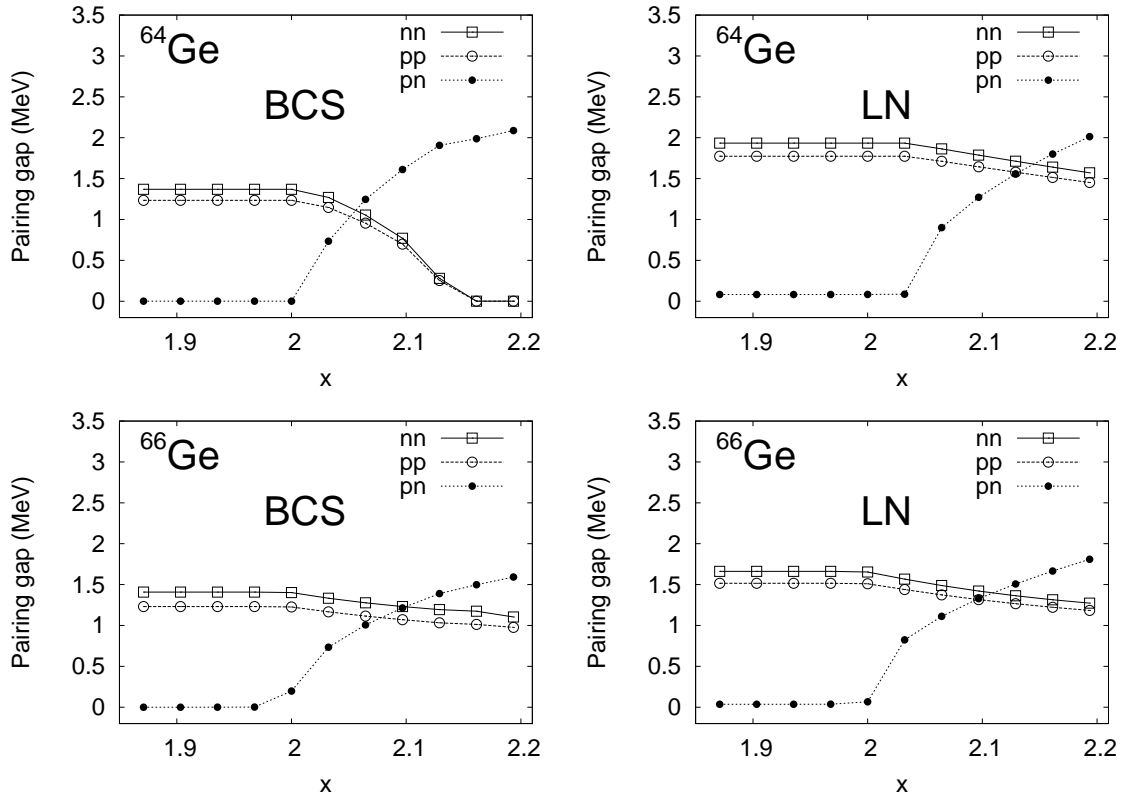
Figure 4.9: Spectral pairing gaps as functions of the $T = 0$ and $T = 1$ pairing strengths ratio x in ^{64}Ge and ^{66}Ge nuclei. The left part of the figure corresponds to BCS calculations, the right part to the Lipkin-Nogami (LN) solutions.
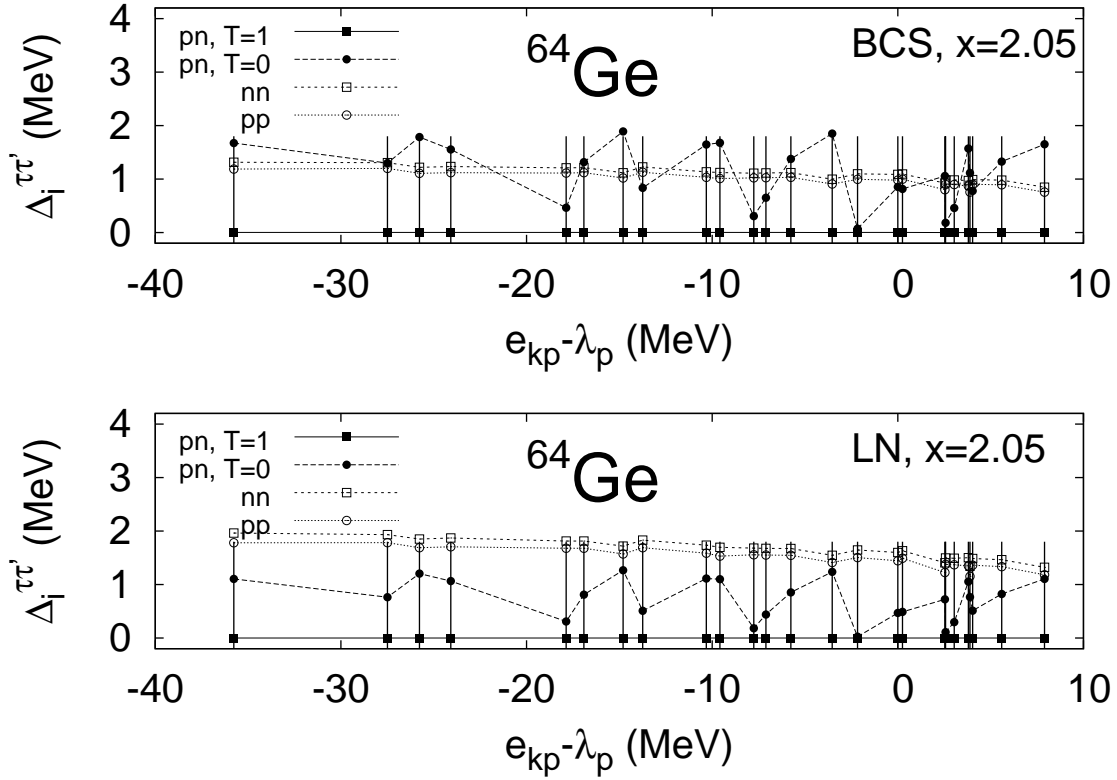
Figure 4.10: State-dependent pairing gaps in ^{64}Ge nucleus vs proton single-particle energies normalized to the Fermi energy. Two results are shown: BCS calculations (upper panel) and LN solutions (lower panel) in the point of the coexistence of nn, pp and pn solutions.

point of the coexistence of the three solutions ($x \sim 2.05$). Two results are reported, of the BCS and Lipkin-Nogami calculations. The magnitudes of pairing solutions for a given x depend on the method, but the results remain qualitatively the same. It is seen that the real, $T = 1$ part of the pn pairing gap is equal to zero for all states. It seems that $T = 0$ and $T = 1$ pn pairing modes are exclusive in our model. It is also observed that the like-particle gaps have a smooth dependence on the energy, slightly decreasing with the growing single-particle energy. The structure of pn pairing parameters is more irregular with magnitudes changing even on 1 MeV for neighbouring levels and reflects the pattern of diagonal matrix elements shown in Fig. 4.7.

Occupation probability

In Fig. 4.11 it is exhibited how the presence of the pn pairing influences the occupation probability

$$v_{i\tau}^2 = \sum_{q=1,2} v_{iq\tau} v_{iq\tau}^\star , \qquad (4.93)$$
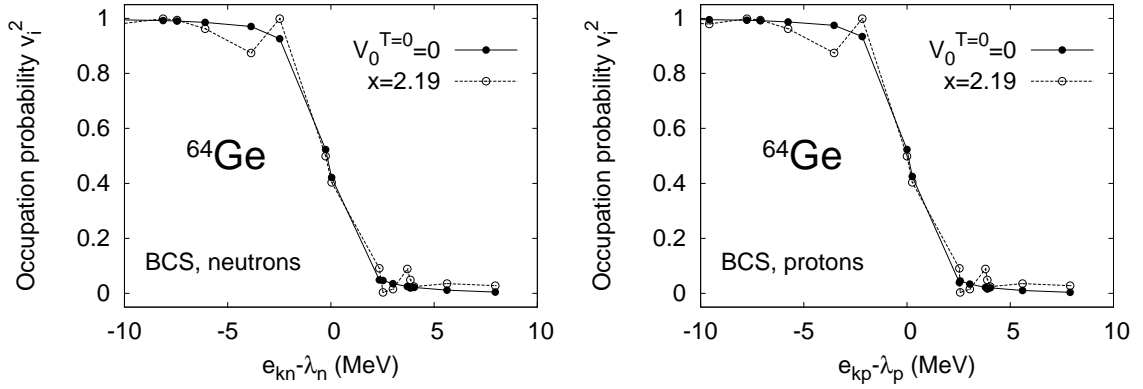
Figure 4.11: Occupation probability $v_{i\tau}^2$ as a function of sp energy normalized to the Fermi energy for neutrons (left panel) and protons (right panel) in the ^{64}Ge. The BCS solutions with (open circles) and without (filled circles) $T = 0$ pairing are shown.
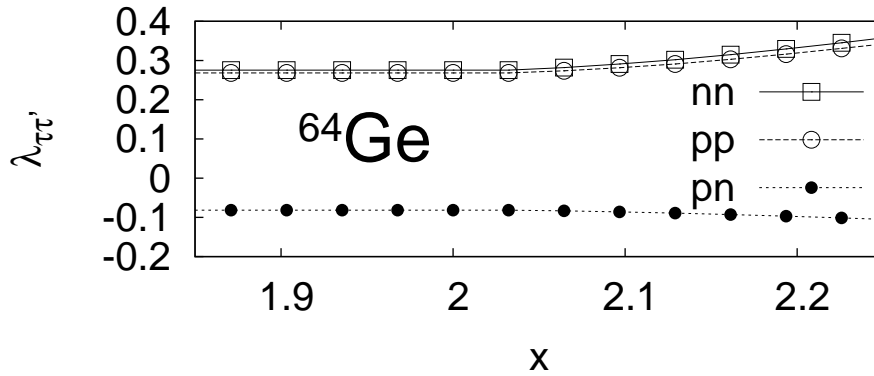
Figure 4.12: Lipkin-Nogami $\lambda_{\tau\tau'}$ parameters as functions of the x ratio in ^{64}Ge nucleus.

in the vicinity of the Fermi level for neutrons and protons in the ^{64}Ge nucleus. We show the dependence of v_i^2 on the sp energy in the case where no pn pairing is present $V_0^{T=0} = 0$ (filled circles) and in the case where there is a pn collectivity (open circles). The solutions are chosen in such a way that the pairing energy in both cases (with and without pn pairing) is approximately the same. In the BCS case it corresponds to the situation where only $T = 0$ pairing is present ($x = 2.19$). It is seen that the smooth diffusivity around the Fermi level is significantly disturbed when the pn pairing is taken into account.

Lipkin-Nogami $\lambda_{\tau\tau'}$ parameters

It is worthwhile to notice that the Lipkin-Nogami parameter λ_{pn} appears negative in numerical calculations thus the correction to the pairing energy associated with the pn mode is positive. Nevertheless, the corrections associated with the like-particle
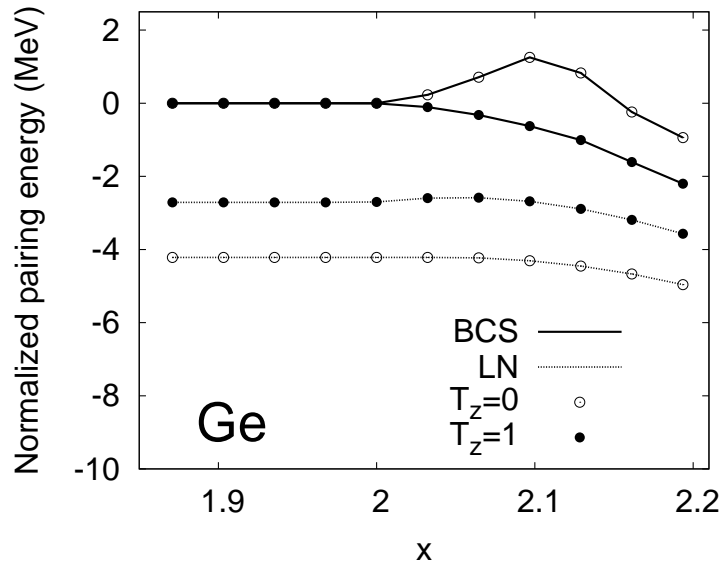
Figure 4.13: Normalized pairing energy as a function of x ratio in LN and BCS methods for ^{64}Ge ($T_z = 0$) and ^{66}Ge ($T_z = 1$) nuclei.

pairing are such that the total Lipkin-Nogami correction is negative and its absolute value increases slightly with the increase of $V_0^{T=0}$ strength.

The $\lambda_{\tau\tau}$ values increase when the pn pairing is activated. The λ_{pn} values as functions of x fulfil roughly the relation

$$\lambda_{pn} \approx -\frac{1}{3}\lambda_{\tau\tau}\,, \qquad\qquad (4.94)$$

therefore the Lipkin-Nogami correction is not symmetric in different pairing channels-the pn pairing is weakened while the pp and nn gaps are enhanced which results in the above mentionned shift of the critical value x_{crit} with respect to the corresponding BCS value. The behaviour of Lipkin-Nogami parameters as functions of x is demonstrated in Fig. 4.12 in the case of the $N = Z$ nucleus.

Pairing energy

In Fig. 4.13 the dependence of the pairing energy normalized to the BCS solution without the pn pairing is plotted as a function of the x ratio for the two studied cases. In the $N = Z$ nucleus the absolute value of the pairing energy decreases when all the three modes are present. Hence, such a system prefers to form only one type of pairs. The LN corrected solution lies on about 4.2 MeV lower than the BCS one. The pairing energy is a decreasing function of x but the gain in energy due to the appearance of the pn mode is very modest. In the $T_z = 1$ case the pairing energy diminishes with growing x value in both models. The LN solution is on about 2.5

MeV lower than the BCS one.

Let us point out the main features of BCS and LN solutions.

1. In the BCS method, the like-particle and the *pn* pairing can coexist in a narrow region of x parameters in the case of the $N = Z$ nucleus. With the increase of the pairing strength in the $T = 0$ channel the system undergoes a phase transition and prefers to form $T = 0$ pairs only. In the $T_z = 1$ nucleus the *pn* pairing mode does appear only in coexsistence with like-particle modes.

2. In the approximately particle-conserving scheme (LN) $T = 0$ and $T = 1$ superfluid phases can coexist in both nuclei for all values of x above x_{crit}.

3. Particle number conservation in the Lipkin-Nogami method acts destructively on the $T = 0$ pairing and enhances like-particle modes. Thence the $T = 0$ phase occurs for a larger x value as compared to the BCS results.

4. No coexistence of the *pn* pairing in $T = 1$ and $T = 0$ channels is found.

5. No *pn* collective solutions are observed for T_z=-1 and T_z=2 nuclei.

4.4.4 Wigner energy

In what follows we apply the method proposed by Chasman [69] which allows to estimate the pairing strength in the $T = 0$ channel basing ourselves on the knowledge of spectroscopic properties of nuclei.

In Sec. 3.1 we have shown how the Wigner energy is defined in terms of different combinations of binding energies of nuclei. To understand better the Wigner term we decompose the binding energies (B) into two parts: the Slater energy and the correlation energy. The Slater energy is the binding energy of the configuration obtained by filling the lowest single-particle levels. The correlation energy, which increase the binding, is the difference between the total binding energy and the Slater energy. This decomposition is useful because the correlation energy is almost constant from one even-even nucleus to the next and we may assume there is no change in the quantity

$$
\begin{aligned}
\delta V(N, Z) \;=\; & \frac{1}{4}\left[B(N, Z) - B(N - 2, Z)\right. \\
& \left. - B(N, Z - 2) + B(N - 2, Z - 2)\right]
\end{aligned} \tag{4.95}
$$

due to the correlations. Hence, we only need to derive the Slater energy for each of the configurations appearing in $\delta V(N, Z)$. The energy of the single Slater determinant wave function is just a sum of the diagonal energies evaluated for the Hamiltonian (4.41). We obtain for even-even $N = Z$ nuclei

$$
\delta V(N, Z) = \frac{1}{2}(G_{ii}^{T=1} + G_{ii}^{T=0}), \tag{4.96}
$$
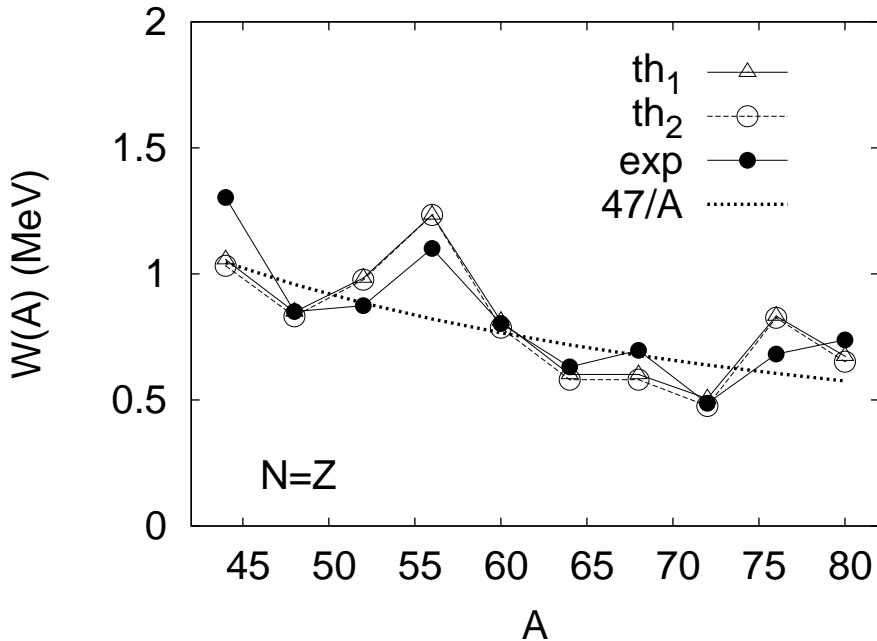
Figure 4.14: Experimental and calculated strength of the Wigner energy of even-even $N = Z$ nuclei. The results of two theoretical calculations are given, see text for details.

where

$$G_{ii}^T = V_0^T g_{ii}^T \tag{4.97}$$

and g_{ii}^T is a bare diagonal pairing matrix element of the proton-neutron interaction. If $N \neq Z$ one has

$$\delta V(N, Z) = 0 \,. \tag{4.98}$$

Plugging in the energies of the relevant configurations we get the Slater approximation to the Wigner energy of even-even $N = Z$ nuclei:

$$W(A) = \frac{1}{2}(G_{ii}^{T=1} + G_{ii}^{T=0}) \,, \tag{4.99}$$

Thence, we may adjust the pairing strength to the Wigner energy having calculated the matrix elements of the pairing interaction. In Ref. [139] we have shown that this method provides similar values for the coupling strengths as fitting them to the *pn* pairing indicators (Eq. (3.15)).

In Fig. 4.14 we show the experimental and calculated (Eq. 4.99) values of $W(A)$ Wigner strength for even-even $N = Z$ nuclei in the vicinity of ^{64}Ge. The general trend $47/A$ is indicated with a dashed line. Theoretical points are shown for the best results of two fits: one with the fixed value $V_0^{T=1}$=310 MeV fm^3 which was adopted in preceding calculations (th$_1$) and of the second, done on a two dimensional mesh of $V_0^{T=1}$ and $V_0^{T=0}$ values (th$_2$). This way we have obtained the subsequent sets of
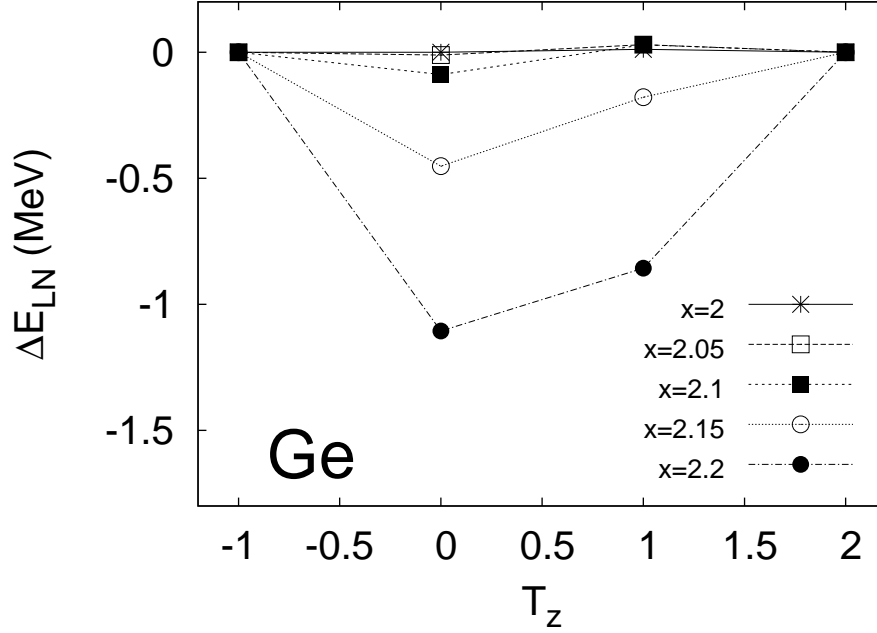
Figure 4.15: Normalized ground state energy ($\Delta E = E(V_0^{T=0} \neq 0) - E(V_0^{T=0} = 0)$) as a function of the reduced isospin $T_z = (N - Z)/2$ for various values of the $T = 0$ and $T = 1$ pairing strengths ratio x obtained in the Lipkin-Nogami approach.

parameters:

$$V_0^{T=1} = 310 \text{ MeV fm}^3, \ V_0^{T=0} = 670 \text{ MeV fm}^3$$

and

$$V_0^{T=1} = 360 \text{ MeV fm}^3, \ V_0^{T=0} = 620 \text{ MeV fm}^3.$$

It is seen that the theoretical results obtained for the two parametrizations given above are close to each other so they give similar deviations for the Wigner energy strength $W(A)$. It is worth pointing out that the calculated values follow nicely the trend of the experimental data.

Although the two sets of values adjusted to the $W(A)$ strength provide similar resuls for this quantity, the second fit (th$_2$) gives the pairing strengths the ratio of which $x = 1.72$ lies below the critical value $x_{\text{crit}} \sim 2$ obtained in our calculations. Thus, no pn collective solution will occur for this parametrization and for that reason it is not appropriate to reproduce the Wigner cusp.

The first set of fitted parameters gives $x \sim 2.15$, a value for which the pn pairing is activated in both BCS and LN approaches. Nevertheless for the BCS method it lies in the region of the $T = 1$ to $T = 0$ pairing phase transition with almost no additional binding due to the pn pairing. In Fig. 4.15 the normalized ground state energy $\Delta E = E(V_0^{T=0} \neq 0) - E(V_0^{T=0} = 0)$ is presented as a function of T_z for various values of the $T = 0$ and $T = 1$ pairing strengths ratio x obtained in the Lipkin-Nogami approach. It is seen that for $x > 2.1$ some additional binding is

gained due to the *pn* pairing and that its value is the largest for the $N = Z$ nucleus. For the value adjusted in this section there is the additional binding attributed to the $T = 0$ pairing, however very modest (of about 0.5 MeV).

Since the mean-field models ignore the explicit proton-neutron coupling they are a priori unable to reproduce the Wigner term (see however [29, 68]). It is known that the deviations in calculated and experimental masses in the vicinity of the $N = Z$ line are of about 2 MeV in an Extended Thomas-Fermi model [146] which is supposed to take into account properly the effects attributed to the particle-hole channel. Thus, the 2 MeV energy offset can be associated with the lack of *pn* correlations. It is seen from our calculations that in principle the BCS(LN) model taking into account the isoscalar pairing might produce a sharp slope discontinuity in the mass parabola that might contribute to the Wigner term. However, the gain in energy is too modest for the residual $T = 0$ interaction to be the solely explanation of the Wigner term. On the other hand, the fit to $W(A)$ value may be questionable due to the uncertainties of the empirical Wigner strengths values.

4.4.5   Summary

Let us summarize the results obtained in this part of the work. In the ground states of several Ge isotopes obtained in the Skyrme-HF model we have performed BCS and Lipkin-Nogami calculations for the pairing Hamiltonian which includes all possible nucleonic pairs in time-reversed orbits. The two-body interaction between nucleons was accounted for with a state dependent interaction. Studying the pairing matrix elements of the δ and $\boldsymbol{k}'\delta\boldsymbol{k}$ forces and basing ourselves on our previous calculations with the proton-neutron pairing we have shown that a reasonable description of the *pn* pairing is yielded by the δ force, that is to say in terms of $T = 1, J = 0$ and $T = 0, J = 1$ coupling. The results of the generalized BCS and LN calculations with the state-dependent force are qualitatively comparable to the results of other authors obtained in BCS(LN) and HFB approaches with schematic pairing interactions. The generic feature of the BCS method is the $T = 1$ to $T = 0$ pairing transition in the $N = Z$ nucleus which is smeared out in the formalism conserving the particle number symmetry. No coexistence of the *pn* pairing in $T = 0$ and $T = 1$ channels is found while the like-particle and $T = 0$ modes do coexist.

Chapter 5

Particle number conserving treatment of correlations

It is well known that the non-conservation of particle number in the BCS method is especially harmful in the case of phase (normal/superfluid) transitions as a function of some continous parameter (deformation, temperature, rotational frequency, and as we have previously seen, pairing strengths ratio in $T = 0$ and $T = 1$ channels). There exists a number of methods to deal with this problem, the first consisting in projecting BCS wave functions onto a good particle number. It is however quite obvious that such an approach will not be of any help in the situations when the level density around the Fermi surface is too low to provide any solution except the trivial HF one. It should be as well stated clearly that these projections are rather complicated and time-consuming in numerical treatment even for like-particle pairing and that completely microscopic calculations of this type are not available on extensive scale (however, see *e.g.* [147, 148]). In practical cases a simpler variant, that is to say projection after variation is performed, often with further approximative schemes [149]. Other approaches used to remove the effects of spurious dispersion of the particle number are Generator Coordinate Method within Gaussian Overlap Approximation (GCM+GOA) [113, 114, 115] and the Lipkin-Nogami [117, 118] method already discussed in this work. However simple in practical treatment, they both allow to treat pairing correlations only in an approximately particle number conserving scheme.

In this part of the work we will describe ground states of $N \sim Z$ nuclei in an approach explicitely conserving particle number, both reliable and tractable. This method, known as the Higher Tamm-Dancoff Approximation (HTDA) [150] has been recently applied successfully to describe GS properties and isomeric states of [178]Hf nucleus [31, 151] and then developed for odd-nuclei [152]. Some work has been done as well to treat pairing correlations in high spin states in a Routhian-HTDA (RHTDA) method [153].

The main purpose of this part of the work is to extend the HTDA method to be able to treat proton-neutron pairing correlations on the same footing as like-particle

correlations. We restrict ourselves to the study of the ground states of even-even nuclei, however the formalism presented in this work and the numerical code are developed to treat as well excited states.

The numerical calculations are performed in the GS of Ge isotopes obtained in the HF+BCS(G) approach described in Sec. 4.4.1.

5.1   HTDA method

The purpose of the method is to describe the pair diffusion phenomenon around the Fermi surface as a particular, yet very important, part of some many quasiparticle excitations of the particle-hole type over a Slater determinant vacuum $|\Psi_0\rangle$. Thus one can consider dealing with a kind of higher Tamm-Dancoff approximation or equivalently with a highly truncated shell model calculation. The latter point of view makes it clear that the success (*i.e.,* the fast convergence in terms of the number of considered quasiparticles) of such a truncation scheme will depend on the realistic character of the vacuum in use. Such a favorable situation may be expected when the vacuum is defined from the mean-field carrying most of the single-particle properties (even those yielded by the correlations) associated with a given effective Hamiltonian. Let us assume that we are describing the nuclear system with an effective interaction $\hat{V}$. It is therefore advisable to choose for the wave function $|\Psi_0\rangle$ the Hartree-Fock solution obtained from the HF potential $\hat{V}_{\mathrm{HF}}$ corresponding to the desired number of particles and possibly taking into account various constraints (*e.g.* deformation) and symmetries (*e.g.* time-reversal symmetry). In some cases when the level density around the Fermi level is not high enough to provide a converged HF solution (oscillations during the iterative process between two almost degenerate minima) some arbitrary amount of pairing correlations may be added *e.g.* in the BCS approximation to get a converged mean-field solution. The detailed outline of the HTDA method is given in the next subsection.

One must remind that performing exact pairing calculation on the top of a Hartree-Fock calculation (or some approximations thereof) has already been achieved [154, 155, 156, 157]. While the authors of [154]-[156] have used a schematic seniority force, in [157] a more realistic interaction has been used. However, both approaches included a simple pairing Hamiltonian involving only matrix elements between pairs of Kramers degenerate orbitals. It should be pointed out that the HTDA is far beyond a method of treating only pairing correlations. Since it admits correlations in the ground state it is as well an approach far more complete than the usual Tamm-Dancoff approximation or even than the RPA method, as it takes into account a larger variety of possible excitations.

5.1.1 Outline of the method

As mentioned above, we use an effective interaction $\hat{V}$ to describe the nuclear system. The nuclear Hamiltonian consists then in two parts, $\hat{V}$ and the kinetic energy $\hat{K}$:

$$\hat{H} = \hat{K} + \hat{V} \, . \tag{5.1}$$

A HF solution resulting from a mean-field calculation is chosen as the vacuum for particle-hole excitations

$$\hat{H}_{\text{HF}}|\Psi_0\rangle = E_0|\Psi_0\rangle \, , \tag{5.2}$$

where

$$\hat{H}_{\text{HF}} = \hat{K} + \hat{V}_{\text{HF}} \, , \tag{5.3}$$

$\hat{V}_{\text{HF}}$ being the one-body reduction of $\hat{V}$ for $|\Psi_0\rangle$.

The $|\Psi_0\rangle$ vacuum may now serve to construct an orthonormal N-body basis in which we will diagonalize Hamiltonian (5.1). In principle to build this basis we should consider the Slater determinant corresponding to the 0p0h state and all the particle-hole excitations: 1p1h, 2p2h, 3p3h and so on. It is, however, obvious that in practice we need to truncate the space of particle-hole excitations. More attention to the subject will be paid in the discussion of numerical aspects and results of this work in Sec 5.2.

The ground state wave function can be decomposed in the following way

$$|\Psi\rangle = \chi_0|\Psi_0\rangle + \sum_{\{1p1h\}} \chi_1|\Psi_1\rangle + \sum_{\{2p2h\}} \chi_2|\Psi_2\rangle + \cdots \, . \tag{5.4}$$

The ensemble of $|\Psi_i\rangle$ Slater determinants represents a complete orthogonal basis with real coefficients χ_i fulfilling the relation

$$\sum_i \chi_i^2 = 1 \tag{5.5}$$

which assure the normalization of the function (5.4). It is clear [151] that this function has a good particle number $\langle \Psi|\hat{N}|\Psi\rangle = N$.

The solution of the problem is equivalent to the diagonalization of the subsequent matrix

$$\begin{pmatrix} H_{00} & H_{01} & H_{02} & \ldots \\ H_{10} & H_{11} & H_{12} & \ldots \\ & & & \\ H_{20} & H_{21} & H_{22} & \ldots \\ \vdots & \vdots & \vdots & \ddots \end{pmatrix} \tag{5.6}$$

where H_{ij} stands for the set of the N-body matrix elements of the Hamiltonian (5.1).

Let us rewrite the Hamiltonian (5.1) in the following form

$$\begin{aligned}
\hat{H} &= \hat{K} + \hat{V}_{\text{HF}} - \langle\Psi_0|\hat{V}|\Psi_0\rangle + \hat{V} - \hat{V}_{\text{HF}} + \langle\Psi_0|\hat{V}|\Psi_0\rangle \\
&= \langle\Psi_0|\hat{H}|\Psi_0\rangle + \hat{H}_{\text{IQP}} + \hat{V}_{\text{res}},
\end{aligned} \tag{5.7}$$

where the independent quasiparticle Hamiltonian $\hat{H}_{\text{IQP}}$ reads

$$\hat{H}_{\text{IQP}} = \sum_i \xi_i \eta_i^\dagger \eta_i, \tag{5.8}$$

where $\eta_i^\dagger$ equals to the particle creation operator $a_i^\dagger$ for i being a particle (unoccupied) state and to the annihilation operator a_i in the case of hole (occupied) states. For ξ_i we have: $\xi_i = e_{\text{p}}^i$ or $\xi_i = e_{\text{h}}^i$, with e^i indicating the single-particle energy corresponding to the particle or hole level, respectively. As seen from Eq. (5.7), the residual interaction reads

$$\hat{V}_{\text{res}} = \hat{V} - \hat{V}_{\text{HF}} + \langle\Psi_0|\hat{V}|\Psi_0\rangle. \tag{5.9}$$

The matrix element H_{ij} of the Hamiltonian above given in the multi-particle multi-hole basis takes the form

$$H_{ij} = \langle\Psi_i|\hat{H}|\Psi_j\rangle = \left(\langle\Psi_0|\hat{H}|\Psi_0\rangle + E_{\text{p}-\text{h}}^i\right)\delta_{ij} + \langle\Psi_i|\hat{V}_{\text{res}}|\Psi_j\rangle \tag{5.10}$$

with

$$E_{\text{p}-\text{h}}^i = \sum_{\text{p}} e_{\text{p}}^i - \sum_{\text{h}} e_{\text{h}}^i \tag{5.11}$$

being the particle-hole excitation energy of the N-body state $|\Psi_i\rangle$ calculated with respect to the Slater determinant of the lowest energy $|\Psi_0\rangle$. The residual interaction (5.9) is defined as a difference of two-body and one-body operators. The matrix elements appearing in (5.10) can be calculated using expressions given in Appendix C.

From now on, the following convention is chosen for indicating the single-particle states: greek letters are used to specify particle states, the latin a, b, c, d letters stand for hole states, the i, j, k, l ones are applied to define one and two-body operators, *i.e.* they may be both, particle or hole states.

Diagonal matrix elements

Let us first consider in detail a diagonal matrix element of (5.7). From Eq. (5.10) one has

$$H_{ii} = \langle\Psi_0|\hat{H}|\Psi_0\rangle + E_{\text{p}-\text{h}}^i + \langle\Psi_i|\hat{V}_{\text{res}}|\Psi_i\rangle \tag{5.12}$$

The last term of (5.12) can be evaluated using formulae (C-17) and (C-22) :

$$\langle\Psi_i|\hat{V}_{\text{res}}|\Psi_i\rangle = \frac{1}{2}\left[\sum_k^{\text{h}(\Psi_i)}\sum_l^{\text{h}(\Psi_i)} + \sum_k^{\text{p}(\Psi_i)}\sum_l^{\text{p}(\Psi_i)} - 2\sum_k^{\text{h}(\Psi_i)}\sum_l^{\text{p}(\Psi_i)}\right]\langle kl|\hat{V}|\widetilde{kl}\rangle, \tag{5.13}$$

where the notation is the same as in the Appendix C, that is to say the summations $\sum_k^{h(\Psi_i)}$ and $\sum_k^{p(\Psi_i)}$ runs respectively over all the hole states in $|\Psi_i\rangle$ with respect to $|\Psi_0\rangle$ and all the particle states in $|\Psi_i\rangle$ with respect to $|\Psi_0\rangle$.

In the case where $|\Psi_i\rangle \equiv |\Psi_0\rangle$, the expression (5.13) for the diagonal matrix element of $\hat{V}_{\mathrm{res}}$ is equal to zero and the first diagonal matrix element of the Hamiltonian (5.1) is a constant

$$H_{00} = \langle \Psi_0 | \hat{H} | \Psi_0 \rangle \,. \tag{5.14}$$

Using relations (5.12), (5.13) and (5.14) we obtain a general expression for any diagonal matrix element of (5.1)

$$\begin{aligned}
H_{ii} &= H_{00} + E_{\mathrm{p-h}}^i \\
&+ \frac{1}{2} \left[\sum_k^{h(\Psi_i)} \sum_l^{h(\Psi_i)} + \sum_k^{p(\Psi_i)} \sum_l^{p(\Psi_i)} -2 \sum_k^{h(\Psi_i)} \sum_l^{p(\Psi_i)} \right] \langle kl | \hat{V} | \widetilde{kl} \rangle \,.
\end{aligned} \tag{5.15}$$

Non-diagonal matrix elements

Since $\hat{H}$ is a sum of one- and two-body operators it is clear that the non-diagonal matrix elements H_{ij} calculated between $|\Psi_i\rangle$ and $|\Psi_j\rangle$ states are equal to zero if $|\Psi_j\rangle$ differs from $|\Psi_i\rangle$ by more than two nucleons. Consequently, we need to consider only the two following cases:

1. $|\Psi_j\rangle$ differs from $|\Psi_i\rangle$ by one nucleon, namely up to a phase factor (due to a possible reordering of the hole states in $|\Psi_i\rangle$ and $|\Psi_j\rangle$)

$$|\Psi_j\rangle = a_\alpha^\dagger a_a |\Psi_i\rangle \,. \tag{5.16}$$

The matrix element of $\hat{V}_{\mathrm{HF}}$ is equal to (Eq. (C-20))

$$\langle \Psi_i | \hat{V}_{\mathrm{HF}} | \Psi_j \rangle = \langle a | \hat{V}_{\mathrm{HF}} | \alpha \rangle = \sum_k^h \langle ka | \hat{V} | \widetilde{k\alpha} \rangle \,, \tag{5.17}$$

while for the two-body operator using Eq. (C-24) we obtain

$$\langle \Psi_i | \hat{V} | \Psi_j \rangle = \left[\sum_k^h + \sum_k^{p(\Psi_i)} - \sum_k^{h(\Psi_i)} \right] \langle ka | \hat{V} | \widetilde{k\alpha} \rangle \,. \tag{5.18}$$

Combining Eqs. (5.17) and (5.18) we find the final expression for the non-diagonal matrix elements in this case

$$H_{ij} = \langle \Psi_i | \hat{V}_{\mathrm{res}} | \Psi_j \rangle = \left[\sum_k^{p(\Psi_i)} - \sum_k^{h(\Psi_i)} \right] \langle ka | \hat{V} | \widetilde{k\alpha} \rangle \,. \tag{5.19}$$

2. $|\Psi_j\rangle$ differs from $|\Psi_i\rangle$ by two nucleons, namely up to a phase factor

$$|\Psi_j\rangle = a_\alpha^\dagger a_\beta^\dagger a_a a_b |\Psi_i\rangle \,. \tag{5.20}$$

In this case we have

$$\langle \Psi_i | \hat{V}_{\mathrm{HF}} | \Psi_j \rangle = 0 \qquad (5.21)$$

and

$$\langle \Psi_i | \hat{V} | \Psi_j \rangle = \langle ba | \hat{V} | \widetilde{\alpha\beta} \rangle . \qquad (5.22)$$

Using the method developed in [152] (presented in the Appendix C) for the calculation of N-body matrix elements, we have shown that simple and double summations over the hole states in $|\Psi\rangle$ disappear in the calculation of matrix elements of $\hat{V}_{\mathrm{res}}$. As we have seen from Eqs. (5.17-5.19) these terms appear in both $\hat{V}$ and $\hat{V}_{\mathrm{HF}}$ components and are automatically cancelled making it so that all Hartree-Fock contributions are removed expliciting therefore the genuinely residual character of the interaction (5.9).

Self-consistent HTDA

It is possible to insert our approach in a self-consistent framework. Assuming that we have at our disposal a correlated wave function $|\Psi\rangle$ (which is *e.g.* after one diagonalization of the matrix) we may compute the matrix element of the one-body reduced density

$$\langle i | \rho | j \rangle = \langle \Psi | a_j^\dagger a_i | \Psi \rangle . \qquad (5.23)$$

Folding this density with the two-body effective potential, in our case a Skyrme interaction with the SIII parametrization, one gets a new mean-field and then diagonalize the associated one-body Hamiltonian $\hat{H}_{\mathrm{HF}}$ yielding a new Slater determinant $|\Psi_0\rangle$. From particle-hole configuration mixing defined in terms of the HF single-particle states associated with $\hat{H}_{\mathrm{HF}}$ one gets a new correlated wave function $|\Psi\rangle$ from which a new density matrix ρ is evaluated from Eq. (5.23) and so on, until the self-consistency is reached. In this way we incorporate in the mean-field all the sp properties resulting from the many-particle correlations.

Time-reversal symmetry

We have used an ensemble of Slater determinants to build the orthonormal basis in which we diagonalize the Hamiltonian (5.1). However, the function (5.4) is not even with respect to time-reversal symmetry in its 1p1h and 2p2h parts (except for the pair excitation for the latter). This may be especially harmful in the case of *pn* correlations where the excitations $(1p1h)_p \otimes (1p1h)_n$ are of particular interest.

To restore the time-reversal symmetry, we use the following combination instead of (5.4)

$$|\Psi_i(\pm)\rangle \Rightarrow \frac{1}{\sqrt{2}}(|\Psi_i\rangle \pm |\bar{\Psi}_i\rangle) \qquad (5.24)$$

and replace the matrix elements

$$\langle \Psi_i | \hat{V}_{\mathrm{res}} | \Psi_j \rangle \qquad (5.25)$$

by

$$\frac{1}{2} \langle \Psi_i \pm \bar{\Psi}_i | \hat{V}_{\text{res}} | \Psi_j \pm \bar{\Psi}_j \rangle \, . \tag{5.26}$$

Considering the time-reversal operator for a system of N_τ particles with a spin $1/2$ like the nucleons in an atomic nucleus we may write

$$\hat{T}^2 = (\Pi_{i=1}^{N_\tau}(-i\sigma_y)K)^2 = (-1)^{N_\tau} \, . \tag{5.27}$$

Since we consider even-even nuclei for which $\hat{T}^2 = 1$ we restrict ourselves to the basis containing only many-body states even under the time-reversal symmetry which limits additionally the size of this basis.

5.1.2 Technicalities

The δ force

In Sec. 5.1.1 we have presented the HTDA method introducing the residual interaction

$$\hat{V}_{\text{res}} = \hat{V} - \hat{V}_{\text{HF}} + \langle \Psi_0 | \hat{V} | \Psi_0 \rangle \, . \tag{5.28}$$

However, most of the effective forces of the Skyrme type, including the SIII force applied in the HF part of this work, are not able to reproduce well the data in the particle-particle channel. Therefore, in practical calculations we replace the effective interaction defining the residual interaction by a δ force. The advantages of the zero-range interaction of this type have already been discussed in Sec. 4.1.

With the use of a δ force, the exact Hamiltonian

$$\hat{H} = \hat{K} + \hat{V} = \langle \Psi_0 | \hat{H} | \Psi_0 \rangle + \hat{H}_{\text{IQP}} + \hat{V}_{\text{res}} \tag{5.29}$$

is substituted with

$$\hat{H}' = \langle \Psi_0 | \hat{H} | \Psi_0 \rangle + \hat{H}_{\text{IQP}} + \hat{V}_\delta - \hat{V}_\delta^{\text{HF}} + \langle \Psi_0 | \hat{V}_\delta | \Psi_0 \rangle \, , \tag{5.30}$$

where $\hat{V}_\delta^{\text{HF}}$ is the one-body reduction of the $\hat{V}_\delta$ interaction. The latter in the isovector ($|T_z| = 1$) channel was defined by Eq. (4.87).

In other words, the real residual interaction is approximated by $\hat{V}_\delta - \hat{V}_\delta^{\text{HF}} + \langle \Psi_0 | \hat{V}_\delta | \Psi_0 \rangle$ so in practice one needs to replace the two-body interaction $\hat{V}$ by the δ interaction when calculating many-body matrix elements in Eqs. (5.13, 5.15, 5.19, 5.22). The exact expressions for two-body matrix elements of $\hat{V}_\delta$ for like-particle interaction are given in Appendix B.

Construction of 0^+ states

In the limit of vanishing proton-neutron coupling the nuclear wave function is a product of two correlated wave functions, one for each charge state. The problem is then decoupled into two separate problems of finding correlated functions for protons and neutrons.
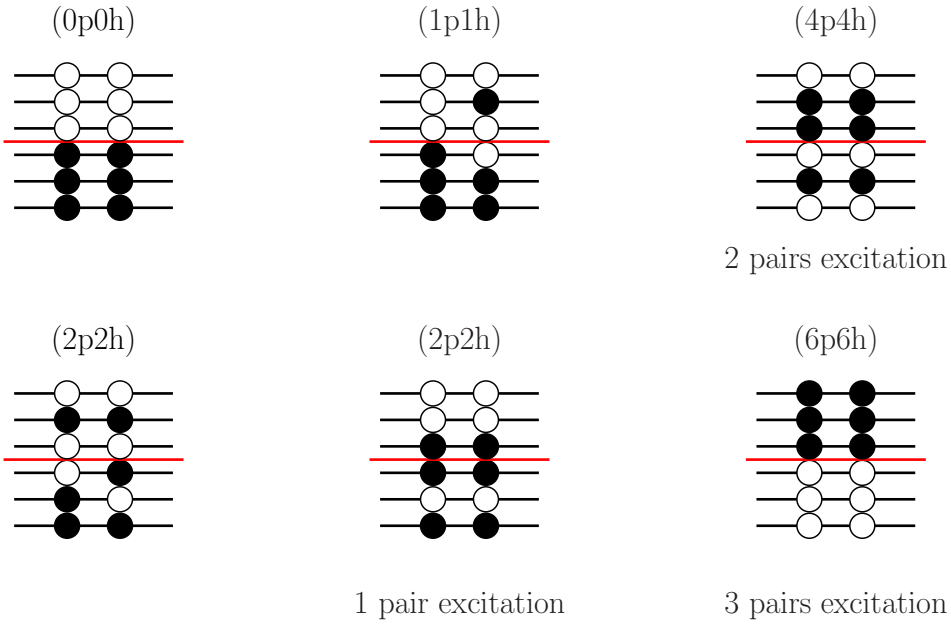
Figure 5.1: Examples of particle-hole excitations considered in this work. Red lines indicate Fermi levels.

It is clear that in practice we need to truncate the space of particle-hole excitations which relevance needs to be checked a posteriori. The global size of the subspace of retained single-particle configurations being defined, the particular choice of i-particle i-holes states to be included in the calculations is then constrained by the symmetries of the many-body state to be described. In what follows we conserve axial symmetry and parity and specify the states by quantum numbers Ω_i^π.

To produce a nuclear state of a given Ω^π number one has to couple proton and neutron configurations $\Omega_n^\pi(\mathrm{mp}-\mathrm{mh})\otimes\Omega_p^\pi(\mathrm{m'p}-\mathrm{m'h})$ of some m(m')-particle m(m')-hole states in such a way that

$$\Omega = \Omega_n(\mathrm{mp} - \mathrm{mh}) + \Omega_p(\mathrm{m'p} - \mathrm{m'h}),$$
$$\pi = \pi_n(\mathrm{mp} - \mathrm{mh})\pi_p(\mathrm{m'p} - \mathrm{m'h}) . \tag{5.31}$$

where

$$\Omega_\tau(\mathrm{mp} - \mathrm{mh}) = \sum_{\mathrm{p}}\Omega_{\tau\mathrm{p}} - \sum_{\mathrm{h}}\Omega_{\tau\mathrm{h}} \tag{5.32}$$

and

$$\pi_\tau(\mathrm{mp} - \mathrm{mh}) = \prod_{\mathrm{p}}\pi_{\tau\mathrm{p}} \times \prod_{\mathrm{h}}\pi_{\tau\mathrm{h}} . \tag{5.33}$$

In the above mentionned decoupling scheme and in view of the scalar and parity-conserving character of the residual interaction (δ force) it is obvious that the states corresponding to various coupling schemes will not mix. In practice, when searching for a GS configuration the discrimination between possible candidates may be

approached on the basis of unperturbed energies. In view of the latter, it is very likely that the ground state of an even-even nucleus, which is of course a 0^+ state, will result from two 0^+ configurations, one for protons and one for neutrons. In that case the correlated wave function will include the following configurations:

- 0p0h (Slater determinant) state;

- 1p1h states such that both the particle and hole states should have the same quantum numbers which limits considerably their number;

- 2p2h states corresponding to a pair excitation, *i.e.* two particles placed in Kramers doubly degenerate hole orbital are promoted to Kramers doubly degenerate particle state;

- 2p2h states where only hole or conversely only particle states are Kramers degenerate;

- 2p2h states where none of the hole or and particle states form a pair;

- multi-pair excitations;

Schematic examples of the particle-hole excitations are shown in Fig. 5.1.

If the physical assumptions behind the usual BCS pairing treatment are to hold, one expects that most of the correlations beyond $|\Psi_0\rangle$ should come from pair excitations, as was found formerly in the HTDA framework studies. Nevertheless, for the completeness of this study we will discuss the role of other excitations for the considered mass region.

Matrix diagonalization

The HTDA method can be viewed as a kind of the shell model calculation thus it is in practice limited by the dimensionality of the configuration space that can be handled by a computer. In practice, to diagonalize matrices (5.6, 5.44) we use the common shell model tool, which is the Lanczös algorithm [158] within the code developed by Parlett and Scott [159]. Such a method allows to search for the lowest energy configurations in a reasonable time. The advantage of the HTDA method is the realistic character of the vacuum in use, that is of the HF solution corresponding to the desired number of particles, deformation etc., which allows for a fast convergence in terms of the number of included quasiparticles. Classifying states according to the invariance groups of the Hamiltonian (*e.g.* the rotation over the z axis) and conserving time-reversal symmetry limits considerably the matrix dimension. As it appears, the matrix diagonalization problem is then far from attaining the difficulty level of the so-called shell model calculations. In the mass region of interest and within the truncation scheme adequate for this type of study, typically we need to handle matrices $\sim 10^4 \times 10^4$.

Table 5.1: Numbers of many-body configurations of different types depending on the number of sp (hole/particle) levels contained in the sp configuration space window for the cut-off value $E_{\mathrm{cut}}^{\mathrm{sp}}$. These numbers correspond to the neutron spectrum of ^{64}Ge.

$E_{\mathrm{cut}}^{\mathrm{sp}}$(MeV)	Number of h/p levels	1p1h	1 pair	2p2h	2pairs	3 pairs
6	4/8	6	32	162	168	224
12	8/12	12	96	1744	1848	12157
15	9/20	48	180	6596	6758	58404
18	11/27	76	297	13706	14230	>100000

5.2 Results: limiting case of nn & pp interactions

Before extending the HTDA framework to accommodate the pn pairing correlations, we apply the formalism for the calculations with nn and pp interactions only and discuss the validity of the HTDA approach with all its advantages and caveats. First, the problems of the basis truncation and a possible way to fix the δ force strength are presented. Some words are devoted to the self-consistency of our approach and its impact on physical quantities. A special attention is paid to the power of the method in its description of pairing correlations.

The departure point of our calculations are deformed mean-fields obtained in HF+BCS(G) calculations in the ground states of several Ge isotopes (see Sec. 4.4.1). These fields are used to initiate the self-consistent HF process thus to obtain the vacuum Slater determinant from which the HTDA particle-hole space is constructed.

5.2.1 Basis truncation and fitting procedure

Having chosen a configuration space size in terms of the complexity of the many-particle many-hole states, one has to further truncate on single-particle levels from which these configurations will be built. In that we are facing a situation met in usual BCS calculations. Typically we will limit our sp subspace to the so-called single-particle configuration space window of the form

$$e_F \pm E_{\mathrm{cut}}^{\mathrm{sp}}, \tag{5.34}$$

e_F being the Fermi energy defined as the average between the single-particle energies of the last occupied and the first empty levels and $E_{\mathrm{cut}}^{\mathrm{sp}}$ the cut-off parameter. Its actual value should be such that the inclusion of further single-particle levels does not introduce any significant physical consequences but only a possible slight renormalization of the relevant quantities.

Let us exemplify the dimension of the matrix to be handled depending on the sp basis size. In Table 5.1 the number of possible configurations of various types depending on the number of hole and particle levels contained in the window of the size $e_F \pm E_{\text{cut}}^{\text{sp}}$ is listed (the numbers concern the neutron spectra of ^{64}Ge).

The δ force for matrix elements calculations being used, it goes without saying a cut-off and a coupling constant have to be given together to define fully the interaction. In the HF+BCS calculations the pairing strengths were adjusted to reproduce the 3-point experimental pairing gaps. Here we may act in the same way to determine the strength of the δ force, however an analog of the BCS pairing gap (quasiparticle energy) in the HTDA case is required. Assuming that the appearance of the pairing gap is related to a breaking of the Cooper pair of the lowest energy we perform for each charge state a calculation with the level closest to the Fermi energy blocked and consider the difference of the expectation value of the residual interaction of blocked and unblocked cases as a proper measure of pairing correlations that can be compared to the empirical gap. Namely, we define

$$\Delta = [E(n) - E_{\text{IQP}}(n)] - [E(n-1) - E_{\text{IQP}}(n-1)] \tag{5.35}$$

where $E_{\text{IQP}} = \langle\Psi|\hat{H}_{\text{IQP}}|\Psi\rangle$, $E = \langle\Psi|\hat{H}|\Psi\rangle$ and n indicates here the number of sp levels contained in the window.

Since we deal with $N \sim Z$ nuclei, similarly like in the BCS(δ) case, coupling constants and cut-off energy values are assumed to be equal for neutrons and protons. The strength of the δ interaction for the HTDA approach in the ground states of considered nuclei is adjusted in non self-consistent calculations, that is to say performing a single diagonalization of the Hamiltonian (5.7) matrix.

For a given sp configuration space with $E_{\text{cut}}^{\text{sp}} = 12\text{MeV}$, we investigate the role of different particle-hole excitations. The discussion is limited to the case of the ^{64}Ge nucleus. The quantity we will refer to in the following is the correlation energy defined in the HTDA approach as the difference of the mean values of the Hamilton operator of the system in the correlated and non-correlated states

$$E_{\text{corr}} = \langle\Psi|\hat{H}|\Psi\rangle - \langle\Psi_0|\hat{H}|\Psi_0\rangle. \tag{5.36}$$

Let us first report the outcome of the calculations performed with 1p1h and 2p2h excitations. In Table 5.2 the percentage of different components is listed in such a case. It is seen that 1p1h component is fully negligible while 2p2h excitations of other types do not contribute to more than 1% of the total amount. As expected, the non-pair components can be neglected in the description of the ground states which introduces a great simplification from the numerical point of view, since the number of pair-excitation type components is highly limited as compared to all possible particle-hole excitations (cf. Table 5.1).

In Table 5.3 a similar presentation is made for calculations with 1 pair, 1 and 2 pairs, and finally, with 1, 2 and 3 pairs embedded in the calculations. The absolute differences in the correlation energy resulting from the addition of the next pair

Table 5.2: Percentage of different components of the ground state correlated wave function of ^{64}Ge. These results concern the case where all types of particle-hole excitations up to the 2nd order are taken into account.

	0p0h	1p1h	1 pair	2p2h (all included)
neutrons	69.6	0.003	29.6	30.4
protons	70.6	0.005	28.3	29.3

mode are given in the last column. As can be seen, the 1 pair element is dominant in each case. The probability for 3 pairs excitations is negligible and their presence does not influence neither the values of the energies nor the percentage of other components. Similarly, the probability for 2 pairs is very small ($\sim 2\%$), yet their presence boosts the population of 1 pair excitations and yields appreciable changes in the correlation energy. This indicates that for such a correlation regime 1 and 2 pairs added to the vacuum are sufficient for further calculations in this nucleus and that, a priori, they need to be taken into account when extending the method for the proton-neutron pairing case.

Some words of caution are necessary when dealing with the interaction strength. Upon using a zero-range force, any change of the configuration space requires a readjustment of the interaction parametrization. Obviously, the results in Tables 5.2, 5.3 were obtained with different interaction strength. Those in Table 5.3 were given for a value adjusted in the calculation accounting for 1 and 2 pairs excitations only ($V_{0\tau} = 300$MeV fm^3 for both charge states), for the sake of simplicity. However, it is reasonable to presume that the adjustment done with 3 pairs would not change this value or eventually would provide a slight decrease of the coupling constant which would even reduce their anyhow insignificant influence on the results. In Fig. 5.2 it is shown how the correlation energy evolves with the increasing interaction strength $V_{0\tau}$ for neutrons and protons when subsequent types of pair excitations are added. The difference between various calculations increasing toward larger values of $V_{0\tau}$, it is still sizable only for the two first cases, precisely for the calculations with 1 pairs only and those including as well 2 pairs excitations.

Figure 5.2 shows also that for weak pairing interactions one pair excitations space is sufficient to account for the full amount of the correlations in the system.

The last, obvious remark suitable here, is that the method of exact diagonalization of the Hamiltonian matrix in the space of pair excitations does not collapse for any weak interactions, contrary to the BCS treatment and some approximate projections, $i.e.$ Lipkin-Nogami, GCM+GOA or Projection After Variation method.
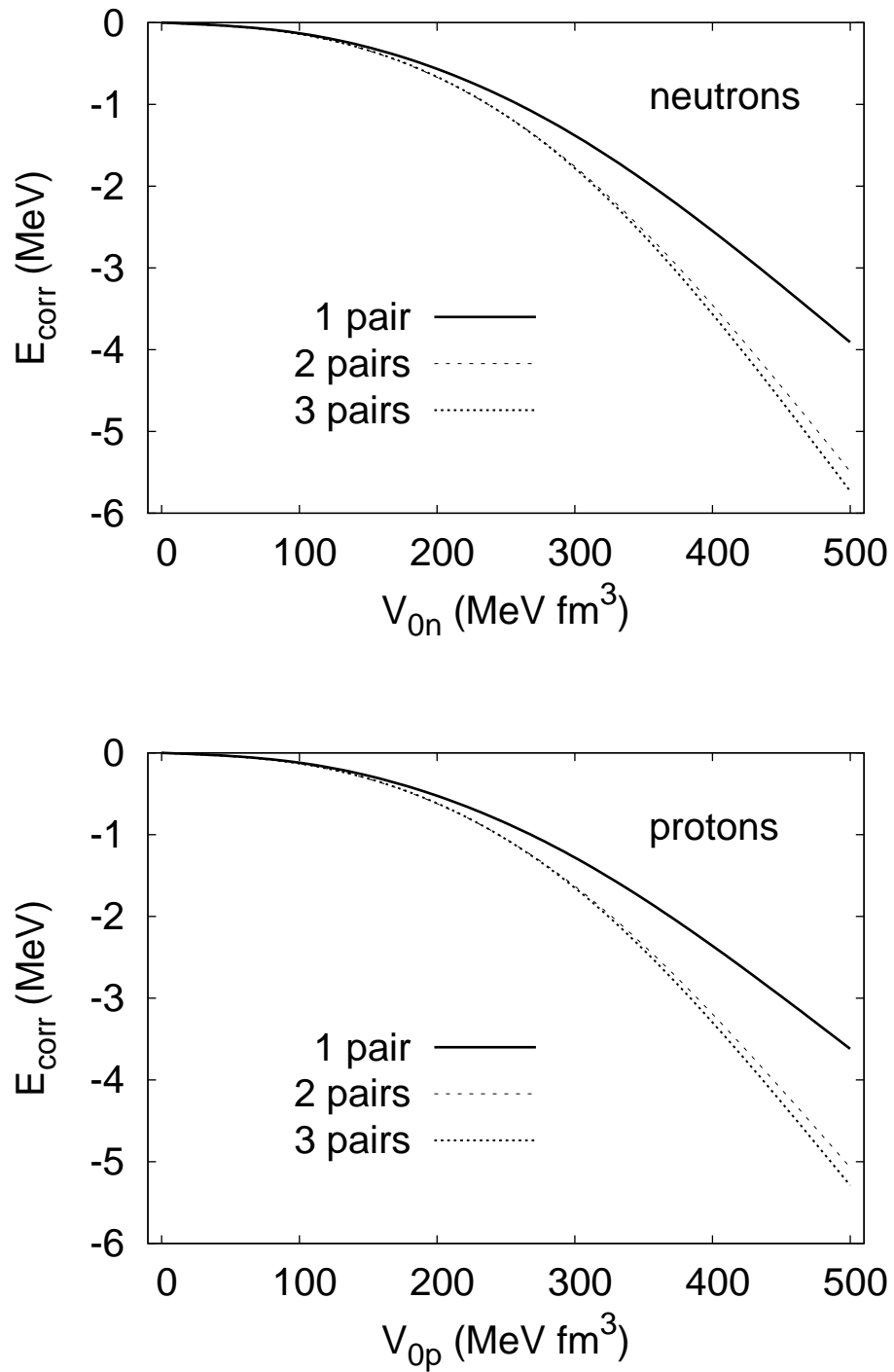
Figure 5.2: Correlation energy vs interaction strength for neutrons and protons in ^{64}Ge. The data concerns calculations with 1 pair excitations (1 pair), 1 and 2 pairs (2 pairs) and finally, 1,2 and 3 pairs (3 pairs) excitations embedded in the calculations.

Table 5.3: Percentage of various components of the correlated wave function and the correlation energy values for neutrons and protons in ^{64}Ge. Results of three calculations are reported: with 1 pair excitations added to the vacuum, with 1 and 2 pairs and with 1, 2 and 3 pairs included. The last column contains the difference in the correlation energy between consecutive calculations.

	0p0h	1 pair	2 pairs	3 pairs	ΔE_{corr} (MeV)
neutrons	65.4	34.6	–	–	0
	49.55	48.5	1.95	–	0.27
	49.0	48.9	2.1	0.02	0.02
protons	65.3	34.7	–	–	0
	47.7	50.2	2.1	–	0.30
	46.9	50.7	2.3	0.04	0.02

5.2.2   Self-consistency

In Sec. 5.1.1 it was described how to insert the HTDA into a self-consistent framework. The self-consistent versions of the HTDA calculations presented in the forthcoming were performed until the accuracy 10^{-6} MeV for the energy and about 10^{-4} b (b^2) for the mass quadrupole and hexadecapole moments, respectively, was achieved. In the case studied here (that is for ^{64}Ge) and in calculations starting with the HF+BCS mean-field the convergence was achieved after ~ 40 iterations. In view of the rigorous convergence conditions assumed here one may consider the HTDA self-consistent process to converge rapidly. It seems to be a consequence of the realistic vacuum and of the size of the valence space in use. However, there is no guarantee that a fully self-consistent calculation with varying deformation would not become problematic and numerically unstable and that a small configuration space chosen here would be adequate to investigate the energy dependence on the deformation.

Let us have a look what are the modifications brought to the mean-field by the self-consistent HTDA process. For the case of the ^{64}Ge nucleus the neutron and proton spectra in the vicinity of the Fermi surface are plotted in Fig. 5.3 and Fig. 5.4 before (HF+BCS) and after the HTDA self-consistent process (scHTDA). The Fermi levels are indicated with dashed lines. Conspiciously, the qualitative and quantitative differences are minor, the energy shifts in single-particle levels being much smaller than 100 keV.

It is clear that self-consistent calculations of that type are a bit time consuming
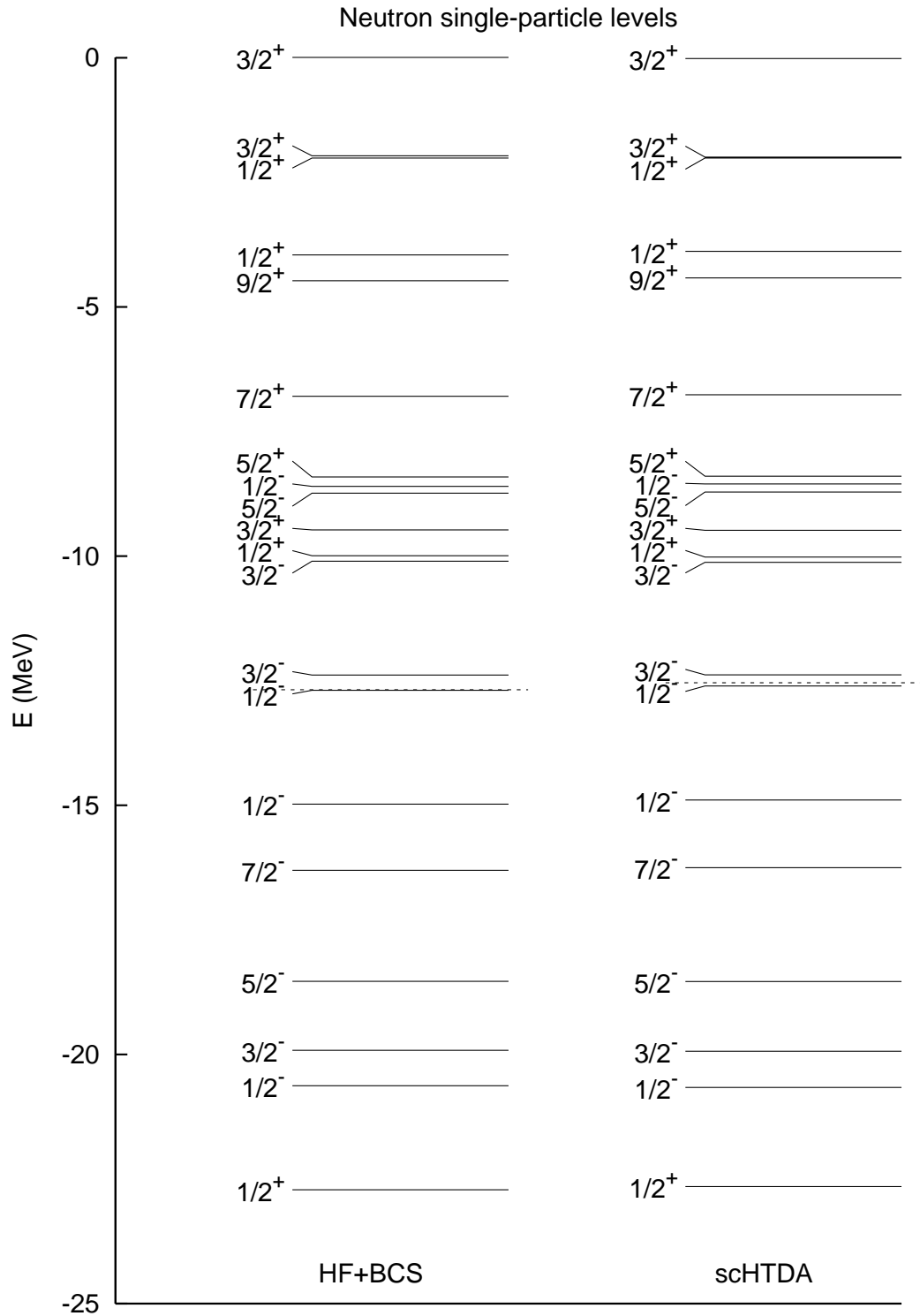
Figure 5.3: Neutron single-particle spectra in the vicinity of the Fermi level resulting HF+BCS and self-consistent HTDA (scHTDA) calculations for ^{64}Ge. Fermi levels are indicated with dashed lines.
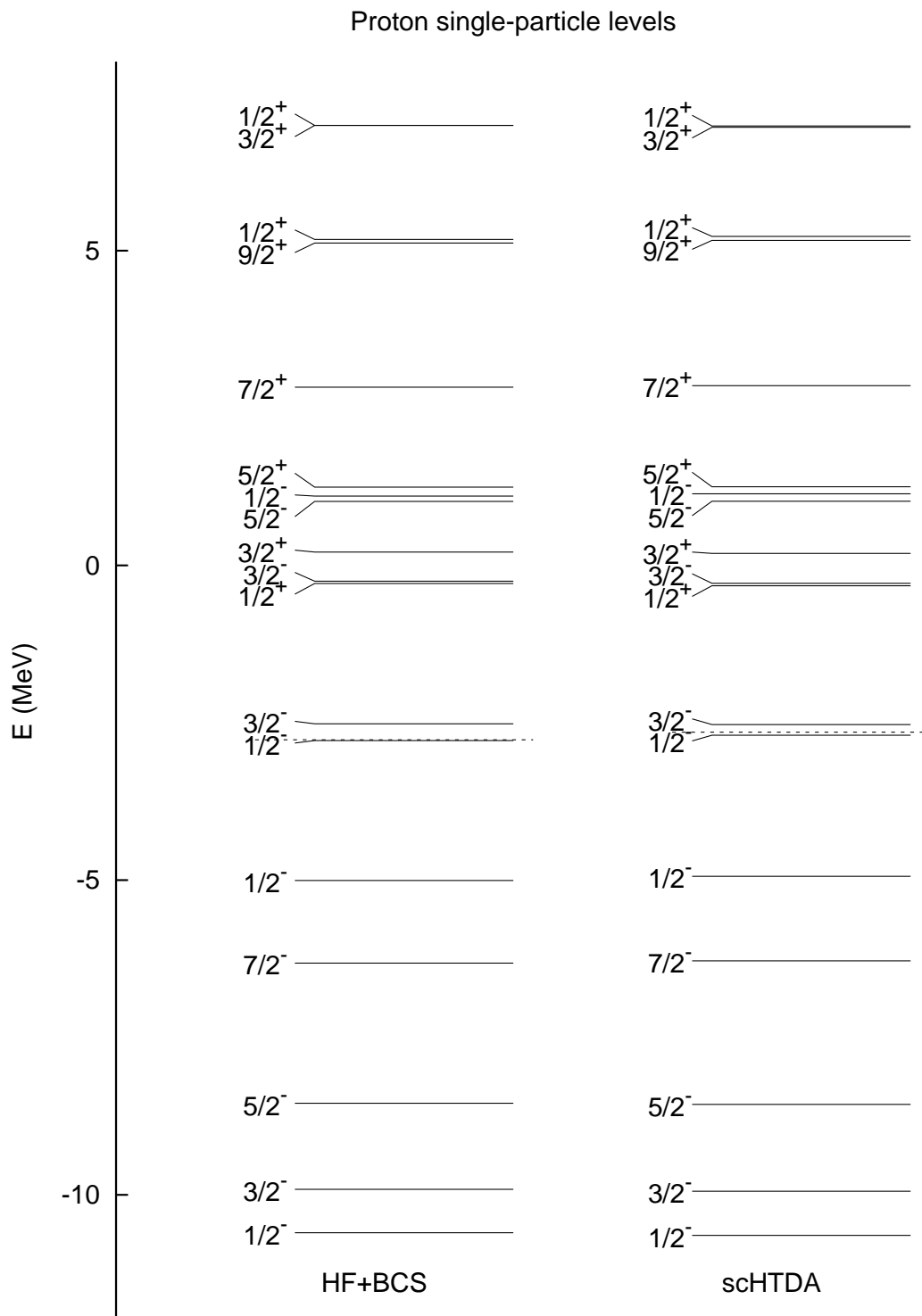
Figure 5.4: Same as in Fig. 5.3 but for protons.
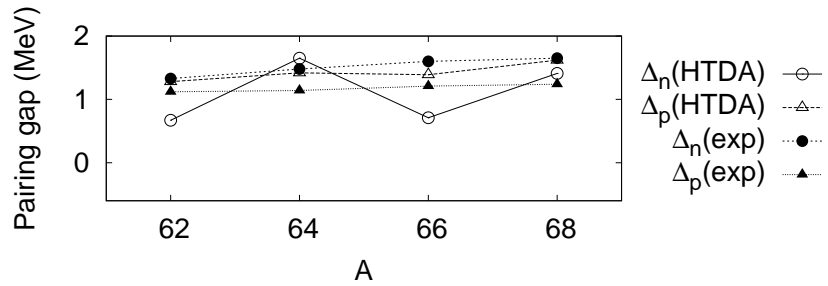
Figure 5.5: Theoretical (HTDA, Eq. (5.35)) and experimental 3-point pairing gaps for neutrons and protons for considered Ge isotopes.

due to the computation of a large number of matrix elements at each iteration. Hence, we limit the further discussion to consider only the results of a single HTDA matrix diagonalization.

5.2.3   Ground states properties of Ge isotopes

Within fixed single-particle ($E_{\text{cut}}^{\text{sp}} = 12\text{MeV}$) and particle-hole excitation spaces (4p4h) the non self-consistent HTDA calculations are now performed. The δ force strength ($V_{0n}=V_{0p}=300$ MeV fm^3) is adjusted to reproduce the 3-point pairing gaps of considered nuclei. Experimental and theoretical gaps for both kinds of particles are plotted in Fig. 5.5. As can be seen, there is an undesirable (and explained below) zigzag in the calculated neutron gaps pattern. The trend in theoretical proton gaps is satisfactory though the gaps are systematically overestimated. Of course it could be cured by reducing the coupling constant for protons, however it is not our aim here to reproduce exactly the phenomenological quantities (for which the uncertainties are quite large anyway) but to discuss the main features of the method within a reasonable and possibly simple parametrization of the interaction.

Equilibrium deformation and radii

In the following the results obtained for quadrupole and hexadecapole mass moments and radii are demonstrated and compared to the HF+BCS ones. Since these properties in the HF+BCS do not differ significantly upon the pairing force in use (see Sec. 4.4.1), the results concern the simple G force pairing.

Let us recall the definitions of quadrupole and hexadecapole moments operators

$$\hat{Q}_{20} = \sum_{i=1}^{A}(2z_i^2 - x_i^2 - y_i^2)\,, \tag{5.37}$$

$$\hat{Q}_{40} = \sum_{i=1}^{A} r_i^4 Y_{40}(\theta_i)\,. \tag{5.38}$$

Table 5.4: Quadrupole (q_2) and hexadecapole (q_4) mass moments and mass radii (r_m) obtained in HF+BCS and HTDA calculations.

nucleus	q_2 (b)		q_4 (b^2)		r_m (fm)	
	HF+BCS	HTDA	HF+BCS	HTDA	HF+BCS	HTDA
^{62}Ge	2.43	2.46	0.0312	0.0301	3.8743	3.8735
^{64}Ge	2.65	2.67	0.0085	0.0051	3.9148	3.9133
^{66}Ge	2.83	2.84	-0.0106	-0.0186	3.9548	3.9518
^{68}Ge	-2.98	-3.00	0.0422	0.0410	3.9970	3.9946

The mean values of the quadrupole and hexadecapole moments calculated in the correlated HTDA state $|\Psi\rangle$

$$q_2 = \langle\Psi|\hat{Q}_{20}|\Psi\rangle, \qquad q_4 = \langle\Psi|\hat{Q}_{40}|\Psi\rangle \tag{5.39}$$

are expressed as matrix elements of these operators between many-body states $|\Psi_i\rangle$. Using formulae of Appendix C these matrix elements can be written as sums of matrix elements calculated between single-particle states.

The root mean square radius r_m is calculated as

$$r_m = \sqrt{\frac{\langle\hat{\boldsymbol{r}}^2\rangle}{A}} \tag{5.40}$$

where the expectation value of the squared position operator $\hat{\boldsymbol{r}}^2$ is obtained by integrating the isoscalar nuclear density $\rho(\boldsymbol{r})$ (neutron+proton) times $\boldsymbol{r}^2$ over the whole space

$$\langle\hat{\boldsymbol{r}}^2\rangle = \int \mathrm{d}^3\boldsymbol{r}\rho(\boldsymbol{r})\boldsymbol{r}^2\,. \tag{5.41}$$

Again, this definition can be translated into the HTDA language if we take proper mean values in the correlated state $|\Psi\rangle$. With the use of Eq. (C-17) we obtain the mean value of the operator in the correlated state as a sum of matrix elements calculated between single-particle states.

In Table 5.4 we list the equilibrium deformations q_2 (in barns), q_4 (in squared barns) as found in HF+BCS and HTDA approaches. As seen the deformation hardly varies in the HTDA calculation and the mass radii remain almost unchanged. This is not surprising in view of the non self-consistent HTDA calculation done in the HF+BCS minimum.

Occupation probability

The occupation probability in the HTDA method is contained in the single-particle density ρ. Let us point out that this density is not diagonal in the HF basis, so one
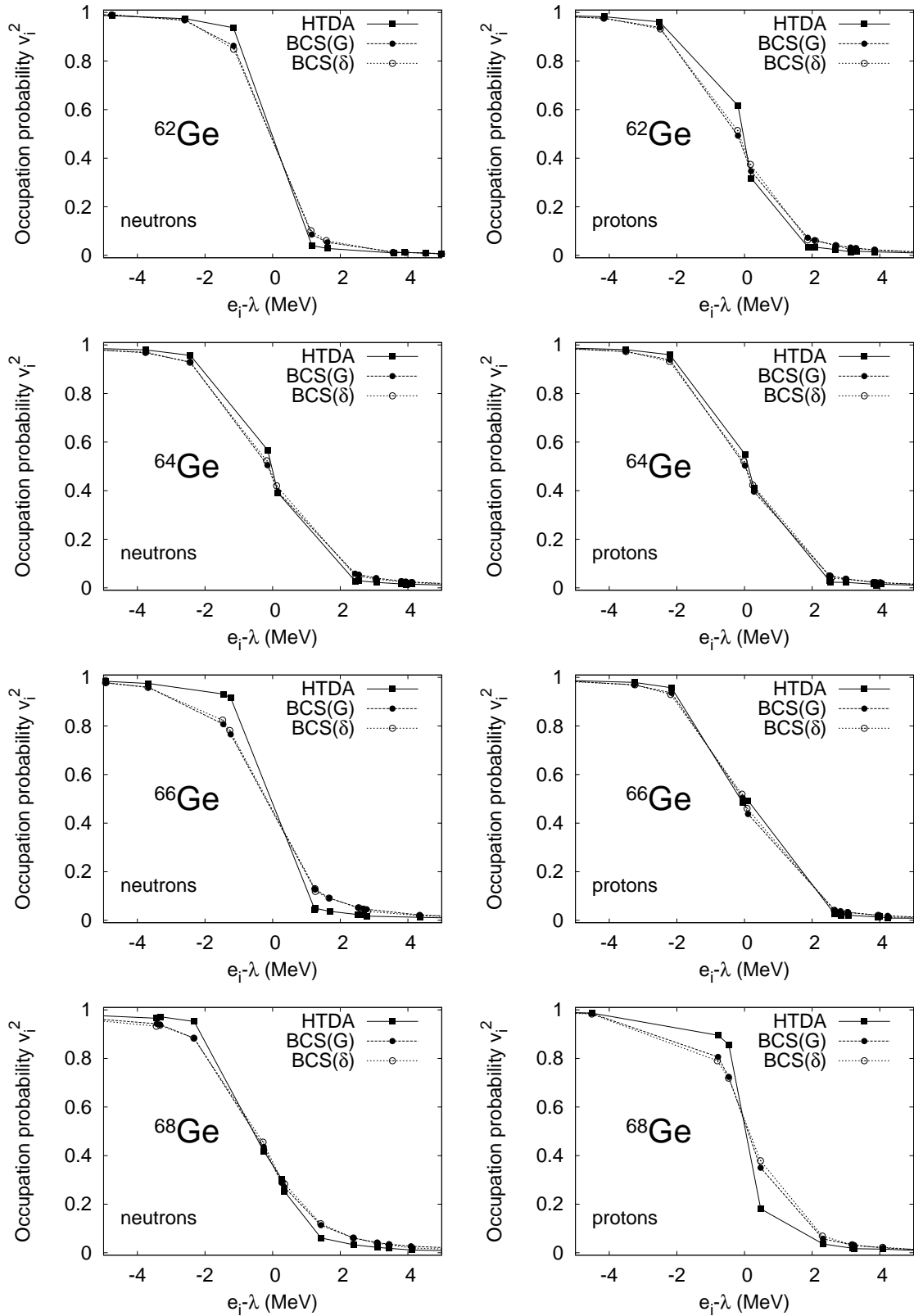
Figure 5.6: Occupation probabilities v_i^2 for neutrons (left panel) and protons (right panel) plotted as functions of normalized sp energies for studied nuclei. The results concern: BCS with seniority pairing (BCS(G)), BCS with the δ-pairing force (BCS(δ)) and HTDA calculations.
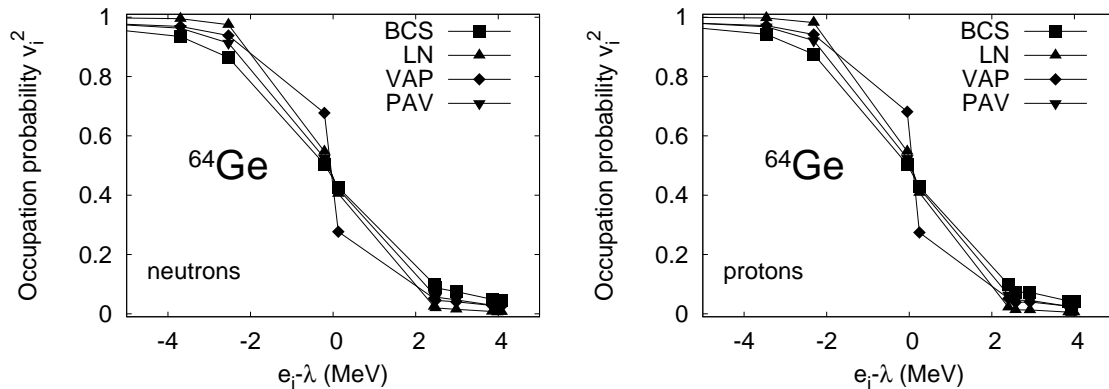
Figure 5.7: Occupation probabilities v_i^2 for neutrons (left panel) and protons (right panel) plotted as functions of normalized sp energies. The results correspond to BCS, Lipkin-Nogami (LN), Projection After Variation (PAV) and Variation After Projection (VAP) calculations performed in the ground state of ^{64}Ge nucleus.

should first find a canonical basis which (by definition) diagonalizes ρ. The diagonal matrix element ρ_{ii} is the occupation probability v_i^2.

In Fig. 5.6 the occupation probabilities for neutrons and protons as functions of the single-particle energy normalized to the Fermi energy are plotted for all studied cases. In addition to the BCS calculations (with seniority pairing and δ forces) the HTDA ones are presented. It can be seen that both BCS approaches give similar values of v_i^2 which, in the majority of cases, are more diffused than those produced in the HTDA method.

For comparison, the results of similar HF+BCS(δ) calculations [160] for this nucleus obtained in other particle-conserving approaches, precisely: Lipkin-Nogami (LN), Projection After Variation (PAV) and Variation After Projection (VAP) results in addition to the corresponding BCS ones are depicted in Fig. 5.7 for neutrons and protons in the ground state of ^{64}Ge. As can be seen, the diminution of pair diffuseness around the Fermi surface is a typical behaviour for particle number conserving approaches. It is seen in Fig. 5.7 that the same effect is observed in LN, PAV and VAP methods, however the changes are far more significant in the exact projection case (VAP) which is equivalent (a priori) with the HTDA case due to the Ritz theorem.

Degree of correlations

To measure the effect on the energies of pairing correlations one can resort to the consideration of the correlation energy, defined in the HTDA approach as the difference of the mean values of the Hamiltonian in correlated and uncorrelated states (see Eq. 5.36). However, this quantity has no realistic analogue to be compared with in the HF+BCS method as used in our case. Another variable that might shed
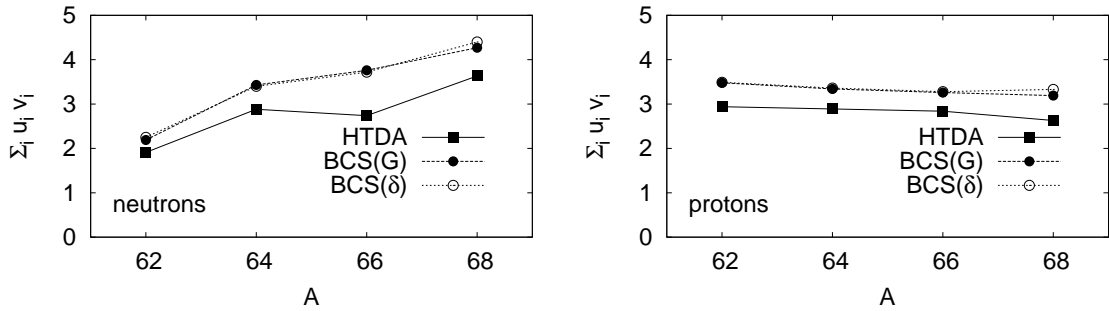
Figure 5.8: Traces of the pairing tensor calculated in BCS with seniority pairing (BCS(G)), BCS with the δ-pairing force (BCS(δ)) and HTDA approaches.
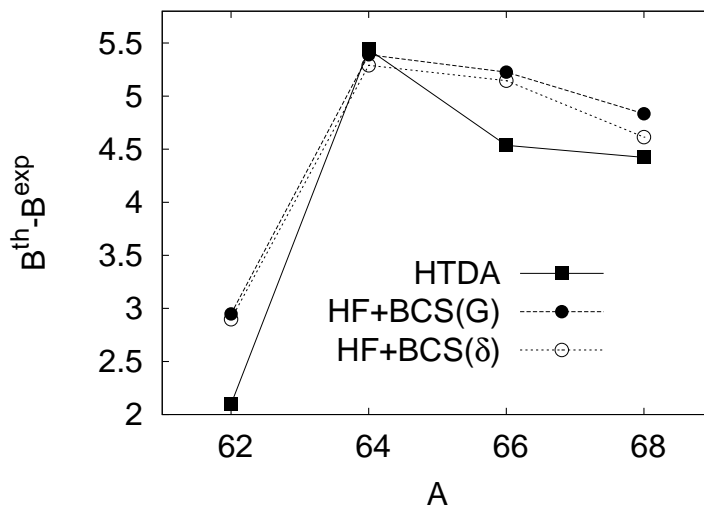
Figure 5.9: Discrepancies in calculated and experimental binding energies (in MeV) for HF+BCS models with seniority and δ-pairing forces and for HTDA method.

light on the degree of the correlations is the trace $\sum_i u_i v_i$ of the pairing tensor κ. In the HTDA approach we may define v_i and u_i amplitudes through the density matrix in the canonical basis. In Fig. 5.8 the traces of pairing tensors as obtained in different approaches are shown for both types of particles. They deviate up to 30 percent in the case of neutrons, the results being closer to each other for protons. Clearly, the diffusivity around the Fermi level reckoned with this quantity turns out to be smaller in the HTDA approach (cf. Fig 5.6).

Let us now consider the total energy of the system. In Fig. 5.9 the discrepancies between calculated and experimental binding energies are shown for the HF+BCS approximation with two pairing models (seniority and δ-pairing) and for the HTDA method. All three methods fail to the same extent in reproducing the extra binding of the $N = Z$ isotope– this problem will be rephrased when discussing the proton-neutron pairing. For other nuclei the binding energy is lower in the HTDA approach

Table 5.5: Percentage of various components of the correlated wave function result-
ing the HTDA calculation for neutrons and protons in studied nuclei.

	neutrons			protons		
nucleus	0p0h	1 pair	2 pairs	0p0h	1 pair	2 pairs
^{62}Ge	87.4	12.1	0.4	54.6	43.4	2.0
^{64}Ge	49.0	48.6	2.3	47.8	49.9	2.3
^{66}Ge	78.6	20.3	1.1	41.0	56.5	2.5
^{68}Ge	68.1	30.2	1.7	71.5	27.2	1.3

by an amount of 0.3-1.0 MeV. It is then seen that interestingly the particle-number
conserving approach yields a similar (or even lower) total energy like the HF+BCS
approximation with a simultaneous reduction of the diffusivity around the Fermi
surface.

5.2.4   Ground state wave function decomposition

We have already examined the amount of different types of particle-hole excitations
in the ground state of ^{64}Ge while discussing the basis truncation. Here, for the
completness of the study, we give the percentage of each type of p-h excitations in
the correlated wave function for all considered nuclei in Table 5.5.

The numbers in Table 5.5 show that together the vacuum and the 1 pair exci-
tation content are the dominant components in all cases and that the 2 pair exci-
tations are less probable. The amounts of vacuum and pair excitations parts differ
considerably for various isotopes which may be clarified by the consideration of the
single-particle spectra.

In Tables 5.6-5.9 particle-hole energy, probability and type of configuration for
the major components of the correlated solution are listed for neutrons and protons
in all cases. The numbers determining the type of the configuration correspond to
the indices of single-particle levels listed in the table. Only the levels contained in the
sp configuration space window are given. Each single-particle level is characterized
by its energy (e_{HF}), quantum numbers Ω^π, mean square radius ($\langle r^2 \rangle$) and the mean
value of the third spin component ($\langle s_z \rangle$) determined for this level. Additionally, the
single particle-spectra normalized to the Fermi level energy are plotted for neutrons
and protons in each case in Figs. 5.10-5.13.

As seen, in all cases the most probable pair excitation is that with the lowest
quasiparticle energy (or the two lowest ones in the case of nearly degenerate single-
particle levels). It may be noted that the large gaps (~ 2.5MeV) in spectra in the
vicinity of the Fermi level diminish the probability of one pair excitations– this is

the case of neutrons in $N=30$, 34 isotopes. The opposite situation found in the other cases leads to the increase of this probability. This also explains the pattern of neutron pairing gaps in Fig. 5.5 obtained with the same value of V_{0n} for all nuclei.

A case demanding some special attention is that of protons in $N=34$ isotope where the pair excitation with the lowest p-h energy is slightly favoured over the vacuum (43% and 41% respectively), that is to say the ground state is a mixture of the dominating 2p2h excitation and the vacuum. This is very easily understood in view of the nearly degenerate character of the last occupied and first unoccupied states ($1/2^-$ and $3/2^-$, respectively) as seen on Fig. 5.12.

In the $N = Z$ nucleus, as may be expected, the decomposition of the correlated wave functions of protons and neutrons is supremely analogous.

Table 5.6: Particle-hole energy (E_{p-h}^i) in MeV, probability χ_i^2 and type of particle-hole excitations contributing the most to the correlated wave functions of neutrons and protons in ^{62}Ge. The numbers describing configuration type correspond to the indices of listed single-particle levels which are contained in the sp configuration space window. Single-particle energies (e_{HF}), quantum numbers (Ω^π), the third spin component ($\langle s_z \rangle$) and mean values of the squared radius ($\langle r^2 \rangle$) are given for each level. Bars indicate time-reversed states.

$$^{62}\textbf{Ge}$$

neutrons			protons		
E_{p-h}^i (MeV)	χ_i^2	type	E_{p-h}^i (MeV)	χ_i^2	type
0.0	0.87	0p0h	0.0	0.54	0p0h
4.6	0.02	$1p_{16}1h_{15}1p_{\overline{16}}1h_{\overline{15}}$	0.8	0.3	$1p_{17}1h_{16}1p_{\overline{17}}1h_{\overline{16}}$
5.5	0.01	$1p_{17}1h_{15}1p_{\overline{17}}1h_{\overline{15}}$	4.1	0.02	$1p_{18}1h_{16}1p_{\overline{18}}1h_{\overline{16}}$
10.1	0.006	$1p_{19}1h_{15}1p_{\overline{19}}1h_{\overline{15}}$	4.5	0.02	$1p_{19}1h_{16}1p_{\overline{19}}1h_{\overline{16}}$
7.5	0.005	$1p_{16}1h_{14}1p_{\overline{16}}1h_{\overline{14}}$	5.4	0.015	$1p_{17}1h_{15}1p_{\overline{17}}1h_{\overline{15}}$

neutrons				protons				
N^o	e_{HF}	Ω^π	$\langle s_z \rangle$	$\langle r^2 \rangle$	N^o	e_{HF}	Ω^π	$\langle s_z \rangle$	$\langle r^2 \rangle$
9	-23.488	$3/2^+$	-0.432	13.607	9	-11.907	$3/2^+$	-0.429	14.012
10	-22.954	$1/2^+$	0.465	13.651	10	-11.213	$1/2^+$	0.467	14.138
11	-20.680	$1/2^-$	0.164	18.966	11	-9.322	$1/2^-$	0.166	19.583
12	-19.882	$3/2^-$	0.334	18.588	12	-8.497	$3/2^-$	0.337	19.191
13	-18.551	$5/2^-$	0.438	17.957	13	-7.093	$5/2^-$	0.436	18.512
14	-16.406	$7/2^-$	0.500	17.197	14	-5.222	$7/2^-$	0.500	17.766
15	-14.972	$1/2^-$	0.058	18.754	15	-3.592	$1/2^-$	0.035	19.939
					16	-1.273	$1/2^-$	0.206	19.856
	Fermi level								
16	-12.653	$1/2^-$	0.193	18.322		Fermi level			
17	-12.190	$3/2^-$	-0.183	18.079	17	-0.883	$3/2^-$	-0.167	19.270
18	-10.238	$3/2^-$	0.349	17.908	18	0.797	$3/2^-$	0.329	20.008
19	-9.903	$1/2^+$	0.107	22.394	19	0.989	$1/2^+$	0.110	23.673
20	-9.290	$3/2^+$	0.263	22.146	20	1.612	$3/2^+$	0.267	23.398
21	-8.813	$1/2^-$	-0.415	18.875	21	2.065	$1/2^-$	-0.408	21.801
22	-8.757	$5/2^-$	-0.438	17.852	22	2.229	$5/2^-$	-0.436	19.094
23	-8.164	$5/2^+$	0.371	21.658	23	2.775	$5/2^+$	0.374	22.934
24	-6.623	$7/2^+$	0.447	21.048	24	4.337	$7/2^+$	0.445	22.353
25	-4.480	$9/2^+$	0.500	20.490	25	6.147	$1/2^+$	0.382	36.030
26	-3.895	$1/2^+$	0.345	26.072	26	6.153	$9/2^+$	0.500	21.939
					27	8.046	$3/2^+$	0.381	38.526
					28	8.065	$1/2^+$	-0.306	38.625
					29	9.168	$1/2^+$	0.365	51.333
					30	9.593	$5/2^+$	0.475	44.485
					31	9.772	$3/2^+$	-0.383	44.117
					32	9.854	$1/2^-$	0.453	69.347
					33	10.728	$1/2^+$	-0.048	40.600
					34	10.873	$3/2^-$	0.424	57.250
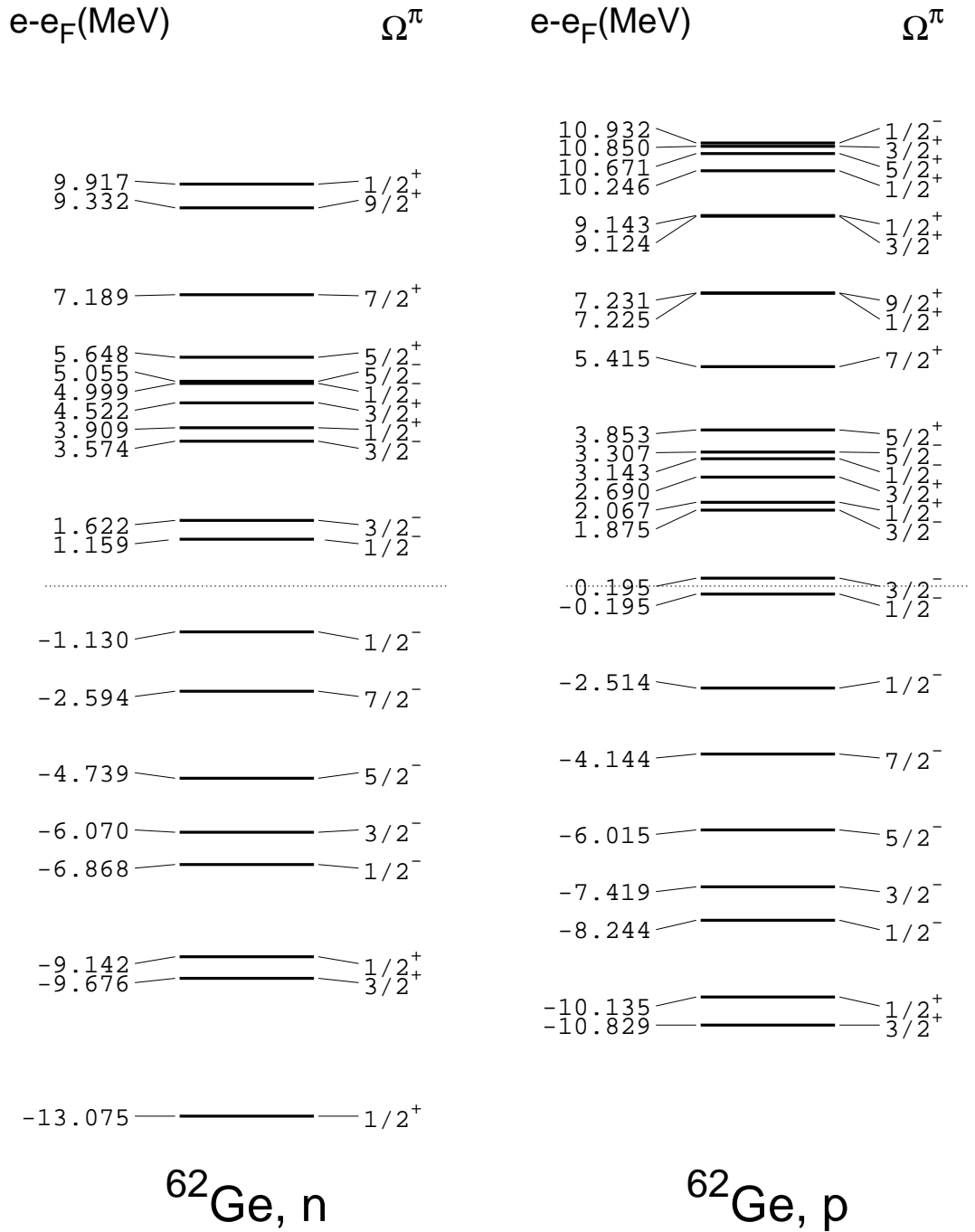
Figure 5.10: Single-particle spectra normalized to the Fermi level energy for neutrons and protons for ^{62}Ge. Fermi levels are indicated with dashed lines.

Table 5.7: Same as in Table 5.6 but for the $N = Z$ Ge isotope.

$$^{64}\text{Ge}$$

	neutrons			protons	
$E^i_{\mathrm{p-h}}$ (MeV)	χ^2_i	type	$E^i_{\mathrm{p-h}}$ (MeV)	χ^2_i	type
0.0	0.49	0p0h	0.0	0.48	0p0h
0.6	0.33	$1\mathrm{p}_{17}1\mathrm{h}_{16}1\mathrm{p}_{\overline{17}}1\mathrm{h}_{\overline{16}}$	0.5	0.35	$1\mathrm{p}_{17}1\mathrm{h}_{16}1\mathrm{p}_{\overline{17}}1\mathrm{h}_{\overline{16}}$
5.1	0.02	$1\mathrm{p}_{18}1\mathrm{h}_{16}1\mathrm{p}_{\overline{18}}1\mathrm{h}_{\overline{16}}$	4.9	0.018	$1\mathrm{p}_{19}1\mathrm{h}_{15}1\mathrm{p}_{\overline{19}}1\mathrm{h}_{\overline{15}}$
5.2	0.017	$1\mathrm{p}_{19}1\mathrm{h}_{16}1\mathrm{p}_{\overline{19}}1\mathrm{h}_{\overline{16}}$	5.0	0.016	$1\mathrm{p}_{18}1\mathrm{h}_{16}1\mathrm{p}_{\overline{18}}1\mathrm{h}_{\overline{16}}$
5.4	0.016	$1\mathrm{p}_{17}1\mathrm{h}_{15}1\mathrm{p}_{\overline{17}}1\mathrm{h}_{\overline{15}}$	5.0	0.015	$1\mathrm{p}_{19}1\mathrm{h}_{16}1\mathrm{p}_{\overline{19}}1\mathrm{h}_{\overline{16}}$

	neutrons				protons			
N^o	e_{HF}	Ω^π	$\langle s_z \rangle$	$\langle r^2 \rangle$	N^o	e_{HF}	Ω^π	$\langle s_z \rangle$	$\langle r^2 \rangle$
9	-23.314	$3/2^+$	-0.437	13.786	9	-13.103	$3/2^+$	-0.438	14.202
10	-22.716	$1/2^+$	0.466	13.730	10	-12.366	$1/2^+$	0.470	14.226
11	-20.630	$1/2^-$	0.149	19.210	11	-10.603	$1/2^-$	0.146	19.729
12	-19.919	$3/2^-$	0.335	18.913	12	-9.914	$3/2^-$	0.334	19.432
13	-18.531	$5/2^-$	0.445	18.320	13	-8.547	$5/2^-$	0.445	18.847
14	-16.303	$7/2^-$	0.500	17.357	14	-6.316	$7/2^-$	0.500	17.891
15	-14.977	$1/2^-$	0.045	18.987	15	-5.008	$1/2^-$	0.036	19.869
16	-12.694	$1/2^-$	0.229	18.621	16	-2.785	$1/2^-$	0.245	19.733

<table>
<tr><td colspan="5">Fermi level</td><td colspan="5">Fermi level</td></tr>
</table>

N^o	e_{HF}	Ω^π	$\langle s_z \rangle$	$\langle r^2 \rangle$	N^o	e_{HF}	Ω^π	$\langle s_z \rangle$	$\langle r^2 \rangle$
17	-12.388	$3/2^-$	-0.220	18.343	17	-2.519	$3/2^-$	-0.234	19.225
18	-10.098	$3/2^-$	0.386	18.074	18	-0.288	$1/2^+$	0.095	23.548
19	-9.992	$1/2^+$	0.095	22.600	19	-0.251	$3/2^-$	0.400	19.668
20	-9.476	$3/2^+$	0.255	22.421	20	0.210	$3/2^+$	0.255	23.343
21	-8.737	$5/2^-$	-0.445	17.982	21	1.017	$5/2^-$	-0.446	18.966
22	-8.600	$1/2^-$	-0.424	19.080	22	1.100	$1/2^-$	-0.428	21.167
23	-8.414	$5/2^+$	0.373	22.046	23	1.242	$5/2^+$	0.374	22.980
24	-6.794	$7/2^+$	0.454	21.458	24	2.830	$7/2^+$	0.455	22.429
25	-4.472	$9/2^+$	0.500	20.647	25	5.122	$9/2^+$	0.500	21.767
26	-3.957	$1/2^+$	0.359	26.410	26	5.177	$1/2^+$	0.385	33.323
27	-2.014	$1/2^+$	-0.195	26.586	27	6.989	$3/2^+$	0.333	33.925
28	-1.968	$3/2^+$	0.273	26.498	28	6.989	$1/2^+$	-0.257	33.698
					29	8.733	$1/2^+$	0.196	46.591
					30	8.831	$3/2^+$	-0.222	35.377
					31	9.124	$5/2^+$	0.424	40.649

Figure 5.11: Same as in Fig. 5.10 but for ^{64}Ge.

Table 5.8: Same as in Table 5.6 but for the ^{66}Ge isotope.

^{66}Ge

neutrons			protons		
$E^i_{\mathrm{p-h}}$ (MeV)	χ^2_i	type	$E^i_{\mathrm{p-h}}$ (MeV)	χ^2_i	type
0.0	0.78	0p0h	0.0	0.41	0p0h
5.0	0.018	$1p_{19}1h_{17}1p_{\overline{19}}1h_{\overline{17}}$	0.3	0.43	$1p_{17}1h_{16}1p_{\overline{17}}1h_{\overline{16}}$
5.0	0.016	$1p_{18}1h_{17}1p_{\overline{18}}1h_{\overline{17}}$	4.0	0.02	$1p_{17}1h_{15}1p_{\overline{17}}1h_{\overline{15}}$
5.4	0.014	$1p_{18}1h_{16}1p_{\overline{18}}1h_{\overline{16}}$	5.9	0.01	$1p_{18}1h_{16}1p_{\overline{18}}1h_{\overline{16}}$
5.4	0.012	$1p_{19}1h_{16}1p_{\overline{19}}1h_{\overline{16}}$	6.4	0.01	$1p_{19}1h_{16}1p_{\overline{19}}1h_{\overline{16}}$

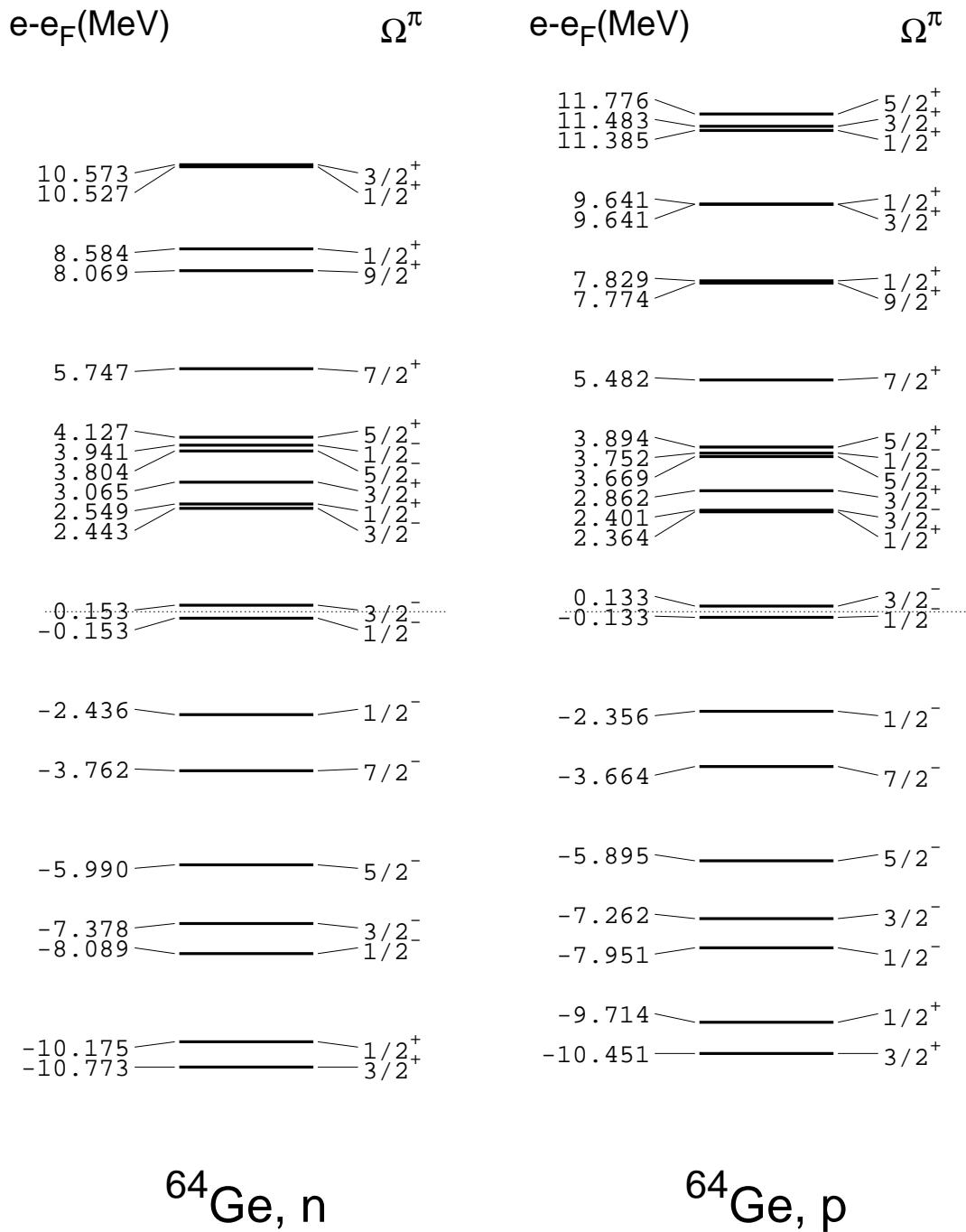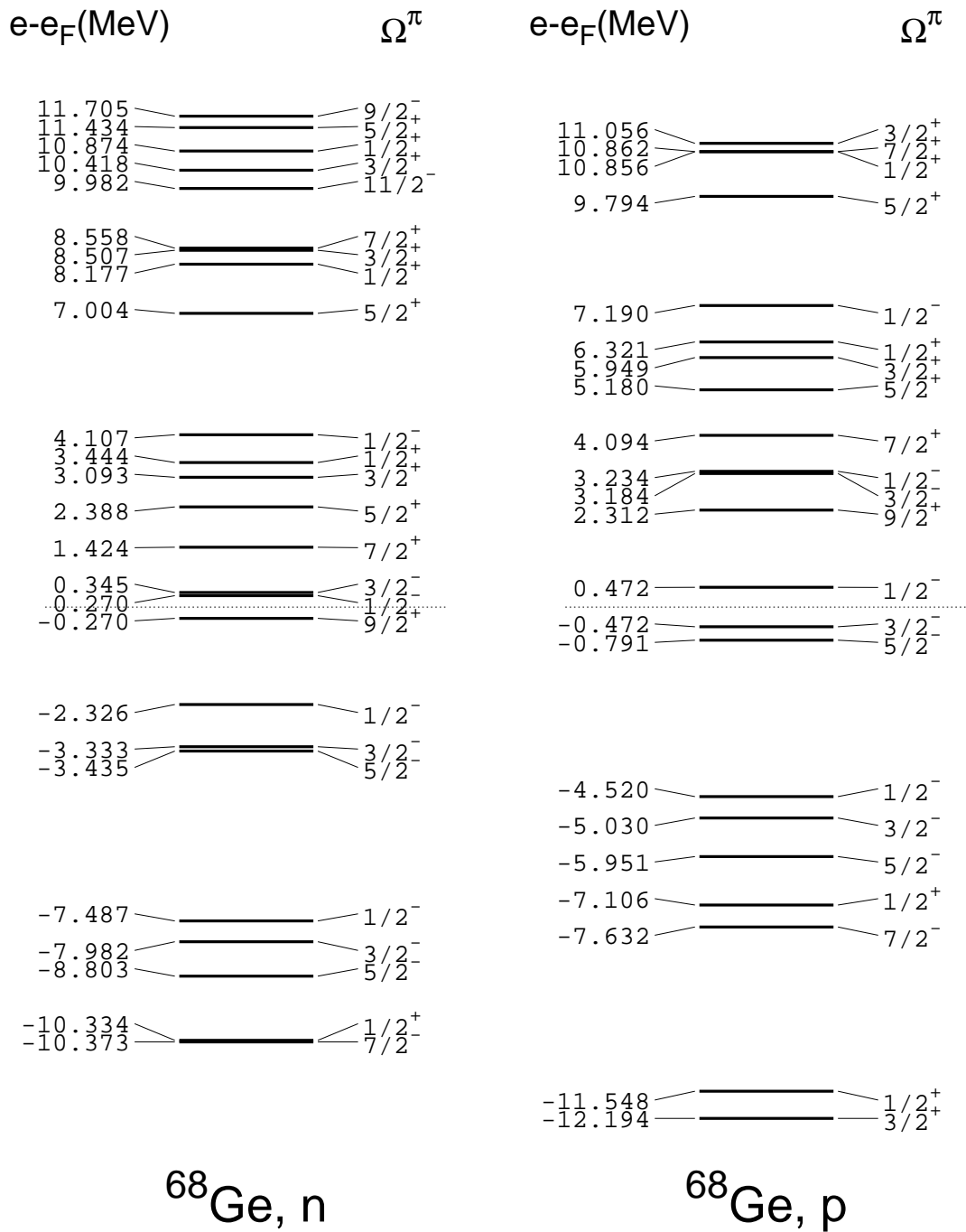| neutrons				protons				
N^o	e_{HF}	Ω^π	$\langle s_z \rangle$	$\langle r^2 \rangle$	N^o	e_{HF}	Ω^π	$\langle s_z \rangle$	$\langle r^2 \rangle$
9	-23.169	$3/2^+$	-0.440	13.957	9	-14.306	$3/2^+$	-0.444	14.395
10	-22.543	$1/2^+$	0.466	13.843	10	-13.524	$1/2^+$	0.473	14.347
11	-20.541	$1/2^-$	0.135	19.437	11	-11.819	$1/2^-$	0.130	19.888
12	-19.907	$3/2^-$	0.335	19.215	12	-11.243	$3/2^-$	0.330	19.655
13	-18.477	$5/2^-$	0.449	18.670	13	-9.931	$5/2^-$	0.452	19.161
14	-16.235	$7/2^-$	0.500	17.548	14	-7.440	$7/2^-$	0.500	18.057
15	-14.959	$1/2^-$	0.045	19.202	15	-6.339	$1/2^-$	0.041	19.864
16	-12.745	$1/2^-$	0.248	18.910	16	-4.234	$1/2^-$	0.267	19.703
17	-12.528	$3/2^-$	-0.235	18.588			Fermi level		
	Fermi level				17	-4.076	$3/2^-$	-0.257	19.302
18	-10.043	$3/2^-$	0.401	18.274	18	-1.512	$1/2^+$	0.083	23.524
19	-10.033	$1/2^+$	0.084	22.823	19	-1.337	$3/2^-$	0.427	19.449
20	-9.603	$3/2^+$	0.247	22.706	20	-1.114	$3/2^+$	0.245	23.399
21	-8.759	$5/2^-$	-0.448	18.144	21	-0.234	$5/2^-$	-0.451	18.954
22	-8.601	$5/2^+$	0.373	22.440	22	-0.195	$5/2^+$	0.372	23.116
23	-8.504	$1/2^-$	-0.428	19.317	23	0.056	$1/2^-$	-0.439	20.820
24	-6.928	$7/2^+$	0.458	21.872	24	1.391	$7/2^+$	0.460	22.608
25	-4.521	$9/2^+$	0.500	20.865	25	4.033	$9/2^+$	0.500	21.783
26	-4.059	$1/2^+$	0.375	26.854	26	4.146	$1/2^+$	0.390	32.264
27	-2.242	$3/2^+$	0.275	26.909	27	5.794	$3/2^+$	0.297	32.603
28	-2.226	$1/2^+$	-0.200	26.971	28	5.795	$1/2^+$	-0.232	32.240
29	-0.267	$3/2^+$	-0.091	27.250	29	7.585	$3/2^+$	-0.134	33.800
30	0.377	$1/2^+$	-0.121	32.978	30	7.738	$1/2^+$	0.090	48.578
31	0.575	$5/2^+$	0.229	30.071					
32	0.607	$1/2^-$	0.067	28.482					
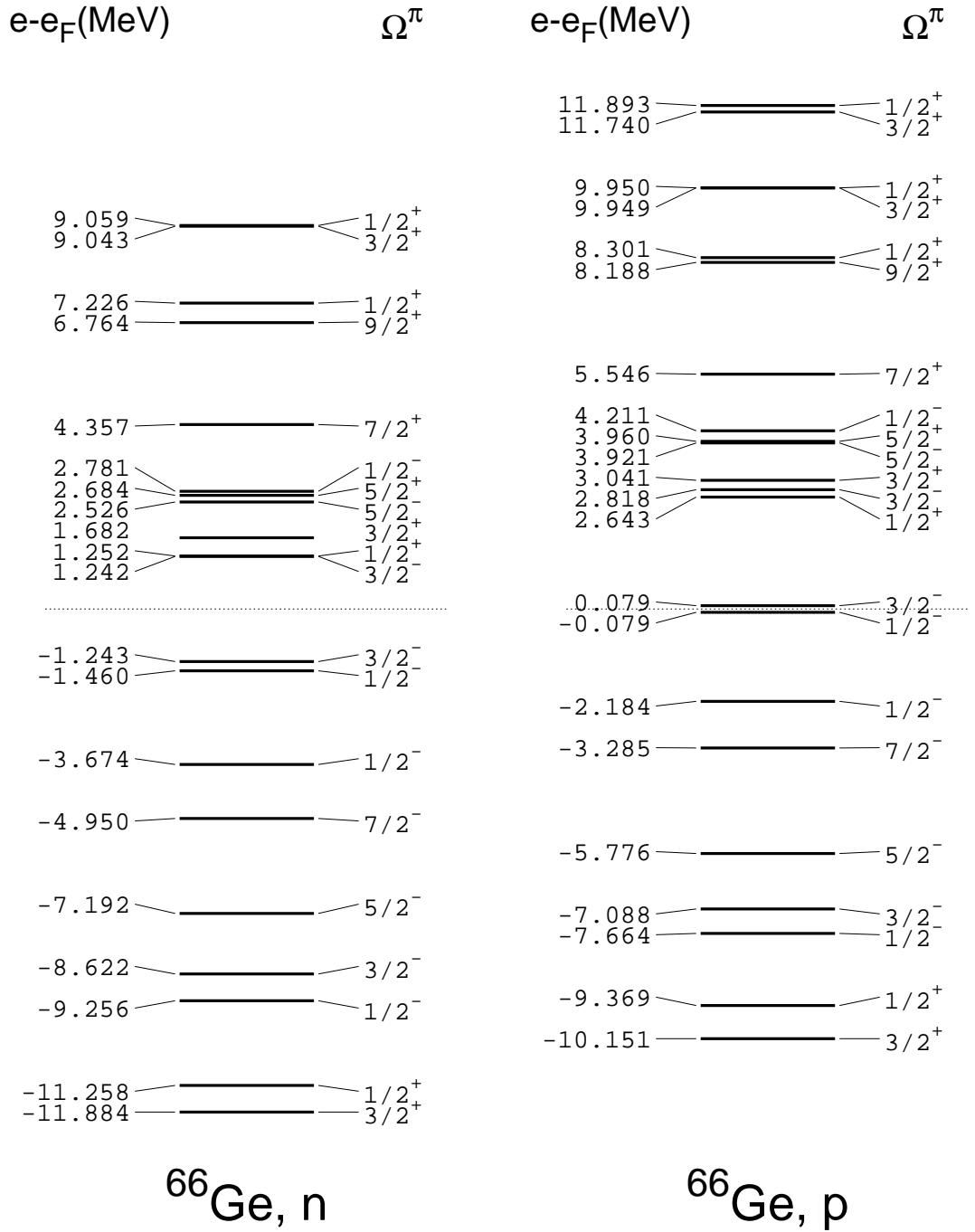
Figure 5.12: Same as in Fig. 5.10 but for ^{66}Ge.

Table 5.9: Same as in Table 5.6 but for the ^{68}Ge isotope.

^{68}Ge

neutrons			protons		
$E^i_{\mathrm{p-h}}$ (MeV)	χ^2_i	type	$E^i_{\mathrm{p-h}}$ (MeV)	χ^2_i	type
0.0	0.68	0p0h	0.0	0.71	0p0h
1.0	0.25	$1p_{19}1h_{18}1p_{\overline{19}}1h_{\overline{18}}$	1.9	0.11	$1p_{17}1h_{16}1p_{\overline{17}}1h_{\overline{16}}$
1.2	0.20	$1p_{20}1h_{18}1p_{\overline{20}}1h_{\overline{18}}$	2.5	0.06	$1p_{17}1h_{15}1p_{\overline{17}}1h_{\overline{15}}$
3.4	0.04	$1p_{21}1h_{18}1p_{\overline{21}}1h_{\overline{18}}$	6.2	0.03	$1p_{18}1h_{15}1p_{\overline{18}}1h_{\overline{15}}$
5.3	0.02	$1p_{22}1h_{18}1p_{\overline{22}}1h_{\overline{18}}$	5.6	0.02	$1p_{18}1h_{16}1p_{\overline{18}}1h_{\overline{16}}$

neutrons				protons			
N^o	e_{HF}	Ω^π	$\langle s_z \rangle$	$\langle r^2 \rangle$	N^o	e_{HF}	Ω^π	$\langle s_z \rangle$	$\langle r^2 \rangle$
10	-20.689	$7/2^-$	0.500	19.760	9	-17.348	$1/2^+$	-0.137	14.900
11	-20.650	$1/2^+$	0.407	13.733	10	-13.432	$7/2^-$	0.500	20.260
12	-19.119	$5/2^-$	0.131	19.086	11	-12.906	$1/2^+$	0.415	14.154
13	-18.298	$3/2^-$	0.175	18.745	12	-11.751	$5/2^-$	0.112	19.608
14	-17.803	$1/2^-$	-0.018	18.563	13	-10.830	$3/2^-$	0.175	19.198
15	-13.751	$5/2^-$	-0.131	18.995	14	-10.320	$1/2^-$	-0.023	18.987
16	-13.649	$3/2^-$	0.157	18.815	15	-6.591	$5/2^-$	-0.112	19.589
17	-12.642	$1/2^-$	-0.192	19.231	16	-6.272	$3/2^-$	0.131	19.296
18	-10.586	$9/2^+$	0.500	23.259		Fermi level			
	Fermi level				17	-5.328	$1/2^-$	-0.170	19.781
19	-10.046	$1/2^-$	-0.127	18.392	18	-3.488	$9/2^+$	0.500	23.746
20	-9.971	$3/2^-$	0.168	18.651	19	-2.616	$3/2^-$	0.194	19.284
21	-8.892	$7/2^+$	0.249	22.661	20	-2.566	$1/2^-$	-0.175	19.042
22	-7.928	$5/2^+$	0.210	22.456	21	-1.706	$7/2^+$	0.240	23.192
23	-7.223	$3/2^+$	0.082	22.320	22	-0.620	$5/2^+$	0.201	23.000
24	-6.872	$1/2^+$	0.056	22.336	23	0.149	$3/2^+$	0.075	22.892
25	-6.209	$1/2^-$	0.338	19.280	24	0.521	$1/2^+$	0.056	22.944
26	-3.312	$5/2^+$	0.344	25.767	25	1.390	$1/2^-$	0.369	20.277
27	-2.139	$1/2^+$	0.378	29.379	26	3.994	$5/2^+$	0.334	27.735
28	-1.809	$3/2^+$	-0.378	28.545	27	5.056	$1/2^+$	0.371	33.607
29	-1.758	$7/2^+$	-0.249	24.715	28	5.062	$7/2^+$	-0.240	25.642
30	-0.334	$11/2^-$	0.500	27.276	29	5.256	$3/2^+$	-0.373	31.308
31	0.102	$3/2^+$	0.209	28.584					
32	0.558	$1/2^+$	-0.242	30.187					
33	1.118	$5/2^+$	-0.053	25.944					
34	1.389	$9/2^-$	0.309	26.970					

Figure 5.13: Same as in Fig. 5.10 but for ^{68}Ge.

5.2.5   Summary

Before extending the HTDA framework which we have to account for *pn* pairing let us summarize the main features of the approach. We have shown that the method proposed here, applied for the calculations in the minima of the deformation of several Ge isotopes, leads to the results being in qualitative agreement with those of the customary HF+BCS approach yet being free of the particle number non-conservation. The unquestionable advantage of the method is that it is valid in any region of the interaction strengths and brings in a reasonable amount of correlations in both, low pairing and superfluid regimes. Thus it seems a proper approach to investigate the $T = 0$ and $T = 1$ pairing correlations which are known to compete with each other in the BCS picture producing the isovector to isoscalar superfluidity transition.

It was shown for the case of ^{64}Ge that the so-called pair excitations are the most important parts of the particle-hole excitations in the ground state. The space of 1 and 2 pair excitations is sufficient to account properly for the ground state superfluidity as the addition of 3 pairs has negligibly influenced the results. The constitution of the correlated wave function for other even-even Ge isotopes suggests that limiting the configuration space to 4p4h excitations of the pair excitation type should be adequate as well in those nuclei.

5.3 Proton-neutron HTDA

We have discussed in detail the HTDA method for the case where only the proton-proton and neutron-neutron correlations are present. However, in the ground states of $N \sim Z$ nuclei the proton-neutron pairing plays a non negligible role. Therefore, in what follows we extend the HTDA approach by including explicitely the *pn* part of the residual interaction.

As expected, (see the results of Sec. 5.2), the main contribution in the ground states of considered nuclei beyond $|\Psi_0\rangle$ comes from the so-called pair excitations, *i.e.* when two particles in Kramers degenerate hole orbitals are promoted to two Kramers degenerate particle states. The 1p1h excitations, as well as other types of excitations are of minor importance. Accordingly, one can expect that the *pn* pair excitation will be also the dominant phenomenon as far as *pn* correlations are concerned.

The extended HTDA method is outlined for the general case where all type of excitations are considered. The expressions for the matrix elements given in the forthcoming are also suitable for the most general case of many-particle many-hole excitations. Nevertheless, mostly for practical reasons, the numerical code with proton-neutron coupling built for the purpose of this work can handle only pair excitations. In this very first approach to *pn* correlations within the HTDA framework the results of numerical calculations with 1 and 2 pairs excitations added to the vacuum are presented.

5.3.1 The method

In the following we still consider Hamiltonian (5.7) but we do not neglect the proton-neutron coupling in the residual interaction $\hat{V}_{\text{res}}$, namely we allow for the correlated wave function the following expansion (indicating by τ and τ' two different charge states):

$$
\begin{aligned}
|\Psi\rangle &\equiv |\Psi^\tau \otimes \Psi^{\tau'}\rangle = \chi_{00}|\Psi_0^\tau \otimes \Psi_0^{\tau'}\rangle + \sum_{\{1p1h\}_\tau} \chi_{10}|\Psi_1^\tau \otimes \Psi_0^{\tau'}\rangle + \sum_{\{1p1h\}_{\tau'}} \chi_{01}|\Psi_0^\tau \otimes \Psi_1^{\tau'}\rangle \\
&+ \sum_{\{1p1h\}_\tau \{1p1h\}_{\tau'}} \chi_{11}|\Psi_1^\tau \otimes \Psi_1^{\tau'}\rangle + \sum_{\{2p2h\}_\tau} \chi_{20}|\Psi_2^\tau \otimes \Psi_0^{\tau'}\rangle + \sum_{\{2p2h\}_{\tau'}} \chi_{02}|\Psi_0^\tau \otimes \Psi_2^{\tau'}\rangle \\
&+ \cdots
\end{aligned}
\tag{5.42}
$$

with the normalization condition given as previously

$$
\sum_I \chi_I^2 = 1 \,.
\tag{5.43}
$$

The solution of the problem involves, as in the decoupled problems, the diagonalization of the Hamiltonian matrix defined in (5.7) which may be written for the

many-body states (5.42):

$$
\begin{pmatrix}
H_{00,00} & H_{00,01} & H_{00,10} & H_{00,11} & H_{00,20} & H_{00,02} & \cdots \\
H_{01,00} & H_{01,01} & H_{01,10} & H_{01,11} & H_{01,20} & H_{01,02} & \cdots \\
H_{10,00} & H_{10,01} & H_{10,10} & H_{10,11} & H_{10,20} & H_{10,02} & \cdots \\
H_{11,00} & H_{11,01} & H_{11,10} & H_{11,11} & H_{11,20} & H_{11,02} & \cdots \\
H_{20,00} & H_{20,01} & H_{20,10} & H_{20,11} & H_{20,20} & H_{20,02} & \cdots \\
H_{02,00} & H_{02,01} & H_{02,10} & H_{02,11} & H_{02,20} & H_{02,02} & \cdots \\
\vdots & \vdots & \vdots & \vdots & \vdots & \vdots & \ddots
\end{pmatrix},
\tag{5.44}
$$

where the pairs of indices signify the numbers of particles and holes in neutron and proton Slater determinants, respectively. The general expression for the matrix element of (5.7) in many-body state (5.42) writes as follows

$$
H_{IJ} = \left(\langle \Psi_0 | \hat{H} | \Psi_0 \rangle + \sum_{\tau=p,n} E_{p-h}^{I\tau} \right) \delta_{IJ} + \langle \Psi_I | \hat{V}_{\text{res}} | \Psi_J \rangle ,
\tag{5.45}
$$

where $|\Psi_I\rangle \equiv |\Psi_k^\tau \otimes \Psi_l^{\tau'}\rangle$, $|\Psi_0\rangle \equiv |\Psi_0^\tau \otimes \Psi_0^{\tau'}\rangle$ and $\sum_{\tau=p,n} E_{p-h}^{I\tau}$ is the total particle-hole excitation energy of $|\Psi_I\rangle$ with respect to the vacuum Slater determinant. In the forthcoming paragraph we repeat the expressions for diagonal and non-diagonal matrix elements (Eqs. (5.15)-(5.22)) upon inserting the modifications due to the presence of the proton-neutron interaction.

Diagonal matrix elements

In what follows the diagonal matrix elements of the Hamiltonian (5.7) are first considered. From Eq. (5.45) the most general diagonal matrix elements writes

$$
H_{II} = \langle \Psi_0 | \hat{H} | \Psi_0 \rangle + \sum_{\tau=p,n} E_{p-h}^{I\tau} + \langle \Psi_I | \hat{V}_{\text{res}} | \Psi_I \rangle .
\tag{5.46}
$$

Following the steps of the paragraph 5.1.1 and using the formula (C-17,C-22) one obtains

$$
\begin{aligned}
\langle \Psi_I | \hat{V}_{\text{res}} | \Psi_I \rangle &= \frac{1}{2} \sum_{\tau=p,n} \left[\sum_i^{h(\Psi_k^\tau)} \sum_j^{h(\Psi_k^\tau)} + \sum_i^{p(\Psi_k^\tau)} \sum_j^{p(\Psi_k^\tau)} - 2 \sum_i^{h(\Psi_k^\tau)} \sum_j^{p(\Psi_k^\tau)} \right] \langle i\tau, j\tau | \hat{V} | \widetilde{i\tau, j\tau} \rangle \\
&+ \frac{1}{2} \sum_{\tau \neq \tau'=p,n} \left[\sum_i^{h(\Psi_k^\tau)} \sum_j^{h(\Psi_l^{\tau'})} + \sum_i^{p(\Psi_k^\tau)} \sum_j^{p(\Psi_l^{\tau'})} - 2 \sum_i^{h(\Psi_k^\tau)} \sum_j^{p(\Psi_l^{\tau'})} \right] \langle i\tau, j\tau' | \hat{V} | \widetilde{i\tau, j}\tau' \rangle ,
\end{aligned}
\tag{5.47}
$$

where the summations $\sum_i^{h(\Psi_k^\tau)} (\sum_i^{p(\Psi_k^\tau)})$ are taken over all hole (particle) states of with respect to the quasi-vacuum.

Since the average of the residual interaction is equal to zero in the non-correlated state $|\Psi_0^\tau \otimes \Psi_0^{\tau'}\rangle$, the diagonal matrix element of (5.7) can be written as (taking into

account Eqs. (5.46, 5.47)):

$$
\begin{aligned}
H_{II} &= H_{00} + \sum_{\tau=p,n} E^{I\tau}_{\mathrm{p-h}} \\
&+ \frac{1}{2} \sum_{\tau=p,n} \left[\sum_i^{\mathrm{h}(\Psi^\tau_k)} \sum_j^{\mathrm{h}(\Psi^\tau_k)} + \sum_i^{\mathrm{p}(\Psi^\tau_k)} \sum_j^{\mathrm{p}(\Psi^\tau_k)} -2 \sum_i^{\mathrm{h}(\Psi^\tau_k)} \sum_j^{\mathrm{p}(\Psi^\tau_k)} \right] \langle i\tau, j\tau | \hat{V} | \widetilde{i\tau, j}\tau \rangle \\
&+ \frac{1}{2} \sum_{\tau\neq\tau'=p,n} \left[\sum_i^{\mathrm{h}(\Psi^\tau_k)} \sum_j^{\mathrm{h}(\Psi^{\tau'}_l)} + \sum_i^{\mathrm{p}(\Psi^\tau_k)} \sum_j^{\mathrm{p}(\Psi^{\tau'}_l)} -2 \sum_i^{\mathrm{h}(\Psi^\tau_k)} \sum_j^{\mathrm{p}(\Psi^{\tau'}_l)} \right] \langle i\tau, j\tau' | \hat{V} | \widetilde{i\tau, j}\tau' \rangle ,
\end{aligned}
$$

with the constant term $H_{00} = \langle \Psi^\tau_0 \otimes \Psi^{\tau'}_0 | \hat{H} | \Psi^\tau_0 \otimes \Psi^{\tau'}_0 \rangle$.

Non-diagonal matrix elements

Let us consider a general matrix element H_{IJ} between different many-body states. It is seen from Eq. (5.45) that only the residual interaction contributes to the matrix element in such a case. Since $\hat{V}_{\mathrm{res}}$ comprises one and two-body operators, we must consider the following cases: $|\Psi_I\rangle$ deviates from $|\Psi_J\rangle$ by one nucleon (one proton or one neutron) or by two nucleons (two protons, two neutrons, one proton and one neutron). All other non-diagonal matrix elements are vanishing.

Using the formulae (5.13) and (5.19) of Sec. 5.1.1 as well as the equation (C-36) we find the matrix element in the case when the two many-body configurations differ by one particle of the type τ (up to a phase factor due to the ordering of sp states in $|\Psi_I\rangle$ and $|\Psi_J\rangle$ which is carefully accounted for in the numerical code)

$$
|\Psi_I\rangle = a^\dagger_{\alpha\tau} a_{a\tau} |\Psi_J\rangle , \tag{5.48}
$$

$$
\begin{aligned}
H_{IJ} &= \frac{1}{2} \left[\sum_i^{\mathrm{h}(\Psi^{\tau'}_l)} \sum_j^{\mathrm{h}(\Psi^{\tau'}_l)} + \sum_i^{\mathrm{p}(\Psi^{\tau'}_l)} \sum_j^{\mathrm{p}(\Psi^{\tau'}_l)} -2 \sum_i^{\mathrm{h}(\Psi^{\tau'}_l)} \sum_j^{\mathrm{p}(\Psi^{\tau'}_l)} \right] \langle i\tau', j\tau' | \hat{V} | \widetilde{i\tau', j}\tau' \rangle \\
&+ \left[\sum_i^{\mathrm{p}(\Psi^\tau_k)} - \sum_i^{\mathrm{h}(\Psi^\tau_k)} \right] \langle i\tau, a\tau | \hat{V} | i\tau, \alpha\tau \rangle \\
&+ \frac{1}{2} \left[\sum_i^{\mathrm{p}(\Psi^{\tau'}_l)} - \sum_i^{\mathrm{h}(\Psi^{\tau'}_l)} \right] \langle i\tau', a\tau | \hat{V} | i\tau', \alpha\tau \rangle . \tag{5.49}
\end{aligned}
$$

Next, in the case when we deal with a two-particle two-hole excitation of two particles of different types, we get (up to a similar phase factor)

$$
|\Psi_I\rangle = a^\dagger_{\beta\tau} a^\dagger_{\alpha\tau'} a_{b\tau} a_{a\tau'} |\Psi_J\rangle . \tag{5.50}
$$

Using Eqs. (5.19) and (C-38) one obtains

$$
H_{IJ} = \left[\sum_i^{\mathrm{p}(\Psi^\tau_k)} - \sum_i^{\mathrm{h}(\Psi^\tau_k)} \right] \langle i\tau, b\tau | \hat{V} | \widetilde{i\tau, \beta}\tau \rangle
$$

$$+ \left[\sum_{i}^{\text{p}(\Psi_l^{\tau'})} - \sum_{i}^{\text{h}(\Psi_l^{\tau'})}\right] \langle i\tau', a\tau' | \hat{V} | i\tau', \widetilde{\alpha\tau'} \rangle$$

$$- \frac{1}{2} \langle a\tau', b\tau | \hat{V} | \alpha\tau', \widetilde{\beta\tau} \rangle . \tag{5.51}$$

The last possibility to be taken into account is a two-particle two-hole excitation of two particles of type τ (two neutrons or two protons)

$$|\Psi_I\rangle = a_{\beta\tau}^{\dagger} a_{\alpha\tau}^{\dagger} a_{b\tau} a_{a\tau} |\Psi_J\rangle , \tag{5.52}$$

inserting Eqs. (5.19,5.22) one obtains

$$H_{IJ} = \frac{1}{2} \left[\sum_{i}^{\text{h}(\Psi_l^{\tau'})} \sum_{j}^{\text{h}(\Psi_l^{\tau'})} + \sum_{i}^{\text{p}(\Psi_l^{\tau'})} \sum_{j}^{\text{p}(\Psi_l^{\tau'})} - 2\sum_{i}^{\text{h}(\Psi_l^{\tau'})} \sum_{j}^{\text{p}(\Psi_l^{\tau'})}\right] \langle i\tau', j\tau' | \hat{V} | i\tau', \widetilde{j\tau'} \rangle$$

$$+ \frac{1}{2} \langle a\tau, b\tau | \hat{V} | \widetilde{\beta\tau}, \widetilde{\alpha\tau} \rangle . \tag{5.53}$$

5.3.2   Remarks on the numerical treatment

Residual interaction

As already stated, the SIII parametrization of the Skyrme force used here for calculations is not suited to yield the correct correlation properties in the particle-particle channel. Hence, when treating the pp and nn correlations in the HTDA method, the effective interaction was replaced by a volume δ interaction in actual calculations. In chapter 4 we have shown that some pn superfluidity in BCS(LN) methods can be obtained in terms of $T = 0, J = 1$ and $T = 1, J = 0$ coupling which is the scenario yielded by the application of the contact force to describe two-body interactions between particles moving in time-reversed orbitals. Since we focus here on the pair diffusion phenomenon around the Fermi surface, the BCS results support the choice of a δ force for further investigations with pn correlations included.

In the calculations a substitution

$$\hat{V} \Rightarrow \hat{V}_\delta = V_0^T \delta(\vec{r}_{12}) \Pi^S \Pi^T \tag{5.54}$$

is therefore done for the residual interaction. The operators $\Pi^S \Pi^T$ project onto spin-isospin subspaces (see Eq. (4.11)), V_0^T is an interaction strength to be adjusted. One should bear in mind that the inclusion of pn pairing opens the $T = 0$ channel for correlations and, therefore, another strength parameter $V_0^{T=0}$ in addition to $V_0^{T=1}$ needs to be determined.

The integral formulae for two-body matrix elements of the δ force in all channels are given in Appendix B.

The 0^+ states

To produce a nuclear state of a given Ω^π one needs to couple proton and neutron configurations. The ground state of an even-even nucleus can be obtained as formerly by coupling two unperturbed 0^+ configurations, one for protons and one for neutrons. However, in view of the inclusion of the pn interaction, 0^+ can be as well reproduced by coupling neutron and proton configurations with opposite Ω^π, provided that the relations (5.31) are fulfilled.

Since we intend to consider only pair excitations in addition to the HF vacuum, the correlated wave function contains the following components

- 0p0h Slater determinant state;

- 2p2h states corresponding to like-particle pair excitations, *i.e.* two particles of the same charge placed in Kramers degenerate hole states are promoted to two Kramers degenerate particle orbitals (like-particle, isovector pairing);

- 2p2h states corresponding to proton-neutron pair excitations. Since protons and neutrons may fill the same spatial orbitals, three different kinds of pairs may be formed:

  - pn pairs: one neutron and one proton placed in the same ($\Omega_{in}^\pi = \Omega_{jp}^\pi$) hole states are promoted to two same particle states- the nucleons in these pairs have aligned spins, they may interact via the δ force in the $T = 0$ channel only. Note that such pairs were excluded in the BCS case for the sake of simplicity;

  - $\bar{p}\bar{n}$ pairs: one neutron and one proton placed in the same Kramers degenerate ($-\Omega_{in}^\pi = -\Omega_{jp}^\pi$) hole states are promoted to two same Kramers degenerate particle states ($T = 0$ channel only);

  - $p\bar{n}$ pairs: one neutron and one proton placed in Kramers degenerate ($\Omega_{in}^\pi = -\Omega_{jp}^\pi$) hole states are promoted to two Kramers degenerate particle states ($T = 0$ and $T = 1$ channels);

- 4p4h excitations corresponding to 2 pairs transfers in all channels;

The sketch of the particle-hole excitations considered here is shown in Fig. 5.3.2.

It should be added that the time-reversal symmetry in the calculations with proton-neutron pairs is restored as it was described in Sec. 5.1.1.

5.4   Results: general case of $T = 0$ & $T = 1$ interactions

In what follows we investigate (full) isovector and isoscalar pairing correlations in a space including up to 4p4h excitations of the pair excitation type. Our approach is
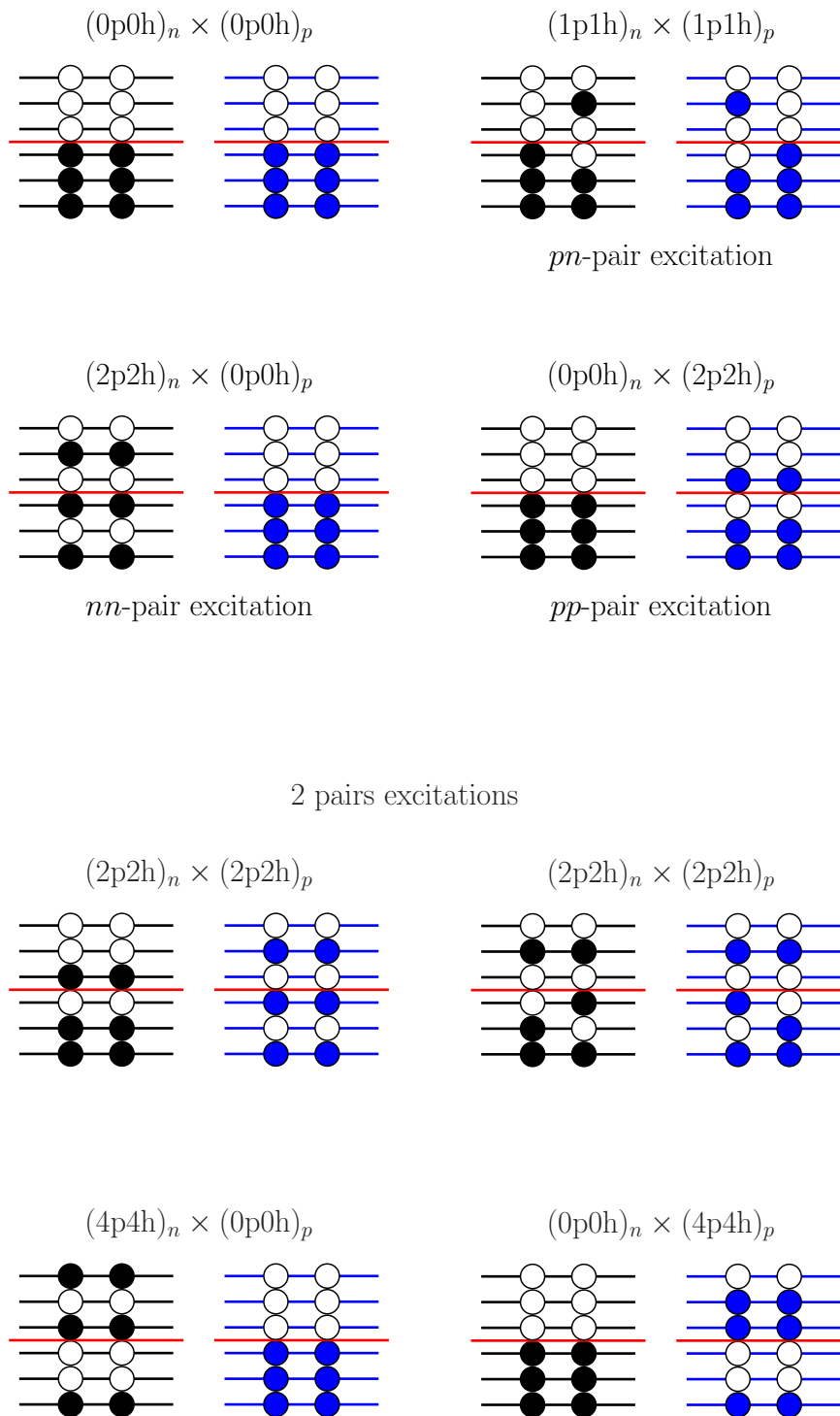
Figure 5.14: Examples of particle-hole excitations considered in this part of the work. The black filled circles represents neutrons, the blue ones protons. Red lines indicate Fermi levels.

phenomenological. Therefore, in principle any change of the configuration space (like embedding proton-neutron pairs) and introducing the full isovector and isoscalar interaction would require a careful study of the basis truncation and the interaction parametrization readjustment once the property of interest is determined. Such applications of our approach in physical problems are reserved for future research. In this preliminary study we investigate the effects of the addition of the proton-neutron pairing in a basis fixed a priori and without fitting from scratch pairing strengths. The behaviour of several quantities as examined in Sec. 5.2 is now analyzed upon varying isoscalar pairing strength treated as a free parameter. This is similar to what has been done in the BCS-type calculations of Sec. 4.4.3. The single-particle configuration space and isovector pairing strength retained here are the same as used before for the isovector ($|T_z| = 1$) case. We impose, as it should be in principle, that all T_z components of the residual interaction in the isovector channel are the same: $V_{0n}^{T=1} = V_{0p}^{T=1} = V_{0pn}^{T=1} = 300 \text{MeV fm}^3$.

In parallel with Sec. 4.4.3 the ratio of two coupling constants $x = V_0^{T=0}/V_0^{T=1}$ is introduced as a tale-telling parameter for further presentation of the results. In the course of the discussion, we will indicate the differences in the Hamiltonian matrix diagonalization as resulting from the use of various particle-hole spaces. Possible analogies or contradictions to the BCS(LN) results will be pointed out.

5.4.1 Decomposition of the correlated wave function

In our discussion of the many-body basis truncation in the case of like particle pairing it was concluded that even though the role of 2 pair excitations is minor in terms of the probability for a nuclear system to be found in such a state, their presence enhances the 1 pair content and has a significant impact on the correlation energy. Table 5.10 displays, for the case of merely one nucleus (^{64}Ge) the percentage of vacuum and paired components as obtained in the calculations in 1 pair and 1 and 2 pairs excitation spaces for several values of x. The boost of the 1 pair content is observed independently on the x value, however the effect is less spectacular than in the previous section. The 2 pair content remains small up to $x = 2$ value. For $x = 2.25$ the probability of 2p2h and 4p4h components becomes equal. It is seen that the majority of the 2 pair excitation percentage belongs to its $\Psi_2^n \otimes \Psi_2^p$ (22) part. It was argued [161] that for two kinds of particles in the same shell the fundamental correlations are α-cluster-like which may be manifested here.

In addition to Table 5.10 the correlation energies obtained as a function of x in the calculations done in the 1 pair excitation space (1 pair) and then in a more complete (2 pairs) particle-hole excitation space are shown in Fig. 5.15 for the $N = Z$ nucleus. Two cases are distinguished: calculations limited to the isoscalar part of the residual interaction ($T = 0$) and with the full pairing interaction ($T = 0$&$T = 1$). As seen, the two $T = 0$ curves are indistiguishable till $x \sim 2$. In the same range of residual interaction intensities the shift between the results obtained with the full residual

Table 5.10: Percentage of various components of the correlated wave function with varying x value for ^{64}Ge. Results of two calculations are reported: with 1 pair excitations added to the vacuum and with 1 and 2 pairs included. The numbers in parenthesis give a detailed percentage for each type of excitations: 20-one neutron pair, 11-one proton-neutron pair, 02-one proton pair, 40-two neutron pairs, 31-one neutron plus one proton-neutron pairs, 22-two proton-neutron pairs, 13-one proton-neutron and one proton pairs, 04-two proton pairs excitations.

x	0p0h	1 pair	(20	11	02)	2 pairs	(40	31	22	13	04)
0.5	73.0	27.0	(13.0	3.0	11.0)	–			–		
	64.0	34.5	(17.0	3.0	14.5)	1.5	(0.7	0.0	0.0	0.0	0.6)
1.0	75.0	25.0	(11.0	3.0	10.0)	–			–		
	67.0	32.0	(16.0	3.0	13.0)	1.0	(0.6	0.0	0.0	0.0	0.4)
2.0	75.5	24.5	(8.5	8.0	8.0)	–			–		
	67.5	29.5	(11.0	9.0	9.5)	3.0	(0.4	0.1	2.1	0.1	0.3)
2.25	75.3	24.7	(8.2	9.0	7.5)	–			–		
	52.0	24.0	(9.0	8.0	7.0)	24.0	(0.4	0.0	23.0	0.0	0.4)

interaction is constant and may come from neglecting 2 pairs excitations of nn and pp types. The rapid growth of the energy difference beyond a certain $T = 0$ interaction strength value ($x \sim 2.25$) suggests a $T = 0$ collectivity emerge there.

In Fig. 5.16 the interplay of different types of particle-hole excitations as functions of x is exhibited for all (four) studied germanium isotopes. On the left side of the figure the total percentage of the vacuum, 1 pair and 2 pair excitations content is shown. As can be seen, in $N = 30$, $N = 34$ and $N = 36$ nuclei the percentage of the vacuum is slightly increasing when the $T = 0$ interaction becomes stronger, at the same time the 2p2h element is reduced. The tiny percentage of 4p4h excitations remains almost unchanged with varying x value. For the $N = Z$ isotope with x larger than 2, the probability of the vacuum component is diminished and the 2 pair content starts playing a significant role. On the right side of the Figure (in different scale) the various components of the 1 pair content are displayed: proton-neutron (11), neutron (20) and proton (02) pairs excitations are distinguished. As could be expected, the probability of the pn pair excitation is the least in the $N = Z + 4$ nucleus and in the other cases becomes nearly equal to that of pp or nn pair excitations for $x \sim 2$ value.

It is worth noting here two analogies with the BCS(LN) results obtained in this work. First, the $x \sim 2$ value beyond which the proton-neutron pair excitation probability becomes comparable to that of like-pairs excitations fits nicely with the one where non-trivial proton-neutron pairing solutions were found in the quasiparticle approach. Second, the probability of proton-neutron pair excitation in the ^{68}Ge
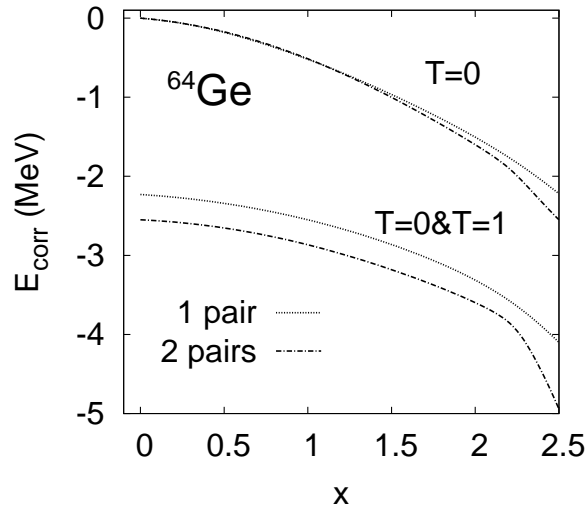
Figure 5.15: Correlation energy obtained in the calculation with 2p2h (1 pair) and 4p4h (2 pairs) spaces of pairs excitations. The results concern the case limited to the isoscalar pairing interaction ($T = 0$) and the case of the full residual interaction ($T = 0$&$T = 1$).

nucleus is found here to be negligible and similarily, it is worth noting that no superfluid solution was found in this nucleus in the BCS(LN) method. This is however no longer the case of $N = 30$ where pn-pairing seems to play a role in the HTDA approach but was no observed in the BCS(LN) calculations.

In spite of the above mentionned nice confirmations of the BCS(LN) results, they should be taken with a grain of salt. First of all, for general reasons the BCS(LN) approach is specifically shaky in the region under scrutiny (low correlation regime for some wave function components). Moreover, the HTDA space of particle-hole excitations is quite restricted. The sufficiency of the 4p4h space in the case of two decoupled problems does not imply that it should automatically be valid in a more general case as here. We have shown in Ref. [162] that even in the space restricted in all channels to 1 pair excitations a visible gain in energy is obtained due to the $T = 0$ pairing and that the HTDA framework is fruitful in investigating pairing correlations in the regions where phase transitions take place in the BCS calculations. The numbers of Table 5.10 suggest however that a proper description of $T = 0$ collective phenomena may demand multi-pair excitations and that this issue stands in need of further investigation. Nevertheless, even at this stage of the work sound conclusions concerning the proton-neutron HTDA approach may be drawn.

We will briefly study, below, the respective role of pn and $\bar{p}\bar{n}$ pairs. In the BCS theory presented in Chapter 4 and actual calculations of Sec. 4 the proton-neutron pairs between particles moving in the same spin-space orbitals were excluded. Such a limitation allowed for a simplification of the quasiparticle transformation and further
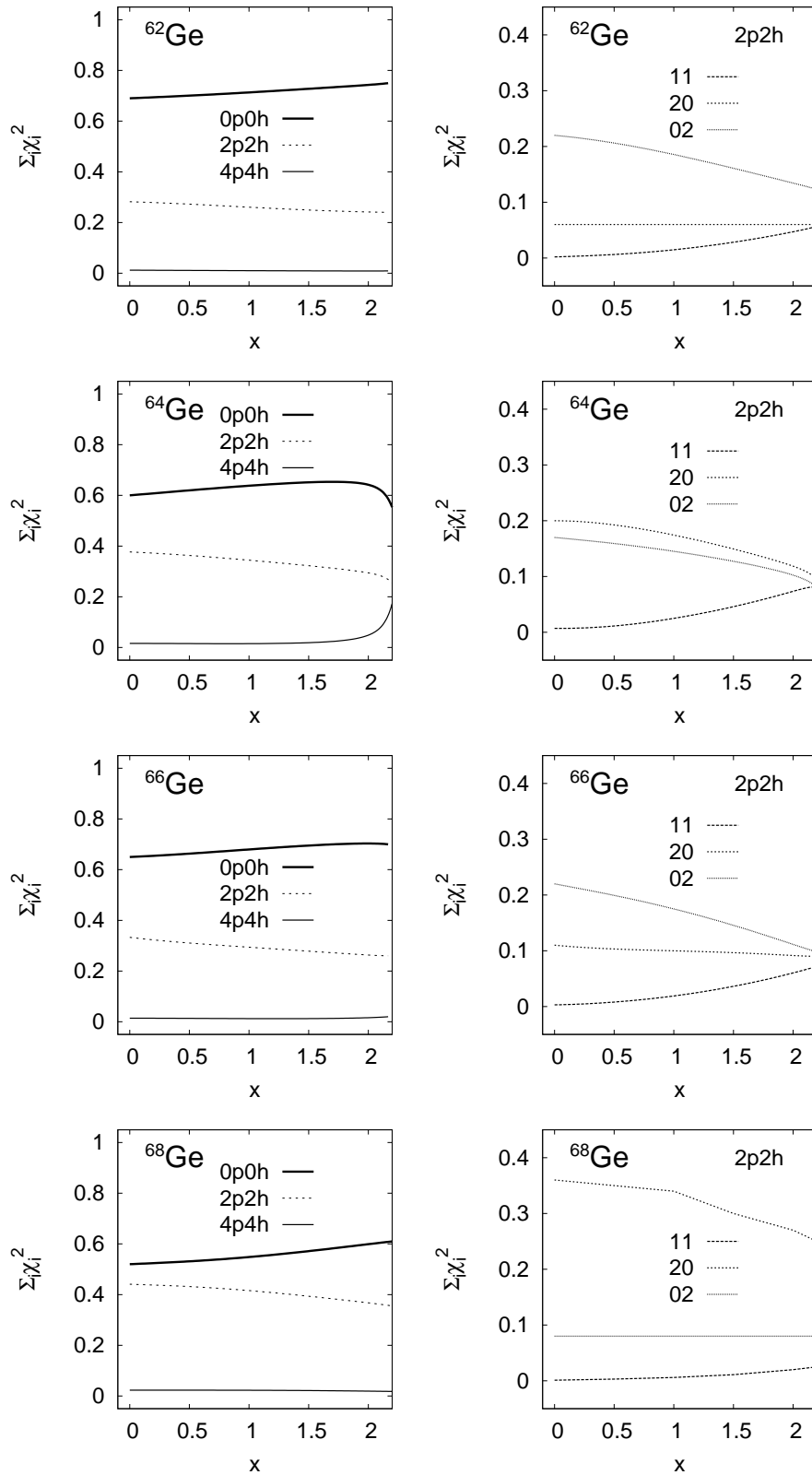
Figure 5.16: Probability of different components in the correlated GS wave function vs x value for studied nuclei. The left side of the figure shows the probability of vacuum (0p0h), 1 pair (2p2h) and 2 pair excitations (4p4h) components. On the right hand side the decomposition of the 2p2h content into proton-neutron (11), neutron (20) and proton (02) pair excitations cases is exhibited. Note different scales of right and left graphs.
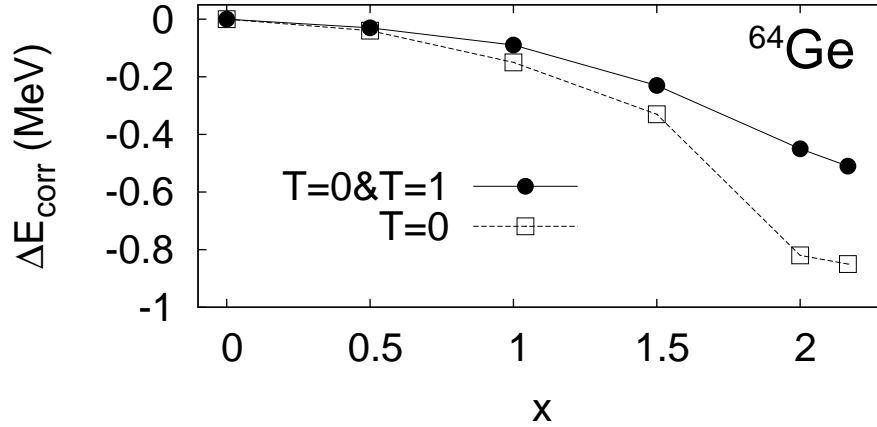
Figure 5.17: Differences in the correlation energies obtained in the complete configuration space and without pn and $\bar{p}\bar{n}$ pairs in calculations with isoscalar (squares) and full pairing interactions (circles).

calculations and was supported by the HFB results of Ref. [11] where such pairs were argued to play a negligible role in axial, non-rotating nuclei.

The easiness of both the HTDA formalism and numerical realisation of particle-hole basis construction has opened the possibility of embedding such pairs without much effort and thus to investigate their role in building correlations. The number of such pairs is of course much smaller than the number of pairs of particles moving in time-reversed orbitals and consequently of minor importance as compared to the total basis size.

In Fig. 5.17 the discrepancies in the correlation energy calculated with all possible pairs and without pn and $\bar{p}\bar{n}$ pairs are shown. Circles mark calculations with the full isovector and isoscalar pairing while the limiting case of the isoscalar pairing is denoted with squares. In both cases the difference is sizable for larger x values.

Let us also study as an example one particular ground state wave function decomposition. For the sake of transparency we will limit ourselves merely to the $T = 0$ interaction case. It is found that the components with the largest probability beyond the vacuum include sizable (if not dominant) pn-pair contributions. For instance, at $x = 2$, we obtain the following decomposition of the ^{64}Ge ground state:

$$
\begin{aligned}
|\Psi\rangle = {} & 0.81\,0p0h \\
& + 0.025(1\mathrm{p}_1)_n(1\mathrm{p}_{\bar{1}})_p(1\mathrm{h}_{15})_n(1\mathrm{h}_{\overline{15}})_p \\
& + 0.025(1\mathrm{p}_{\bar{1}})_n(1\mathrm{p}_1)_p(1\mathrm{h}_{\overline{15}})_n(1\mathrm{h}_{15})_p \\
& + 0.021(1\mathrm{p}_5)_n(1\mathrm{p}_3)_p(1\mathrm{h}_{15})_n(1\mathrm{h}_{15})_p \\
& + 0.021(1\mathrm{p}_{\bar{5}})_n(1\mathrm{p}_{\bar{3}})_p(1\mathrm{h}_{\overline{15}})_n(1\mathrm{h}_{\overline{15}})_p \\
& + 0.005(1\mathrm{p}_5)_n(1\mathrm{p}_3)_p(1\mathrm{h}_{13})_n(1\mathrm{h}_{13})_p \\
& + 0.005(1\mathrm{p}_{\bar{5}})_n(1\mathrm{p}_{\bar{3}})_p(1\mathrm{h}_{\overline{13}})_n(1\mathrm{h}_{\overline{13}})_p + \cdots,
\end{aligned}
$$

<div align="right">(5.55)</div>

where the numbers determining the configuration type correspond to the indices of single-particle levels of Table 5.7 and bars indicate time-reversed states.

5.4.2 Correlation energy

Let us now investigate in more detail the behaviour of the correlation energy upon increasing of the isoscalar pairing interaction strength.

In Fig. 5.18 the dependence of the correlation energy on x is compared for the $T = 0$ as well as for the $T = 0$ and $T = 1$ cases.[1] A constant increase of the two plotted correlation energies (absolute values) is observed. Furthermore, the slopes of the energy curves are shown to differ considerably as a function of T_z. The gain in energy due to the occurence of the proton-nutron coupling concerns the whole range of the isoscalar pairing strength which is opposite to BCS(LN) results where no pn pairing gap, and therefore no energy due to the pn pairing, emerged below some critical value $x \sim 2$. Another point of difference is that in the BCS(LN) approach no collective pn solution was found for $N = 30, 36$ isotopes. Here, even if no $T = 0$ collectivity occurs, the $T = 0$ part of the residual interaction contributes in a distinguishable way to the ground state energy of these systems.

Discussing the yield in energy due to the isoscalar pairing one is tempted to revisit the problem of the Wigner term. In Sec. 4.4.3 we have shown that a kind of the Wigner cusp emerges in the BCS(LN) calculations due to the isoscalar pairing, however the gain in energy is rather modest. The situation found here is quite analogous: the correlation energy increases due to the isoscalar pairing contribution with magnitudes dependent on the $|N - Z|$ difference. It suggests that a kind of the Wigner cusp can be obtained in the present calculations with the $T = 0$ pairing. Indeed, the energy modifications are the largest for the $N = Z$ system which is shown in Fig. 5.19 where the difference of the ground state HTDA energies $\Delta E = E(V_0^{T=0} \neq 0) - E(V_0^{T=0} = 0)$ are plotted. The scale of the Figure is the same as that of Fig. 4.15 displaying the results obtained in the BCS(LN) case. The similarity of the two plots is conspicious. However, the energy shifts between neighbouring nuclei and ΔE values for a given x in two methods are different. From the comparison of the two plots it may be concluded that the behaviour of the BCS(LN) results depend much stronger on the $T = 0$ strength while the HTDA, as expected, provides far more stable picture of pairing correlations. The inclusion of the $T = 0$ pairing in the HTDA method leads to an extra stability of the $N = Z$

---

[1]Note that the configuration space is limited here to 4p4h excitations which means the 8p8h component resulting from coupling of neutron and proton Slater determinants $\Psi_4^n \otimes \Psi_4^p$ has been neglected. Thus in the limit of no pn coupling ($V_{0pn}^{T=1} = V_{0pn}^{T=0} = 0$) the correlation energy is not equal to the sum of neutron and proton correlation energies of two separate calculations $E_{\text{corr}} \neq E_{\text{corr}}^n + E_{\text{corr}}^p$. Therefore, direct comparisons of values from Sec. 5.2 with those obtained here should not be done.
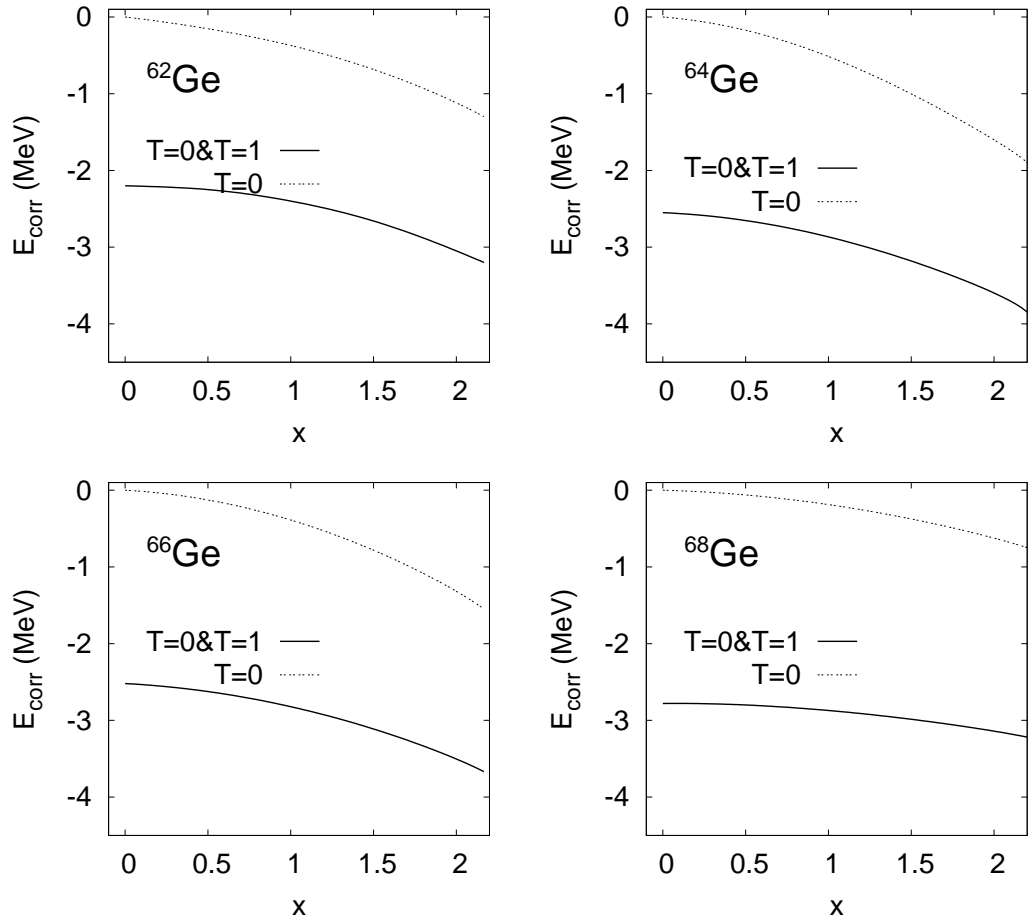
Figure 5.18: Correlation energy vs the isoscalar and isovector pairing strengths ratio x in $N \sim Z$ Ge isotopes. The cases of barely isoscalar interaction ($T = 0$) and full pairing interaction ($T = 0$&$T = 1$) are distinguished.
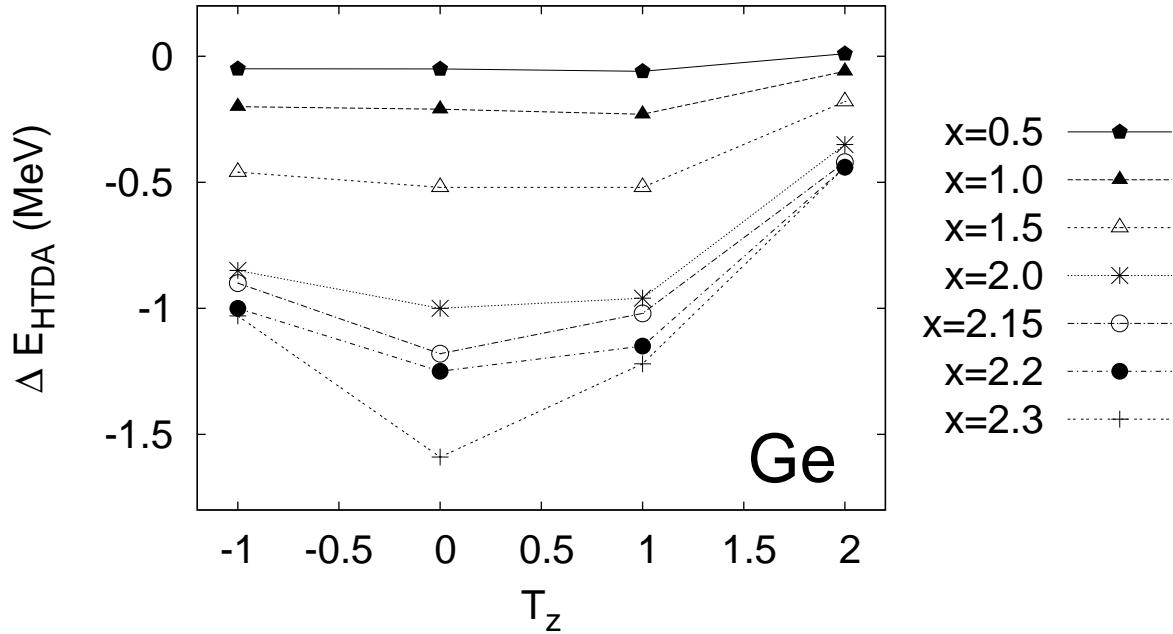
Figure 5.19: Normalized ground state energy ($\Delta E = E(V_0^{T=0} \neq 0) - E(V_0^{T=0} = 0)$) as a function of the reduced isospin $T_z = (N - Z)/2$ for various values of the $T = 0$ and $T = 1$ pairing strengths ratio x obtained in the HTDA approach.

system but it is likely other types of correlations, not included here, should appear necessary to obtain the experimentally observed spike in the isobaric mass parabola.

5.4.3   Summary

In the present section we have applied the HTDA formalism to evaluate pairing correlations upon using isovector and isoscalar residual interactions. Our main emphasis was to study the basic features of proton-neutron correlations in this novel approach and confronting them with the standard treatments based on the BCS method. It was shown that the qualitative behaviour of the energies obtained in the two approaches is similar however the $T = 0$ part of the residual give rise to an additional binding for all studied nuclei and for all x values in the HTDA method whereas BCS(LN) calculations do not. The presence of the isoscalar pairing in the HTDA method leads to a spike in the binding energy in the vicinity of the $N = Z$ nucleus.

The HTDA results confirm the crucial role of the particle number conservation in the description of proton-neutron correlations. However, the point of the role of multi-pair excitations in the description of the $T = 0$ superfluidity in the HTDA method needs to be explored in further studies.

Chapter 6

Summary and perspectives for future research

The central attention of the presented dissertation was focused on the investigation of the correlations beyond the mean-field, especially the proton-neutron pairing which is now extensively studied both experimentally and theoretically. In the present work two different approaches to pairing correlations were exploited. First, the customary BCS treatment was generalized to take into account proton-neutron pairs in time-reversed orbitals in the case of a state-dependent pairing interaction. Of course the generalizations of the independent quasiparticle theory have already a long history, nevertheless most of the calculations so far were carried out only with schematic pairing forces. Similarly, based on the existing work concerning the Lipkin-Nogami method we improved our BCS approach with *pn* pairing by the approximate particle number projection of this type. In the second part of the work a novel approach to correlations, known as the Higher Tamm-Dancoff Approximation, was studied in both like-particle pairing and proton-neutron pairing contexts. Such questions like the role of the particle number conservation in the studies of the proton-neutron pairing, the possibility of the existence of the $T = 0$ collectivity and the origin of the Wigner energy were referred to while discussing consecutive methods applied and developed in this work.

The detailed conclusions that may be derived from investigations of $N \sim Z$ Ge isotopes were already written down in the summaries of each chapter. The main issues may be shortly outlined as follows. First, we have shown that the extension of the nuclear pairing interaction by adding a space-odd component to the δ force does not influence considerably the picture obtained with the single δ force, thus the rest of the calculations were performed in terms of $T = 0, J = 1$ and $T = 1, J = 0$ couplings. The results of the generalized BCS and LN calculations with the state-dependent force turned out to be qualitatively comparable to the results of other authors obtained in BCS(LN) and HFB approaches with schematic pairing interactions. However, the phase transition from $T = 1$ to $T = 0$ mode is less sharp when using a state-dependent force. No coexistence of the *pn* pairing in $T = 0$ and

$T = 1$ channels was found while the like-particle and the $T = 0$ modes coexistence was obtained. The calculations with the approximate particle number projection have shown that the restoration of the particle number symmetry is crucial for the description of pairing correlations in $N = Z$ nuclei for which in the BCS picture the competition of different pairing phases leads to the already mentioned normal-superfluid transitions.

The investigations of the proton-neutron pairing in the HTDA framework were prefaced with the applications of the formalism in the case of protons and neutrons treated as separate systems. It was shown that in the simple basis of the particle-hole excitations of the 2 pair excitation type, with the δ force used for the residual interaction, the ground state and superfluid properties of the studied nuclei can be reproduced. The fingerprints of the $T = 0$ superfluidity in the HTDA method appeared to be very similar as in the BCS(LN) approaches. It seems that the $T = 0$ superfluidity occurs in both methods above some critical value of the isoscalar interaction strength but the HTDA method is effective as well in the low pairing regimes which is not the case of BCS or even Lipkin-Nogami approaches. The inclusion of the $T = 0$ pairing lead to the appearance of the extra binding in the vicinity of the $N = Z$ nucleus which may be recognized as a contribution to the Wigner cusp, however the relative energy gains in the two methods are substantially different.

The presented study, especially when it deals with the HTDA framework, is far from being complete. Further investigations and embedding other types of particle-hole excitations in the numerical code may be in order to describe properly the proton-neutron collectivity or at least, to judge their role in this aspect. It is of course unclear what impact on all the results of this work might have broken symmetries, *i.e.* breaking of the angular momentum symmetry and spurious (due to the BCS approximation) contributions to the breaking of the isospin symmetry. In fact those are current difficulties encountered in mean-field approaches and most of the calculations carried out on extensive scale suffer from both or at least one of these symmetries non-conservation.

Despite its possible drawbacks, the HTDA formalism provides a possibility to be applied in many interesting aspects of nuclear physics. From the opposite point of view, they may be a robust test for the presented theory. The HTDA method was already applied to examine the K-isomerism in the ^{178}Hf nucleus. The discussion of isomeric and superdeformed states in $N \sim Z$ even-even nuclei can be relatively easily entered within the already developed formalism.

Another important issue is the investigation of the high spin states. It is well known that the usual cranked HFB formalism does not "see" the proton-neutron pairing and is not very efficient in the low pairing regime which leads to the discrepancies in the measured and calculated yrast bands. As we mentioned, the treatment of pairing correlations in high spins in the Routhian-HTDA method was already undertaken. Since the rotation has a different impact on like-particle and proton-

neutron pairs, it may be judicious to enrich the RHTDA by including the proton-neutron coupling.

A great challenge for the HTDA theory would be its application in the β and $\beta\beta$-decay problems, since it requires a precise knowledge of the ground and several excited states of the parent and granddaughter nuclei, both even-even, plus a detailed description of the intermediate odd-odd nucleus. While first attempts to describe odd nuclei in the HTDA method already have been done, they wait for further development.

Appendix A

Definitions and notations

A.1 Axially symmetrical harmonic oscillator basis

The Hamiltonian of an axially deformed harmonic oscillator in the cylindrical coordinates read

$$\hat{H}_{\text{axial}} = \frac{\hbar^2}{2m}\Delta + \frac{1}{2}m\left(\omega_z^2 z^2 + \omega_\perp^2 r^2\right).$$ (A-1)

Let us define auxiliary (stretched) variables η, ξ related to r and z as

$$\xi = zc_z \qquad c_z = \sqrt{\frac{m\omega_z}{\hbar}}$$

$$\eta = \rho^2 c_\perp^2 \qquad c_\perp = \sqrt{\frac{m\omega_\perp}{\hbar}},$$ (A-2)

where $\rho^2 = x^2 + y^2$. We have

$$r^2 = x^2 + y^2 + z^2 = \frac{\eta}{c_\perp^2} + \frac{\xi^2}{c_z^2}$$ (A-3)

therefore the volume element in the stretched coordinates is given by

$$2\pi\rho\mathrm{d}\rho\mathrm{d}z = \pi\mathrm{d}\frac{\eta}{c_\perp^2}\mathrm{d}\frac{\xi}{c_z} = \frac{\pi}{c_\perp^2 c_z}\mathrm{d}\eta\mathrm{d}\xi.$$ (A-4)

Introducing auxiliary variables one can express the eigenfunctions of the Hamiltonian (A-1) as a product of three functions

$$\psi_{n_r}^\Lambda(\eta)\psi_{n_z}(\xi)\psi_\Lambda(\varphi),$$ (A-5)

where the three quantum numbers: n_r (number of nodes into the r direction), n_z (number of nodes into the z direction) and Λ (projection on the z axis of the orbital angular momentum) are sufficient to characterize an eigenstate of (A-1). The

components of (A-5) are given by

$$
\begin{aligned}
\psi_{n_r}^\Lambda(\eta) &= \sqrt{2}N_{n_r}^\Lambda c_\perp \eta^{|\Lambda|/2} e^{-\eta/2} L_{n_r}^{|\Lambda|}(\eta) \\
\psi_{n_z}(\xi) &= N_{n_z}\sqrt{c_z}e^{-\xi^2/2}H_{n_z}(\xi) \\
\psi_\Lambda(\varphi) &= \frac{1}{\sqrt{2\pi}}e^{i\Lambda\varphi},
\end{aligned}
\tag{A-6}
$$

where H_{n_z} and $L_{n_r}^{|\Lambda|}$ are the Hermite and Laguerre polynomials respectively and the normalization constants $N_{n_r}^\Lambda$, N_{n_z} are defined as

$$
N_{n_r}^\Lambda = \left[\frac{n_r!}{(n_r + |\Lambda|)!}\right]^{1/2} \qquad N_{n_z} = \left[\sqrt{\pi}2^{n_z}n_z!\right]^{-1/2}.
\tag{A-7}
$$

A.2 Hartree-Fock single-particle states

In the case of axially-deformed even-even nuclei considered in this work the third component J_z of the total angular momentum is a good quantum number for a single-particle state Φ_i. In other words if we denote by Ω_i the eigenvalue of J_z associated with the single-particle state $|i\rangle = |n_r, n_z, \Lambda, \Sigma\rangle$ the wave function has the form

$$
\Phi_i = \Phi_i^+|+\rangle + \Phi_i^-|-\rangle = f_i^+ e^{i\Lambda^-\varphi}|+\rangle + f_i^- e^{i\Lambda^+\varphi}|-\rangle,
\tag{A-8}
$$

where

$$
\Lambda^\pm = \Omega_i \pm \frac{1}{2}
\tag{A-9}
$$

and f^+, f^- spatial functions depend only on the absolute value of Λ. The spinor components $\Phi_i^\pm$ can be written explicitely as

$$
\Phi_i^\pm = \left[\frac{c_z c_\perp^2}{2\pi}e^{-(\xi^2+\eta)}\right]^{1/2} \sum_\alpha C_\alpha^i e^{i\Lambda^\pm\varphi}\eta^{|\Lambda|/2}H_{n_z}(\xi)L_{n_r}^{|\Lambda|}(\eta).
\tag{A-10}
$$

Due to the time-reversal invariance we may consider in the HF calculations only the states with positive Ω_i values. The time-reversed states $|\bar{i}\rangle$ ($\Omega_i < 0$) belonging to the same eigenvalues e_i, are obtained by acting on $|i\rangle$ with the time-reversal operator

$$
\hat{T} = -i\sigma_y K,
\tag{A-11}
$$

where K denotes the complex conjugation operator. The time-reversed partner of (A-8) has then the form

$$
\bar{\Phi}_i = \Phi^{-\star}|+\rangle - \Phi^{+\star}|-\rangle = f_i^- e^{-i\Lambda^+\varphi}|+\rangle - f_i^+ e^{-i\Lambda^-\varphi}|-\rangle.
\tag{A-12}
$$

A.3 Gradient operator in cylindrical coordinates

The components of the gradient operator $\vec{\nabla} = (\nabla_r, \nabla_z, \nabla_\varphi)$ in cylindrical coordinates are given by

$$\nabla_r = \frac{\partial}{\partial r}, \quad \nabla_z = \frac{\partial}{\partial z}, \quad \nabla_\varphi = \frac{1}{r}\frac{\partial}{\partial \varphi} = \frac{i\hat{l}_z}{r}, \tag{A-13}$$

where $\hat{l}_z$ is the operator of the projection of the angular momentum. Acting with operators (A-13) on the spinor components (A-10) one obtains

$$
\begin{aligned}
\nabla_r \Phi_i^\pm &= \left[\frac{c_z c_\perp^4}{2\pi} e^{-(\xi^2+\eta)}\right]^{1/2} \sum_\alpha C_\alpha^i e^{i\Lambda^\pm \varphi} \eta^{(|\Lambda|-1)/2} H_{n_z}(\xi) \bar{L}_{n_r}^{|\Lambda|}(\eta) \\
\nabla_z \Phi_i^\pm &= \left[\frac{c_z^3 c_\perp^2}{2\pi} e^{-(\xi^2+\eta)}\right]^{1/2} \sum_\alpha C_\alpha^i e^{i\Lambda^\pm \varphi} \eta^{(|\Lambda|)/2} \bar{H}_{n_z}(\xi) L_{n_r}^{|\Lambda|}(\eta) \\
\nabla_\varphi \Phi_i^\pm &= i\left[\frac{c_z c_\perp^4}{2\pi} e^{-(\xi^2+\eta)}\right]^{1/2} \sum_\alpha C_\alpha^i e^{i\Lambda^\pm \phi} \Lambda \eta^{(|\Lambda|-1)/2} H_{n_z}(\xi) L_{n_r}^{|\Lambda|}(\eta).
\end{aligned}
\tag{A-14}
$$

Using the expressions for the derivatives of the Hermite and associated Laguerre polynomials and their recursion formulae one finds that

$$
\begin{aligned}
\bar{H}_{n_z}(\xi) &= \xi H_{n_z}(\xi) - H_{n_z+1}(\xi) \\
\bar{L}_{n_r}^{|\Lambda|}(\eta) &= 2(n_r+1)L_{n_r+1}^{|\Lambda|}(\eta) - (2n_r + \Lambda + 2 - \eta)L_{n_r}^{|\Lambda|}(\eta).
\end{aligned}
\tag{A-15}
$$

Appendix B

Two-body matrix elements

In the following we consider antisymmetrized matrix elements of the two-body interaction between like particles as well as between protons and neutrons. The residual interaction we take in the form (Eq. (4.8), Sec. 4.1)

$$
\begin{aligned}
\hat{V}_{12} &= \hat{V}_\delta + \hat{V}_{\boldsymbol{k}'\delta\boldsymbol{k}} \\
&= \sum_T V_{0\tau}^T [\delta(\vec{r}_{12}) + \mathrm{x}\boldsymbol{k}'\delta(\vec{r}_{12})\boldsymbol{k}]\Pi^S\Pi^T,
\end{aligned} \tag{B-1}
$$

where

$$
\boldsymbol{k}'\delta(\vec{r}_{12})\boldsymbol{k} = \frac{-1}{2i}(\overleftarrow{\nabla}_1 - \overleftarrow{\nabla}_2)\delta(\vec{r}_1 - \vec{r}_2)\frac{1}{2i}(\overrightarrow{\nabla}_1 - \overrightarrow{\nabla}_2), \tag{B-2}
$$

$V_{0\tau}^T, \mathrm{x}$ determine the strength of the interaction and Π^S, Π^T are the operators projecting onto spin-isospin subspaces (4.11).

B.1 Integral formulae for two-body matrix elements

B.1.1 $\delta(\vec{r}_{12})$ force

First, consider the δ part of the above interaction

$$
\hat{V}_\delta = \sum_T V_{0\tau}^T \delta(\vec{r}_{12})\Pi^S\Pi^T . \tag{B-3}
$$

Due to the properties of the force, which is effective only when two particles are in contact $(\vec{r}_1 = \vec{r}_2)$ and the requirement that the wave function of two fermions needs to be antisymmetric, we need to consider only the cases: $S = 0$, $T = 1$ channel, for both like-particle and proton-neutron interaction and $S = 1$, $T = 0$ channel for the proton-neutron coupling.

T=1, L=0, S=0 channel

The antisymmetrized matrix element of (B-3) between like-particle states read

$$
\langle ab|\hat{V}_\delta|\widetilde{cd}\rangle = \langle ab|\hat{V}_\delta|cd - dc\rangle
$$

$$
\begin{aligned}
&= \frac{V_{0\tau}^T}{2}\langle ab|(1-P^\sigma)(1-P^M P^\sigma P^\tau)\delta(\vec{r}_{12})|cd\rangle \\
&= \frac{V_{0\tau}^T}{2}\langle ab|\delta(\vec{r}_{12})(1-P^\sigma)^2|cd\rangle \\
&= V_{0\tau}^T\langle ab|\delta(\vec{r}_{12})(1-P^\sigma)|cd\rangle \\
&= V_{0\tau}^T\int \mathrm{d}^3 r(\Phi_a^+\Phi_b^- - \Phi_a^-\Phi_b^+)(\Phi_c^+\Phi_d^- - \Phi_c^-\Phi_d^+) \\
&= V_{0\tau}^T\int e^{i(-\Omega_a-\Omega_b+\Omega_c+\Omega_d)\varphi}\mathrm{d}\varphi\int(f_a^+f_b^- - f_a^-f_b^+)(f_c^+f_d^- - f_c^-f_d^+)\mathrm{d}\rho\mathrm{d}z \\
&= \frac{V_{0\tau}^T\pi}{c_z c_\perp^2}\delta_{\Omega_a+\Omega_b,\Omega_c+\Omega_d}\int(f_a^+f_b^- - f_a^-f_b^+)(f_c^+f_d^- - f_c^-f_d^+)\mathrm{d}\eta\mathrm{d}\xi\,, \qquad \text{(B-4)}
\end{aligned}
$$

where a,b,c,d are single-particle states and $\Phi_a,\Phi_b,\Phi_c,\Phi_d$ their corresponding wave functions. The f_a,f_b,f_c,f_d are the spatial functions that depend only on absolute values of Λ.

We have an analogous expression for proton-neutron matrix elements where we denote *e.g.* lowercase for proton and uppercase for neutron states:

$$
\begin{aligned}
\langle aB|\hat{V}_\delta|\widetilde{cD}\rangle = \;\; &= \frac{V_{0\tau}^T}{4}\langle aB|(1-P^\sigma)(1+P^\tau)(1-P^M P^\sigma P^\tau)\delta(\vec{r}_{12})|cD\rangle \\
&= \frac{V_{0\tau}^T}{2}\langle aB|(1-P^\sigma)\delta(\vec{r}_{12})|cD\rangle \\
&= \frac{V_{0\tau}^T}{2}\int \mathrm{d}^3 r(\Phi_a^+\Phi_B^- - \Phi_a^-\Phi_B^+)(\Phi_c^+\Phi_D^- - \Phi_c^-\Phi_D^+) \\
&= \frac{V_{0\tau}^T\pi}{2c_z c_\perp^2}\delta_{\Omega_a+\Omega_B,\Omega_c+\Omega_D}\int(f_a^+f_B^- - f_a^-f_B^+)(f_c^+f_D^- - f_c^-f_D^+)\,\mathrm{d}\eta\mathrm{d}\xi\,.
\end{aligned}
$$
$$\text{(B-5)}$$

T=0, L=0, S=1 channel

Similarily we find the expression for proton-neutron two-body matrix elements:

$$
\begin{aligned}
\langle aB|\hat{V}_\delta|\widetilde{cD}\rangle \;=\;\; & \langle aB|V_\delta|cD - Dc\rangle \\
=\;\; & \frac{V_{0\tau}^T}{4}\langle aB|(1+P^\sigma)(1-P^\tau)(1-P^M P^\sigma P^\tau)\delta(\vec{r}_{12})|cD\rangle \\
=\;\; & \frac{V_{0\tau}^T}{2}\langle aB|\delta(\vec{r}_{12})(1+P^\sigma)|cD\rangle \\
=\;\; & \frac{V_{0\tau}^T}{2}\int \mathrm{d}^3 r(\Phi_a^{+\star}\Phi_B^{-\star} + \Phi_a^{-\star}\Phi_B^{+\star})(\Phi_c^+\Phi_D^- + \Phi_c^-\Phi_D^+) \\
+\;\; & \Phi_a^{+\star}\Phi_B^{+\star}\Phi_c^+\Phi_D^+ + \Phi_a^{-\star}\Phi_B^{-\star}\Phi_c^-\Phi_D^- \\
=\;\; & \frac{V_{0\tau}^T\pi}{2c_z c_\perp^2}\delta_{\Omega_a+\Omega_B,\Omega_c+\Omega_D}\int(f_a^+f_B^- + f_a^-f_B^+)(f_c^+f_D^- + f_c^-f_D^+) \\
+\;\; & f_a^+f_B^+f_c^+f_D^+ + f_a^-f_B^-f_c^-f_D^-\,\mathrm{d}\eta\mathrm{d}\xi\,.
\end{aligned}
$$
$$\text{(B-6)}$$

B.1.2 Matrix elements of the $k'\delta(\vec{r}_{12})k$ force

Let us now derive the formulae for two-body matrix elements of the gradient part of the interaction (4.8), that is to say of the interaction

$$\hat{V}_{k'\delta k} = \sum_T \mathrm{x} V_{0\tau}^T k' \delta(\vec{r}_{12}) k \Pi^S \Pi^T \,. \tag{B-7}$$

This force has only space-odd components ($L = 1$), therefore due to the antisymmetrization of the two-nucleon wave function one has to consider $S = 1$, $T = 1$ channel and $S = 0$, $T = 0$ channel.

T=1, L=1, S=1 channel

In the $T = 1$ channel we have three kinds of nucleonic pairs: proton-proton, neutron-neutron and proton-neutron pairs. First, we consider the like-particle matrix elements of (B-7)

$$
\begin{aligned}
\langle ab|\hat{V}_{k'\delta k}|\widetilde{cd}\rangle &= \frac{\mathrm{x}V_{0\tau}^T}{2}\langle ab|k'\delta(\vec{r}_{12})k(1 - P^M P^\tau P^\sigma)(1 + P^\sigma)|cd\rangle \\
&= \frac{\mathrm{x}V_{0\tau}^T}{8}\langle ab|(\overleftarrow{\nabla}_1 - \overleftarrow{\nabla}_2)\delta(\vec{r}_{12})(\overrightarrow{\nabla}_1 - \overrightarrow{\nabla}_2)(1 + P^\sigma)^2|cd\rangle \\
&= \frac{\mathrm{x}V_{0\tau}^T}{4}\langle \nabla_1 ab - a\nabla_2 b|\delta(\vec{r}_{12})(1 + P^\sigma)|\nabla_1 cd - c\nabla_2 d\rangle \\
&= \frac{\mathrm{x}V_{0\tau}^T}{4}\int \mathrm{d}^3 r \sum_{i=r,z,\varphi} \left\{ (\gamma_{(ab)_i}^{+-})^\star \gamma_{(cd)_i}^{+-} + (\gamma_{(ab)_i}^{-+})^\star \gamma_{(cd)_i}^{-+} + (\gamma_{(ab)_i}^{+-})^\star \gamma_{(cd)_i}^{-+} \right. \\
&\quad + \left. (\gamma_{(ab)_i}^{-+})^\star \gamma_{(cd)_i}^{+-} + 2(\gamma_{(ab)_i}^{++})^\star \gamma_{(cd)_i}^{++} + 2(\gamma_{(ab)_i}^{--})^\star \gamma_{(cd)_i}^{--} \right\} \,, \tag{B-8}
\end{aligned}
$$

where

$$
\begin{aligned}
\gamma_{(kl)_i}^{++} &= \nabla_i \Phi_k^+ \Phi_l^+ - \Phi_k^+ \nabla_i \Phi_l^+ \\
\gamma_{(kl)_i}^{--} &= \nabla_i \Phi_k^- \Phi_l^- - \Phi_k^- \nabla_i \Phi_l^- \\
\gamma_{(kl)_i}^{+-} &= \nabla_i \Phi_k^+ \Phi_l^- - \Phi_k^+ \nabla_i \Phi_l^- \\
\gamma_{(kl)_i}^{-+} &= \nabla_i \Phi_k^- \Phi_l^+ - \Phi_k^- \nabla_i \Phi_l^+ \,, \tag{B-9}
\end{aligned}
$$

where index i denotes r, z or φ gradient components. For the proton-neutron part one has an analogous expression in which, as earlier, we denote the lowercase for proton and uppercase for neutron states:

$$
\begin{aligned}
\langle aB|\hat{V}_{k'\delta k}|\widetilde{cD}\rangle &= \frac{\mathrm{x}V_{0\tau}^T}{8}\int \mathrm{d}^3 r \sum_{i=r,z,\varphi} \left\{ (\gamma_{(aB)_i}^{+-})^\star \gamma_{(cD)_i}^{+-} + (\gamma_{(aB)_i}^{-+})^\star \gamma_{(cD)_i}^{-+} + (\gamma_{(aB)_i}^{+-})^\star \gamma_{(cD)_i}^{-+} + \right. \\
&\quad + \left. (\gamma_{(aB)_i}^{-+})^\star \gamma_{(cD)_i}^{+-} + 2(\gamma_{(aB)_i}^{++})^\star \gamma_{(cD)_i}^{++} + 2(\gamma_{(aB)_i}^{--})^\star \gamma_{(cD)_i}^{--} \right\} \,. \tag{B-10}
\end{aligned}
$$

T=0, L=1, S=0 channel

For proton-neutron pairs coupled to $T = 0$ one obtains:

$$
\begin{aligned}
\langle aB|\hat{V}_{\boldsymbol{k}'\delta\boldsymbol{k}}|\widetilde{cD}\rangle &= \frac{\mathrm{x}V_{0\tau}^T}{4}\langle aB|\boldsymbol{k}'\delta(\vec{r}_{12})\boldsymbol{k}(1-P^M P^\tau P^\sigma)(1-P^\sigma)(1-P^\tau)|cD\rangle \\
&= \frac{\mathrm{x}V_{0\tau}^T}{8}\langle aB|(\overleftarrow{\nabla}_1-\overleftarrow{\nabla}_2)\delta(\vec{r}_{12})(\overrightarrow{\nabla}_1-\overrightarrow{\nabla}_2)(1-P^\sigma)|cD\rangle \\
&= \frac{\mathrm{x}V_{0\tau}^T}{8}\int \mathrm{d}^3 r \sum_{i=r,z,\varphi}\left\{(\gamma^{+-}_{(aB)_i})^\star\gamma^{+-}_{(cD)_i}+(\gamma^{-+}_{(aB)_i})^\star\gamma^{-+}_{(cD)_i}\right) \\
&\quad - (\gamma^{+-}_{(aB)_i})^\star\gamma^{-+}_{(cD)_i}-(\gamma^{-+}_{(aB)_i})^\star\gamma^{+-}_{(cD)_i}\Big\}
\end{aligned}
\tag{B-11}
$$

with $\gamma_{(kl)_i}$ defined as in Eq. (B-9).

B.2   Two-body matrix elements in the asymptotic basis

In the following we remind shortly the formulae necessary to calculate the matrix elements of interest in the asymptotic basis. A more detailed presentation of the problem as well as the discussion of the Moshinsky transformation brackets can be found *e.g.* in Refs. [105, 163, 164] and references quoted therein.

B.2.1   Asymptotic basis

The kets of this basis are formed by the eigenvectors of the axially symmetrical oscillator Hamiltonian (A-1) and the third component of the orbital and spin angular momenta. A ket can be labelled

$$
|n_z n_\perp \Lambda \Sigma\rangle\,,
\tag{B-12}
$$

where the number of quanta on x and y axes $n_\perp = 2n_r + |\Lambda|$. There also exist boson operators b_α^+, b_β^+ in such a way that

$$
|n_\perp \Lambda\rangle = |\alpha\beta\rangle = (-1)^\beta (b_\alpha^+)^\alpha (b_\beta^+)^\beta \frac{\sqrt{\alpha!}}{\sqrt{\beta!}}|00\rangle\,,
\tag{B-13}
$$

where

$$
\alpha = \frac{n_\perp + \Lambda}{2} \qquad \beta = \frac{n_\perp - \Lambda}{2}\,.
\tag{B-14}
$$

B.2.2   Matrix elements of the δ force

For the interaction of the form

$$
\hat{V}_{12} = a_0 \delta(\vec{r})\,,
\tag{B-15}
$$

where the coefficient a_0 may be a spin operator of the type $a_i = t_i(1 + x_i P^\sigma)$ one has

$$\langle n|\delta(z)|n'\rangle = \frac{c_z}{\sqrt{2\pi}} A(n)A(n') , \tag{B-16}$$

where

$$A(n) = \delta_{n,\text{even}} \frac{(-1)^{n/2}\sqrt{n!}}{2^{n/2}(n/2)!}$$

$$\delta_{n,\text{even}} = 0(n \text{ odd}) \qquad \delta_{n,\text{even}} = 1(n \text{ even}) . \tag{B-17}$$

For the rest of the wave function ($\vec{x}$ being the projection of $\vec{r}$ on the xOy plane) we have

$$\langle ab|\delta(\vec{x})|a'b'\rangle = \frac{c_\perp^2}{2\pi}\delta_{a,b}\delta_{a',b'} . \tag{B-18}$$

One then deduces (i standing for $\{n_i, \alpha_i, \beta_i, \Sigma_i\}$)

$$\langle 12|a_0\delta(\vec{r})|34\rangle = \frac{a_0 c_0^3}{(2\pi)^{3/2}}\left(\sum_n f^n A(n)A(n')\right)\left(\sum_{a,b} g^{a,b}\delta_{a,b}\delta_{a',b'}\right) \tag{B-19}$$

with

$$f^n \equiv f^n(n_1, n_2, n_3, n_4) = \langle n_1 n_2||nN\rangle\langle n_3 n_4||n'N\rangle \tag{B-20}$$

$$\begin{aligned} g^{a,b} &\equiv g^{a,b}(\alpha_1, \beta_1, \alpha_2, \beta_2, \alpha_3, \beta_3, \alpha_4, \beta_4) \\ &= \langle \alpha_1\alpha_2||aA\rangle\langle\beta_1\beta_2||bB\rangle\langle\alpha_3\alpha_4||a'A\rangle\langle\beta_3\beta_4||b'B\rangle , \end{aligned} \tag{B-21}$$

where $c_0 = c_z c_\perp^2$ is the spherical harmonic oscillator constant. From a given n (resp. a, b) one deduces n', N (resp. a', A and b', B) by means of selection rules for the Moshinsky coefficients. The one dimensional brackets appearing in the formulae above are calculated as

$$\langle n_1 n_2||nN\rangle = \delta_{n_1+n_2,n+N}\sqrt{\frac{n_1! n_2! n! N!}{2^{n_1+n_2}}} \sum_{l=\max(0,n_2-N)}^{\min(n_2,n)} \frac{(-1)^l}{(n_2-l)!(N-n_2+l)!l!(n-l)!} . \tag{B-22}$$

B.2.3 Matrix elements of the $\overleftarrow{\nabla} \delta \overrightarrow{\nabla}$ force

Let us now deal with the interaction

$$\hat{V}_{12} = a_1 \overleftarrow{\nabla} \delta(\vec{r}) \overrightarrow{\nabla} , \tag{B-23}$$

where a_1 as previously may be a spin operator and $\overleftarrow{\nabla}$ acts on the left. The matrix element of (B-23) read

$$\langle 12|a_1 \overleftarrow{\nabla} \delta(\vec{r}) \overrightarrow{\nabla} |34\rangle = \frac{2c_0^3 a_1}{(2\pi)^{3/2}}$$

$$\times \left[c_z^2 \left(\sum_n f^n A(n-1)A(n'-1)\sqrt{n}\sqrt{n'}\right)\left(\sum_{a,b} g^{a,b}\delta_{a,b}\delta_{a',b'}\right) + c_\perp^2 \left(\sum_n f^n A(n)A(n)\right) \right.$$

$$\times \left. \sum_{a,b} g^{a,b}(\sqrt{a+1}\sqrt{a'+1}\delta_{a+1,b}\delta_{a'+1,b'} + \sqrt{a}\sqrt{a'}\delta_{a-1,b}\delta_{a'-1,b'}) \right] , \tag{B-24}$$

with c_0, f^n, $g_{a,b}$ defined as in Sec. B.2.2.

B.3 Matrix elements of the pairing interaction

In the case of BCS-like calculations (Sec. 4) we considered the antisymmetrized matrix elements of the interaction (4.8) but acting only between particles in time-reversed orbitals (pairing interaction). The formulae given here are the special cases of Eqs. (B-4–B-11) in which we have replaced the b, d states by the time-reversed partners of the states a, c.

B.3.1 Matrix elements of the $\delta(\vec{r}_{12})$ force

T=1, L=0, S=0 channel

The antisymmetrized matrix element of (B-3) force between like-particles in time-reversed states read

$$
\begin{aligned}
\langle a\bar{a}|\hat{V}_\delta|\widetilde{b\bar{b}}\rangle &= \langle a\bar{a}|V_\delta|b\bar{b} - \bar{b}b\rangle \\
&= \frac{V_{0\tau}^T}{2}\langle a\bar{a}|(1 - P^\sigma)(1 - P^M P^\sigma P^\tau)\delta(\vec{r}_{12})|b\bar{b}\rangle \\
&= \frac{V_{0\tau}^T}{2}\langle a\bar{a}|\delta(\vec{r}_{12})(1 - P^\sigma)^2|b\bar{b}\rangle \\
&= V_{0\tau}^T\langle a\bar{a}|\delta(\vec{r}_{12})(1 - P^\sigma)|b\bar{b}\rangle \\
&= V_{0\tau}^T\int \mathrm{d}^3 r(\Phi_a^-\Phi_a^{-\star} + \Phi_a^+\Phi_a^{+\star})(\Phi_b^-\Phi_b^{-\star} + \Phi_b^+\Phi_b^{+\star}) \\
&= V_{0\tau}^T\int \mathrm{d}^3 r(|\Phi_a^+|^2 + |\Phi_a^-|^2)(|\Phi_b^-|^2 + |\Phi_b^+|^2),
\end{aligned}
\tag{B-25}
$$

with the wave function of a time-reversed state $|\bar{a}\rangle$ given by

$$
\Phi_a = \Phi_a^{-\star}|+\rangle - \Phi_a^{+\star}|-\rangle.
\tag{B-26}
$$

Similarly, for the proton-neutron part one obtains

$$
\langle a\bar{A}|\hat{V}_\delta|\widetilde{b\bar{B}}\rangle = \frac{V_{0\tau}^T}{2}\int \mathrm{d}^3 r(\Phi_A^+\Phi_a^{+\star} + \Phi_A^-\Phi_a^{-\star})(\Phi_b^-\Phi_B^{-\star} + \Phi_b^+\Phi_B^{+\star})
\tag{B-27}
$$

where a, b denote *e.g.* proton and A, B neutron states.

T=0, L=0, S=1 channel

In this case, we deal with proton-neutron Cooper pairs. One has:

$$
\begin{aligned}
\langle a\bar{A}|\hat{V}_\delta|\widetilde{b\bar{B}}\rangle &= \langle a\bar{A}|V_\delta|b\bar{B} - \bar{B}b\rangle \\
&= \frac{V_{0\tau}^T}{2}\langle a\bar{A}|(1 + P^\sigma)(1 - P^\tau)(1 - P^M P^\sigma P^\tau)\delta(\vec{r}_{12})|b\bar{B}\rangle \\
&= \frac{V_{0\tau}^T}{2}\langle a\bar{A}|\delta(\vec{r}_{12})(1 + P^\sigma)|b\bar{B}\rangle
\end{aligned}
$$

$$
\begin{aligned}
&= \frac{V_{0\tau}^T}{2} \int \mathrm{d}^3 r \left((\Phi_a^+ \Phi_A^{+\star} - \Phi_a^- \Phi_A^{-\star})(\Phi_b^+ \Phi_B^{+\star} - \Phi_b^- \Phi_B^{-\star}) \right. \\
&+ \left. 2\Phi_a^{+\star}\Phi_A^-\Phi_b^+\Phi_B^{-\star} + 2\Phi_a^{-\star}\Phi_A^+\Phi_b^-\Phi_B^{+\star} \right),
\end{aligned}
$$
$$(\text{B-28})$$

where a, b are proton states and $\bar{A}, \bar{B}$ denote the states of their neutron time-reversed partners.

B.3.2   Matrix elements of the $k'\delta(\vec{r}_{12})k$ force

T=1, L=1, S=1 channel

The space-odd antisymmetrized matrix element between like nucleons in time-reversed states is given by

$$
\begin{aligned}
\langle a\bar{a}|\hat{V}_{k'\delta k}|\widetilde{b\bar{b}}\rangle &= \frac{\mathrm{x}V_{0\tau}^T}{2} \langle a\bar{a}|k'\delta(\vec{r}_{12})k(1 - P^M P^\tau P^\sigma)(1 + P^\sigma)|b\bar{b}\rangle \\
&= \frac{\mathrm{x}V_{0\tau}^T}{8} \langle a\bar{a}|(\overleftarrow{\nabla}_1 - \overleftarrow{\nabla}_2)\delta(\vec{r}_{12})(\overrightarrow{\nabla}_1 - \overrightarrow{\nabla}_2)(1 + P^\sigma)^2|b\bar{b}\rangle \\
&= \frac{\mathrm{x}V_{0\tau}^T}{4} \langle \nabla_1 a\bar{a} - a\nabla_2\bar{a}|\delta(\vec{r}_{12})(1 + P^\sigma)|\nabla_1 b\bar{b} - b\nabla_2\bar{b}\rangle \\
&= \frac{\mathrm{x}V_{0\tau}^T}{4} \int \mathrm{d}^3 r \sum_{i=r,z,\varphi} \left\{ -\gamma_{(aa)_i}^{++}\gamma_{(bb)_i}^{++} - \gamma_{(aa)_i}^{--}\gamma_{(bb)_i}^{--} + \gamma_{(aa)_i}^{++}\gamma_{(bb)_i}^{--} + \gamma_{(aa)_i}^{--}\gamma_{(bb)_i}^{++} \right. \\
&- \left. 2\gamma_{(aa)_i}^{+-}\gamma_{(bb)_i}^{-+} - 2\gamma_{(aa)_i}^{-+}\gamma_{(bb)_i}^{+-} \right\},
\end{aligned}
$$
$$(\text{B-29})$$

where:

$$
\begin{aligned}
\gamma_{(kl)_i}^{++} &= \nabla_i\Phi_k^{+\star}\Phi_l^+ - \Phi_k^{+\star}\nabla_i\Phi_l^+ \\
\gamma_{(kl)_i}^{--} &= \nabla_i\Phi_k^{-\star}\Phi_l^- - \Phi_k^{-\star}\nabla_i\Phi_l^- \\
\gamma_{(kl)_i}^{+-} &= \nabla_i\Phi_k^{+\star}\Phi_l^- - \Phi_k^{+\star}\nabla_i\Phi_l^- \\
\gamma_{(kl)_i}^{-+} &= \nabla_i\Phi_k^{-\star}\Phi_l^+ - \Phi_k^{-\star}\nabla_i\Phi_l^+.
\end{aligned}
$$
$$(\text{B-30})$$

For the like-particle pairing only $\gamma_{(kk)_\varphi}$ components are non-zero thus the final expression for the matrix element has the form

$$
\begin{aligned}
\langle a\bar{a}|\hat{V}_{k'\delta k}|\widetilde{b\bar{b}}\rangle &= \frac{xV_{0\tau}^T}{4} \int \mathrm{d}^3 r \left\{ -\gamma_{(aa)_\varphi}^{++}\gamma_{(bb)_\varphi}^{++} - \gamma_{(aa)_\varphi}^{--}\gamma_{(bb)_\varphi}^{--} + \gamma_{(aa)_\varphi}^{++}\gamma_{(bb)_\varphi}^{--} + \gamma_{(aa)_\varphi}^{--}\gamma_{(bb)_\varphi}^{++} \right. \\
&- \left. 2\gamma_{(aa)_\phi}^{+-}\gamma_{(bb)_\phi}^{-+} - 2\gamma_{(aa)_\phi}^{-+}\gamma_{(bb)_\phi}^{+-} \right\}.
\end{aligned}
$$
$$(\text{B-31})$$

Analogously, for the proton-neutron part one obtains

$$
\begin{aligned}
\langle a\bar{A}|\hat{V}_{k'\delta k}|\widetilde{b\bar{B}}\rangle &= \frac{\mathrm{x}V_{0\tau}^T}{4} \langle a\bar{A}|k'\delta(\vec{r}_{12})k(1 - P^M P^\tau P^\sigma)(1 + P^\sigma)(1 + P^\tau)|b\bar{B}\rangle \\
&= \frac{\mathrm{x}V_{0\tau}^T}{8} \langle a\bar{A}|(\overleftarrow{\nabla}_1 - \overleftarrow{\nabla}_2)\delta(\vec{r}_{12})(\overrightarrow{\nabla}_1 - \overrightarrow{\nabla}_2)(1 + P^\sigma)|b\bar{B}\rangle
\end{aligned}
$$

$$
= \frac{\mathrm{x}V_{0\tau}^T}{8} \langle \nabla_1 a\bar{A} - a\nabla_2\bar{A}|\delta(\vec{r}_{12})(1+P^\sigma)|\nabla_1 b\bar{B} - b\nabla_2\bar{B}\rangle
$$

$$
= \frac{\mathrm{x}V_{0\tau}^T}{8} \int \mathrm{d}^3r \sum_{i=r,z,\varphi} \left\{ \gamma_{(aA)_i}^{++}(\gamma_{(bB)_i}^{++})^\star + \gamma_{(aA)_i}^{--}(\gamma_{(bB)_i}^{--})^\star \right.
$$

$$
\left. - \gamma_{(aA)_i}^{++}(\gamma_{(bB)_i}^{--})^\star - \gamma_{(aA)_i}^{--}(\gamma_{(bB)_i}^{++})^\star + 2\gamma_{(aA)_i}^{+-}(\gamma_{(bB)_i}^{-+})^\star + 2\gamma_{(aA)_i}^{-+}(\gamma_{(bB)_i}^{+-})^\star \right\},
$$

$$
\text{(B-32)}
$$

wit $\gamma_{(kl)_i}$ defined in Eq. (B-30).

T=0, L=1, S=0 channel

Component which we need to take into account is the two-body proton-neutron matrix element for the particles coupled to $T = 0$. We have

$$
\langle a\bar{A}|\hat{V}_{\boldsymbol{k}'\delta\boldsymbol{k}}|\widetilde{b\bar{B}}\rangle = \frac{\mathrm{x}V_{0\tau}^T}{4} \langle a\bar{A}|\boldsymbol{k}'\delta(\vec{r}_{12})\boldsymbol{k}(1 - P^M P^\tau P^\sigma)(1 - P^\sigma)(1 - P^\tau)|b\bar{B}\rangle
$$

$$
= \frac{\mathrm{x}V_{0\tau}^T}{8} \langle a\bar{A}|(\overleftarrow{\nabla}_1 - \overleftarrow{\nabla}_2)\delta(\vec{r}_{12})(\overrightarrow{\nabla}_1 - \overrightarrow{\nabla}_2)(1 - P^\sigma)|b\bar{B}\rangle
$$

$$
= \frac{\mathrm{x}V_{0\tau}^T}{8} \langle \nabla_1 a\bar{A} - a\nabla_2\bar{A}|\delta(\vec{r}_{12})(1 - P^\sigma)|\nabla_1 b\bar{B} - b\nabla_2\bar{B}\rangle
$$

$$
= \frac{\mathrm{x}V_{0\tau}^T}{8} \int \mathrm{d}^3r \sum_{i=r,z,\varphi} \left\{ \gamma_{(aA)_i}^{++}(\gamma_{(bB)_i}^{++})^\star + \gamma_{(aA)_i}^{--}(\gamma_{(bB)_i}^{--})^\star \right.
$$

$$
\left. + \gamma_{(aA)_i}^{++}(\gamma_{(bB)_i}^{--})^\star + \gamma_{(aA)_i}^{--}(\gamma_{(bB)_i}^{++})^\star \right\}
$$

$$
\text{(B-33)}
$$

with $\gamma_{(kl)_i}$ defined as formerly.

Since the time-reversed partners here are protons and neutrons, their spatial wave functions corresponding to *e.g.* $a, \bar{A}$ states are not identical. Therefore, contrary to the *nn* and *pp* cases, all the three $\gamma_{(kl)_{r,z,\phi}}$ components have non-zero values.

Appendix C

Many-body matrix elements

In this appendix the calculations of matrix elements of one-body and two-body operators in many-body basis which are crucial for the HTDA method are described. We remind some theoretical aspects that are necessary to understand the application of the Wick theorem to the calculations with quasi-contractions performed in this work.

C.1 Wick theorem

Consider an even number of operators $c_1, c_2, ..., c_{2n}$ which can be either particle creation $a_i^\dagger$ or annihilation a_j operators. The normal ordered product of these $2n$ operators, which we denote

$$: c_1 c_2 ... c_{2n} : \tag{C-1}$$

is defined as a product in which all the creation operators are on the right and all the destruction ones stand on the left side, all multiplied by the phase factor ± 1 according as the necessary rearrangement requires an even or an odd number of permutations, respectively $e.g.$

$$: a_1^\dagger a_2 := a_1^\dagger a_2 \qquad : a_2 a_1^\dagger := -a_1^\dagger a_2 \,. \tag{C-2}$$

It is then trivial to notice that the mean value of a normal product in the vacuum state is always equal to zero.

Using the definition of the normal product the so-called contraction of two operators may be now introduced

$$\underline{c_1 c_2} = c_1 c_2 - : c_1 c_2 : \,. \tag{C-3}$$

Taking into account the anticommutation rules for fermionic operators one has

$$\underline{a_1 a_2} = \underline{a_1^\dagger a_2^\dagger} = \underline{a_1^\dagger a_2} = 0 \qquad \underline{a_1 a_2^\dagger} = \delta_{12} \,, \tag{C-4}$$

thus the contractions of any two fermionic operators are real numbers and we can identify them as a mean value of a product of two operators in the particle vacuum

state $|0\rangle$:

$$\underline{a_1 a_2^\dagger} = \langle 0 | a_1 a_2^\dagger | 0 \rangle \,. \qquad\qquad (\text{C-5})$$

The Wick theorem states that a set of creation and destruction operators can be expressed as a sum of these operators arranged in the normal product for all possible contractions. The weak version of the Wick theorem concerns the same way the mean value of a product of annihilation and creation operators evaluated in the particle vacuum.

C.2   Quasiparticle transformation

C.2.1   Bogoliubov transformation

Suppose we perform a linear transformation which connects the $(a_i^\dagger, a_i)$ operators with an other ensemble of the operators $(\alpha_i^\dagger, \alpha_i)$ so that

$$\alpha_i^\dagger = \sum_k A_{ki} a_k^\dagger + B_{ki} a_k \,, \qquad\qquad (\text{C-6})$$

where A, B are complex matrices. Demanding that the two sets of operators obey the same anticommutation rules we define the canonical transformation in which the matrices A, B fulfil the conditions

$$A\tilde{B} + \tilde{A}B = 0 \qquad\qquad (\text{C-7})$$

and

$$AA^\dagger + BB^\dagger = 1 \,, \qquad\qquad (\text{C-8})$$

where $\tilde{A}$, $A^\dagger$ are transposed and Hermite conjugate matrices, respectively. If there exists such a normalized state that

$$\alpha_i |\tilde{0}\rangle = 0, \qquad \forall i \qquad\qquad (\text{C-9})$$

we may call α_i quasiparticle operators, the state $|\tilde{0}\rangle$ quasiparticle vacuum or quasi-vacuum and the linear canonical transformation performed here– the Bogoliubov transformation.

Particle-hole quasiparticle transformation

Given a Slater determinant $|\Psi\rangle$ a following linear transformation can be defined

$$\begin{aligned} b_i^\dagger &= a_i, \qquad \forall i \in |\Psi\rangle \\ b_i &= a_i^\dagger, \qquad \forall i \notin |\Psi\rangle \,, \end{aligned} \qquad\qquad (\text{C-10})$$

where the single-particle states contained in the Slater determinant $i \in |\Psi\rangle$ are dubbed hole levels and the others– particle levels.

Since a pair of the operators $(a_i^\dagger, a_i)$ is invariant under the transformation (C-10), the anticommutation relations of $(a_i^\dagger, a_i)$ remain the same for $(b_i^\dagger, b_i)$ therefore the canonical conditions are satisfied. The Slater determinant $|\Psi\rangle$ is then in this case the quasi-vacuum for $b_i^\dagger, b_i$ which we will refer to as particle and hole quasiparticle operators. It is seen that creating a quasiparticle in the hole state (that is to say in the occupied single-particle state) means annihilating a particle in the Slater determinant $|\Psi\rangle$ thus the creation of a hole. Analogously, creating a quasiparticle in the particle (unoccupied) state is adding one particle to $|\Psi\rangle$, thus creating a particle. Consequently, this transformation is called particle-hole quasiparticle transformation.

C.2.2 Quasi-contraction

We have defined a contraction of two operators as a mean value of a pair of operators in the particle vacuum state $|0\rangle$. Similarily, we define a quasi-contraction as a mean value of a pair of quasiparticle operators in the particle vacuum state $|0\rangle$ (or a mean value of two particle opertors in a quasi-vacuum state $|\tilde{0}\rangle$). In the Bogoliubov transformation, noting indifferently c_i, c_j for any particle operators $a, a^\dagger$ and d_i, d_j for any quasiparticle operators $b, b^\dagger$ we have

$$\underline{\underline{c_i c_j}} = \langle\tilde{0}|c_i c_j|\tilde{0}\rangle \tag{C-11}$$

$$\underline{\underline{d_i d_j}} = \langle 0|d_i d_j|0\rangle. \tag{C-12}$$

One can show that for all Bogoliubov transformations the mean value of a product of an even number of quasiparticle operators in the particle vacuum state (or inversly, the product of an even number of particle operators in the quasi-vacuum state) is formally given by the weak Wick theorem in which we replace the contractions of the operators by the corresponding quasi-contractions.

In the case of particle-hole excitations, relying on the anticommutation rules of particle operators, one finds that

$$\underline{\underline{a_i^\dagger a_j^\dagger}} = \underline{\underline{a_i a_j}} = 0 \tag{C-13}$$

$$\underline{\underline{a_i^\dagger a_j}} = \delta_{ij}^{(\mathrm{h})} \tag{C-14}$$

$$\underline{\underline{a_i a_j^\dagger}} = \delta_{ij}^{(\mathrm{p})}. \tag{C-15}$$

Kronecker symbols $\delta_{ij}^{(\mathrm{h})}$ and $\delta_{ij}^{(\mathrm{p})}$ indicate that i, j should be identical and both hole or particle states, respectively.

One possible choice for the quasi-vacuum is the particle-hole HF vacuum $|\mathrm{HF}\rangle$. However, we may construct other Slater determinants $|A\rangle$, $|B\rangle$ on the basis of a HF quasi-vacuum via particle-hole excitations. This choice is arbitrary and in certain cases we may treat $|A\rangle$ and $|B\rangle$ states as quasi-vacua as it will be applied in the calculations of many-body matrix elements in the coming paragraphs.

C.3 One-body operator

Hereafter, we use greek letters to specify the particle states and latin letters for hole states. Only the indices i, j, k, l are used to define one and two-body operators.

In the formalism of the second quantization a one-body operator Θ is given by

$$\Theta = \sum_{ij} \langle i|\theta|j\rangle a_i^\dagger a_j \,, \tag{C-16}$$

where the summation runs over all single-particle states. Let us now consider the diagonal matrix element of the operator (C-16) in the many-body state $|A\rangle$. Using Eq. (C-14) we have

$$\langle A|\Theta|A\rangle = \sum_{ij} \langle i|\theta|j\rangle \langle A|a_i^\dagger a_j|A\rangle = \sum_{ij} \langle i|\theta|j\rangle \delta_{ij}^{(h_A)} \,, \tag{C-17}$$

where the index A was added to h_A to point out that the final summation runs over all the states occupied with respect to the quasi-vacuum $|A\rangle$. Concerning that the set of occupied states of $|A\rangle$ is obtained on the basis of the Hartree-Fock vacuum by adding the particle and removing the hole states, the final summation takes the form

$$\sum_i^{h_A} = \sum_i^{h_{HF}} - \sum_i^{h(A)} + \sum_i^{p(A)} \,. \tag{C-18}$$

For a nondiagonal matrix element $\langle A|\Theta|B\rangle$ where $|B\rangle$ differs from $|A\rangle$ by one nucleon, that is to say $|B\rangle$ is a one-particle one-hole excitation of the state $|A\rangle$

$$|B\rangle = a_\alpha^\dagger a_a|A\rangle \tag{C-19}$$

one obtains (using formulae (C-14) and (C-15))

$$
\begin{aligned}
\langle A|\Theta|B\rangle &= \sum_{ij} \langle i|\theta|j\rangle \langle A|a_i^\dagger a_j a_\alpha^\dagger a_a|A\rangle \\
&= \sum_{ij} \langle i|\theta|j\rangle \delta_{ia}^{(h_A)} \delta_{j\alpha}^{(p_A)} = \langle a|\theta|\alpha\rangle \,.
\end{aligned}
\tag{C-20}
$$

It is easy to notice that other non-diagonal elements, where $|B\rangle$ differs from $|A\rangle$ by more than one nucleon, are all equal to zero.

C.4 Two-body operator

In the following we consider matrix elements of the two-body operator Θ represented in the formalism of the second quantization by its antisymmetrized matrix elements $\tilde{\theta}_{ijkl}$ and defined as

$$\Theta = \frac{1}{4} \sum_{ijkl} \langle i\tau, j\tau'|\theta|\widetilde{k\tau, l\tau'}\rangle a_{i\tau}^\dagger a_{j\tau'}^\dagger a_{l\tau'} a_{k\tau} = \frac{1}{4} \sum_{ijkl} \tilde{\theta}_{ijkl} a_{i\tau}^\dagger a_{j\tau'}^\dagger a_{l\tau'} a_{k\tau} \tag{C-21}$$

between m-hole m-particle states $|A\rangle, |B\rangle$. The indices $\{\tau, \tau'\} = \{p, n\}$ are added to consider the like-particle and proton-neutron interactions.

First we calculate the diagonal matrix element of (C-21) in the N-body state $|A\rangle$ which can be treated as a quasi-vacuum for particle-hole excitations. Using the Wick theorem we obtain

$$
\begin{aligned}
\langle A|\Theta|A\rangle &= \frac{1}{4}\sum_{ijkl}\langle i\tau, j\tau'|\theta|\widetilde{k\tau, l\tau'}\rangle\langle A|a_{i\tau}^\dagger a_{j\tau'}^\dagger a_{l\tau'}a_{k\tau}|A\rangle \\
&= \frac{1}{4}\sum_{ijkl}\langle i\tau, j\tau'|\theta|\widetilde{k\tau, l\tau'}\rangle\left(\delta_{ik}^{(h_A)\tau}\delta_{jl}^{(h_A)\tau'} - \delta_{il}^{(h_A)}\delta_{\tau\tau'}\delta_{jk}^{(h_A)}\delta_{\tau'\tau}\right) \\
&= \frac{1}{4}\sum_{ijkl}\langle i\tau, j\tau'|\theta|\widetilde{k\tau, l\tau'}\rangle\left(\delta_{ik}^{(h_A)\tau}\delta_{jl}^{(h_A)\tau'} - \delta_{il}^{(h_A)}\delta_{jk}^{(h_A)}\delta_{\tau\tau'}\right). \quad \text{(C-22)}
\end{aligned}
$$

In an analogous way one may calculate non-diagonal elements: $\langle A|\Theta|B\rangle$. If $|A\rangle$ differs from $|B\rangle$ by one nucleon

$$
|B\rangle = a_{\alpha\tau}^\dagger a_{a\tau}|A\rangle \quad \text{(C-23)}
$$

we have

$$
\begin{aligned}
\langle A|\Theta|B\rangle &= \frac{1}{4}\sum_{ijkl}\langle i\tau, j\tau'|\theta|\widetilde{k\tau, l\tau'}\rangle\langle A|a_{i\tau}^\dagger a_{j\tau'}^\dagger a_{l\tau'}a_{k\tau}a_{\alpha\tau}^\dagger a_{a\tau}|A\rangle \\
&= \frac{1}{4}\sum_{ijkl}\langle i\tau, j\tau'|\theta|\widetilde{k\tau, l\tau'}\rangle \\
&\quad \langle A|\delta_{ia}^{(h_A)\tau}(a_{j\tau'}^\dagger a_{l\tau'}a_{k\tau}a_{\alpha\tau}^\dagger) - \delta_{ja}^{(h_A)}\delta_{\tau\tau'}(a_{i\tau}^\dagger a_{l\tau'}a_{k\tau}a_{\alpha\tau}^\dagger)|A\rangle \\
&= \frac{1}{4}\sum_{ijkl}\langle i\tau, j\tau'|\theta|\widetilde{k\tau, l\tau'}\rangle\left(\delta_{ia}^{(h_A)\tau}(\delta_{jl}^{(h_A)\tau'}\delta_{k\alpha}^{(p_A)\tau} - \delta_{jk}^{(h_A)}\delta_{l\alpha}^{(p_A)}\delta_{\tau\tau'})\right. \\
&\quad + \left.\delta_{ja}^{(h_A)}\delta_{\tau\tau'}(\delta_{ik}^{(h_A)}\delta_{l\alpha}^{(p_A)} - \delta_{il}^{(h_A)}\delta_{k\alpha}^{(p_A)})\right). \quad \text{(C-24)}
\end{aligned}
$$

When $|B\rangle$ is a two-particle two-hole excitation of $|A\rangle$, *i.e.*

$$
|B\rangle = a_{\alpha\tau}^\dagger a_{\beta\tau'}^\dagger a_{a\tau}a_{b\tau'}|A\rangle \quad \text{(C-25)}
$$

the matrix element read

$$
\begin{aligned}
\langle A|\Theta|B\rangle &= \frac{1}{4}\sum_{ijkl}\langle i\tau, j\tau'|\theta|\widetilde{k\tau, l\tau'}\rangle\langle A|a_{i\tau}^\dagger a_{j\tau'}^\dagger a_{l\tau'}a_{k\tau}a_{\alpha\tau}^\dagger a_{\beta\tau'}^\dagger a_{a\tau}a_{b\tau'}|A\rangle \\
&= \frac{1}{4}\sum_{ijkl}\langle i\tau, j\tau'|\theta|\widetilde{k\tau, l\tau'}\rangle(\delta_{l\beta}^{(p_A)\tau'}\delta_{k\alpha}^{(p_A)\tau} - \delta_{l\alpha}^{(p_A)}\delta_{k\beta}^{(p_A)}\delta_{\tau\tau'}) \\
&\quad (\delta_{ib}^{(h_A)\tau}\delta_{ja}^{(h_A)\tau'} - \delta_{jb}^{(h_A)}\delta_{ia}^{(h_A)}\delta_{\tau\tau'}).
\end{aligned}
$$
$$
\text{(C-26)}
$$

If $|B\rangle$ differ from $|A\rangle$ on more than two nucleons then $\langle A|\Theta|B\rangle = 0$.

Generally, $|A\rangle$ and $|B\rangle$ states should be understood here as Kronecker products of proper many-particle many-hole states for protons and neutrons, *e.g.*

$$
|A\rangle = |(N_p N_h)_n \otimes (N'_p N'_h)_p\rangle. \quad \text{(C-27)}
$$

In the case of no *pn* coupling, when the neutrons and protons can be treated separately, the quasi-vacua $|A\rangle$ and $|B\rangle$ can be viewed as single neutron or proton Slater determinants.

C.4.1   Proton-proton and neutron-neutron interaction

First, consider like-particle interaction. In this case $\tau=\tau'$ in the operator (C-21) and $\delta_{\tau\tau'} = 1$.

For two identical many-body states

$$|B\rangle \equiv |A\rangle \tag{C-28}$$

we have from Eq. (C-22)

$$
\begin{aligned}
\langle A|\Theta|A\rangle &= \frac{1}{4}\sum_{ijkl}\langle ij|\theta|\widetilde{kl}\rangle\langle A|a_i^\dagger a_j^\dagger a_l a_k|A\rangle \\
&= \frac{1}{4}\sum_{ijkl}\langle ij|\theta|\widetilde{kl}\rangle\left(\delta_{ik}^{(\mathrm{h_A})}\delta_{jl}^{(\mathrm{h_A})} - \delta_{il}^{(\mathrm{h_A})}\delta_{jk}^{(\mathrm{h_A})}\right) \\
&= \frac{1}{2}\sum_{kl}\langle kl|\theta|\widetilde{kl}\rangle \\
&= \frac{1}{2}\sum_{k}^{\mathrm{h-h}(A)+\mathrm{p}(A)}\sum_{l}^{\mathrm{h-h}(A)+\mathrm{p}(A)}\langle kl|\theta|\widetilde{kl}\rangle.
\end{aligned}
\tag{C-29}
$$

In the case when two many-body states differ from each other by one nucleon, *i.e.*

$$|B\rangle = a_\alpha^\dagger a_a|A\rangle \tag{C-30}$$

the formula (C-24) takes the form

$$
\begin{aligned}
\langle A|\Theta|B\rangle &= \frac{1}{4}\sum_{ijkl}\langle ij|\theta|\widetilde{kl}\rangle\langle A|a_i^\dagger a_j^\dagger a_l a_k a_\alpha^\dagger a_a|A\rangle \\
&= \frac{1}{4}\sum_{ijkl}\langle ij|\theta|\widetilde{kl}\rangle\left(\delta_{ia}^{(\mathrm{h_A})}(\delta_{jl}^{(\mathrm{h_A})}\delta_{k\alpha}^{(\mathrm{p_A})} - \delta_{jk}^{(\mathrm{h_A})}\delta_{l\alpha}^{(\mathrm{p_A})})\right. \\
&\quad + \left.\delta_{ja}^{(\mathrm{h_A})}(\delta_{ik}^{(\mathrm{h_A})}\delta_{l\alpha}^{(\mathrm{p_A})} - \delta_{il}^{(\mathrm{h_A})}\delta_{k\alpha}^{(\mathrm{p_A})})\right) \\
&= \sum_{k}\langle ka|\theta|\widetilde{k\alpha}\rangle \\
&= \sum_{k}^{\mathrm{h-h}(A)+\mathrm{p}(A)}\langle ka|\theta|\widetilde{k\alpha}\rangle.
\end{aligned}
\tag{C-31}
$$

For non-diagonal elements between two many-body states which differ by two nucleons

$$|B\rangle = a_\alpha^\dagger a_\beta^\dagger a_a a_b|A\rangle \tag{C-32}$$

one obtains from Eq. (C-26)

$$
\begin{aligned}
\langle A|\Theta|B\rangle &= \frac{1}{4}\sum_{ijkl}\langle ij|\theta|\widetilde{kl}\rangle\langle A|a_i^\dagger a_j^\dagger a_l a_k a_\alpha^\dagger a_\beta^\dagger a_a a_b|A\rangle \\
&= \frac{1}{4}\sum_{ijkl}\langle ij|\theta|\widetilde{kl}\rangle(\delta_{l\beta}^{(\mathrm{PA})}\delta_{k\alpha}^{(\mathrm{PA})} - \delta_{l\alpha}^{(\mathrm{PA})}\delta_{k\beta}^{(\mathrm{PA})})(\delta_{ib}^{(\mathrm{h_A})}\delta_{ja}^{(\mathrm{h_A})} - \delta_{jb}^{(\mathrm{h_A})}\delta_{ia}^{(\mathrm{h_A})}) \\
&= \langle ba|\theta|\widetilde{\alpha\beta}\rangle.
\end{aligned}
\tag{C-33}
$$

C.4.2   Proton-neutron interaction

For the residual proton-neutron interaction $\tau \neq \tau'$ in Eq. (C-21) thus $\delta_{\tau\tau'} = 0$ and the formulae C-22, C-24, C-26 reduce to shorter forms.

For the elements calculated between the same many-body states $|B\rangle \equiv |A\rangle$ one obtains

$$
\begin{aligned}
\langle A|\Theta|A\rangle &= \frac{1}{4}\sum_{ijkl}\langle ij|\theta|\widetilde{kl}\rangle\langle A|a_{i\tau}^\dagger a_{j\tau'}^\dagger a_{l\tau'} a_{k\tau}|A\rangle \\
&= \frac{1}{4}\sum_{ijkl}\langle ij|\theta|\tilde{kl}\rangle\delta_{ik}^{(\mathrm{h_A})\tau}\delta_{jl}^{(\mathrm{h_A})\tau'} \\
&= \frac{1}{4}\sum_{kl}\langle k\tau, l\tau'|\theta|\widetilde{k\tau, l\tau'}\rangle \\
&= \frac{1}{4}\sum_{k}^{\mathrm{h}_\tau - \mathrm{h}_\tau(A) + \mathrm{p}_\tau(A)}\ \sum_{l}^{\mathrm{h}_{\tau'} - \mathrm{h}_{\tau'}(A) + \mathrm{p}_{\tau'}(A)}\langle k\tau, l\tau'|\theta|\widetilde{k\tau, l\tau'}\rangle.
\end{aligned}
\tag{C-34}
$$

If $|A\rangle$ and $|B\rangle$ differ by one nucleon, neutron or proton:

$$
|B\rangle = a_{\alpha\tau}^\dagger a_{a\tau}|A\rangle
\tag{C-35}
$$

Eq. (C-24) reduces to

$$
\begin{aligned}
\langle A|\Theta|B\rangle &= \frac{1}{4}\sum_{ijkl}\langle i\tau, j\tau'|\theta|\widetilde{k\tau, l\tau'}\rangle\langle A|a_{i\tau}^\dagger a_{j\tau'}^\dagger a_{l\tau'} a_{k\tau} a_{\alpha\tau}^\dagger a_{a\tau}|A\rangle \\
&= \frac{1}{4}\sum_{ijkl}\langle i\tau, j\tau'|\theta|\widetilde{k\tau, l\tau'}\rangle\delta_{ia}^{(\mathrm{h_A})\tau}\delta_{jl}^{(\mathrm{h_A})\tau'}\delta_{k\alpha}^{(\mathrm{PA})\tau} \\
&= \frac{1}{4}\sum_{j}^{\mathrm{h}_{\tau'} - \mathrm{h}_{\tau'}(A) + \mathrm{p}_{\tau'}(A)}\langle a\tau, j\tau'|\theta|\widetilde{\alpha\tau, j\tau'}\rangle.
\end{aligned}
\tag{C-36}
$$

And last, consider the case $|B\rangle$ is a 2p2h excitation of the state $|A\rangle$

$$
|B\rangle = a_{\alpha\tau}^\dagger a_{\beta\tau'}^\dagger a_{a\tau} a_{b\tau'}|A\rangle.
\tag{C-37}
$$

We have from Eq. (C-26)

$$
\begin{aligned}
\langle A|\Theta|B\rangle &= \frac{1}{4}\sum_{ijkl}\langle i\tau, j\tau'|\theta|\widetilde{k\tau, l\tau'}\rangle\langle A|a_{i\tau}^\dagger a_{j\tau'}^\dagger a_{l\tau'} a_{k\tau} a_{\alpha\tau}^\dagger a_{\beta\tau'}^\dagger a_{a\tau} a_{b\tau'}|A\rangle \\
&= -\frac{1}{4}\sum_{ijkl}\langle i\tau, j\tau'|\theta|\widetilde{k\tau, l\tau'}\rangle\delta_{l\beta}^{(\mathrm{PA})\tau'}\delta_{k\alpha}^{(\mathrm{PA})\tau}\delta_{ia}^{(\mathrm{h_A})\tau}\delta_{jb}^{(\mathrm{h_A})\tau'} \\
&= -\frac{1}{4}\langle a\tau, b\tau'|\theta|\widetilde{\alpha\tau, \beta\tau'}\rangle.
\end{aligned}
\tag{C-38}
$$

Other many-body matrix elements, not given in this appendix, are all equal to zero.

Appendix D

Exact solutions of Lipkin-Nogami equations

The Lipkin-Nogami equations of Sec. 4.3 can be expressed as

$$\vec{\mathcal{G}} = \mathcal{N}\vec{\mathcal{L}}, \tag{D-1}$$

where we have introduced three components vectors $\vec{\mathcal{G}} = (\mathcal{G}^{nn}, \mathcal{G}^{pp}, \mathcal{G}^{pn})$ and $\vec{\mathcal{L}} = (\lambda_2^{nn}, \lambda_2^{pp}, \lambda_2^{pn})$. The solution of Eq. (D-1) is therefore given as

$$\vec{\mathcal{L}} = -\mathcal{N}^{-1}\vec{\mathcal{G}}. \tag{D-2}$$

We need now to evaluate $\mathcal{G}^{\tau\tau'}$ and $\mathcal{N}_{\rho\rho'}^{\tau\tau'}$ elements defined as averages of eight quasi-particle operators in the BCS vacuum, see Eqs. (4.80)-(4.81). After straightforward but tedious calculations we obtain them in quite compact forms [165]:

$$\mathcal{G}^{\tau\tau'} = 2\sum_{ij>0} g_{ij,\tau\tau'}[(\kappa^\star\rho)_{i\bar{i}}^{(\tau} (\kappa(1-\rho^\star))_{j\bar{j}}^{\tau')} - \chi_{ij}^{(\tau} \chi_{i\bar{j}}^{\tau')}], \tag{D-3}$$

where

$$\chi \equiv \kappa\kappa^\star. \tag{D-4}$$

We have applied here the notation in which the symmetrization of the product of two factors with two indices is indicated by two parenthesis, *e.g.*,

$$x^{(r}...z^{s)} \equiv x^r...z^s + x^s...z^r. \tag{D-5}$$

In this way the symmetry in τ and τ' is explicitly emphasized. The final result for $\mathcal{N}_{\rho\rho'}^{\tau\tau'}$ is as before symmetric in both (τ, τ') and (ρ, ρ') pairs of indices and reads

$$\mathcal{N}_{\rho\rho'}^{\tau\tau'} = 8 \left[\mathrm{Tr}^> \chi^{\tau(\rho'} \mathrm{Tr}^> \chi^{\tau'\rho)} - \mathrm{Tr}^> (\chi^\tau \chi^{\tau'})^{(\rho\rho')} \right], \tag{D-6}$$

where we denoted

$$\mathrm{Tr}^>(a) = \sum_{i>0} a_{ii}. \tag{D-7}$$

Using both Eq. (D-3) and (D-6) one easily finds the solutions $\lambda_2^{\tau\tau'}$ of the Lipkin-Nogami equations in the following special cases.

- State dependent BCS pairing in the case of one type of nucleons $(\tau = \tau')$.

$$
\begin{aligned}
\lambda_2 &= \frac{1}{4} \frac{\sum_{ij>0} g_{ij} \left[(\kappa^\star \rho)_{i\bar{i}} (\kappa(1-\rho^\star))_{j\bar{j}} - (\chi_{ji} \chi_{\bar{j}\bar{i}}) \right]}{\mathrm{Tr}^> \chi^2 - (\mathrm{Tr}^> \chi)^2} \\
&= \frac{1}{4} \frac{\sum_{ij>0} g_{ij} \left[(u_i v_i^3)(u_j^3 v_j) - (u_i v_i)^4 \right]}{\left(\sum_{i>0} (u_i v_i)^2 \right)^2 - \sum_{i>0} (u_i v_i)^4} \, ,
\end{aligned}
\tag{D-8}
$$

where

$$
\mathrm{Tr}^<(a) \equiv \sum_{i>0} a_{i\bar{i}} \, .
\tag{D-9}
$$

- Seniority pairing: $G \equiv g_{ij} = \mathrm{const}$, in the case of one type of nucleons $(\tau = \tau')$ (see Ref. [121])

$$
\begin{aligned}
\lambda_2 &= \frac{G}{4} \frac{\mathrm{Tr}^<(\kappa^\star \rho) \mathrm{Tr}^<(\kappa(1-\rho^\star)) - \sum_{ji>0} (\chi_{ji} \chi_{\bar{j}\bar{i}})}{\mathrm{Tr}^> \chi^2 - (\mathrm{Tr}^> \chi)^2} \\
&= \frac{G}{4} \frac{\left[\sum_{i>0} (u_i v_i^3) \sum_{j>0} (u_j^3 v_j) - \sum_{i>0} (u_i v_i)^4 \right]}{\left(\sum_{i>0} (u_i v_i)^2 \right)^2 - \sum_{i>0} (u_i v_i)^4} \, .
\end{aligned}
\tag{D-10}
$$

Appendix E

Isospin operator

Consider the operator of the total isospin $\hat{\mathrm{T}}$ of A particles in a nucleus. In the formalism of the second quantization one has

$$\hat{\mathrm{T}} = \sum_{kl,\tau\tau'} \langle k\tau|\hat{\mathrm{t}}_x + \hat{\mathrm{t}}_y + \hat{\mathrm{t}}_z|l\tau'\rangle a^\dagger_{k\tau} a_{l\tau'} , \tag{E-1}$$

where τ is the eigenvalue of the $\hat{\mathrm{t}}_z$ operator. We adopt the convention: $\tau = -1$ for protons and $\tau = 1$ for neutrons.

We aim at calculating the mean value of the operator (E-1) in the quasiparticle vacuum (BCS) state. For z component we obtain:

$$\langle \hat{\mathrm{T}}_z \rangle = \sum_{kl,\tau\tau'} \langle k\tau|\hat{\mathrm{t}}_z|l\tau'\rangle \langle a^\dagger_{k\tau} a_{l\tau'} \rangle . \tag{E-2}$$

The operator $\hat{\mathrm{t}}_z$ does not have non-zero elements between proton and neutron states and we have by definition (see Eq. (4.21)) $\langle a^\dagger_{k\tau} a_{l\tau'} \rangle = \rho^{\tau\tau'}_{lk}$ which implies

$$
\begin{aligned}
\langle \hat{\mathrm{T}}_z \rangle &= \sum_k \frac{1}{2}\delta_{\tau',n}\rho^{\tau'\tau'}_{kk} - \frac{1}{2}\delta_{\tau,p}\rho^{\tau\tau}_{kk} \\
&= \frac{1}{2}\sum_k \rho^{nn}_{kk} - \rho^{pp}_{kk} = (N-Z)/2 .
\end{aligned}
\tag{E-3}
$$

To evaluate mean values of x and y components of the total isospin operator we introduce rising and lowering operators, as it is customary in any angular momentum algebra

$$\hat{\mathrm{t}}_+ \equiv \hat{\mathrm{t}}_x + i\hat{\mathrm{t}}_y, \qquad \hat{\mathrm{t}}_- \equiv \hat{\mathrm{t}}_x - i\hat{\mathrm{t}}_y , \tag{E-4}$$

thus

$$\hat{\mathrm{t}}_x = \frac{1}{2}(\hat{\mathrm{t}}_+ + \hat{\mathrm{t}}_-), \qquad \hat{\mathrm{t}}_y = \frac{1}{2i}(\hat{\mathrm{t}}_+ - \hat{\mathrm{t}}_-) . \tag{E-5}$$

The operators $\hat{\mathrm{t}}_+$, $\hat{\mathrm{t}}_-$ have non-zero non-diagonal elements: $\langle p|\hat{\mathrm{t}}_+|n\rangle = 1$ and $\langle n|\hat{\mathrm{t}}_-|p\rangle = 1$. The mean value of $\hat{\mathrm{T}}_x$ reads

$$\langle \hat{\mathrm{T}}_x \rangle = \sum_{kl,\tau\tau'} \langle k\tau|\hat{\mathrm{t}}_x|l\tau'\rangle \langle a^\dagger_{k\tau} a_{l\tau'} \rangle$$

$$
= \quad \frac{1}{2} \sum_{kl,\tau\tau'} \langle k\tau|\hat{t}_+|l\tau'\rangle \langle a_{k\tau}^\dagger a_{l\tau'}\rangle + \frac{1}{2} \sum_{kl,\tau\tau'} \langle k\tau|\hat{t}_-|l\tau'\rangle \langle a_{k\tau}^\dagger a_{l\tau'}\rangle
$$

$$
= \quad \frac{1}{2} \sum_{kl} (\delta_{\tau,p}\delta_{\tau',n} + \delta_{\tau',p}\delta_{\tau,n})\delta_{kl}\rho_{kl}^{\tau\tau'}
$$

$$
= \quad \frac{1}{2} \sum_{k} (\rho_{kk}^{pn} + \rho_{kk}^{np}) . \tag{E-6}
$$

Since $\rho_{kk}^{np} = \rho_{kk}^{pn\star}$ we obtain

$$
\langle \hat{T}_x \rangle = \Re e \sum_{k} \rho_{kk}^{pn} . \tag{E-7}
$$

Analogously like for $\hat{T}_x$ we may evaluate the mean value of $\hat{T}_y$ as

$$
\langle \hat{T}_y \rangle = \frac{1}{2i} \sum_{k} (\rho_{kk}^{pn} - \rho_{kk}^{np}) = \Im m \sum_{k} \rho_{kk}^{pn} . \tag{E-8}
$$

Bibliography

[1] A. Bohr, B. Mottelson, and D. Pines. *Phys. Rev.*, 110:936, 1958.

[2] S.T. Belyaev. *Mat. Fys. Medd. Dan. Vid. Selsk.*, 31:no. 11, 1959.

[3] F. Barranco, B.F. Bortignon, R.A. Broglia, G. Colo, P. Schuck, E. Vigezzi, and X. Viñas. *Phys. Rev.*, C72:054314, 2005.

[4] A.M. Lane. *Nuclear Theory.* Benjamin, New York, 1964.

[5] A. Goswami. *Nucl. Phys.*, 60:228, 1964.

[6] P. Camiz, A. Covello, and M. Jean. *Nuovo Cimento*, 36:663, 1965.

[7] A. Goswami and L. Kisslinger. *Phys. Rev.*, 140:B26, 1965.

[8] P. Camiz, A. Covello, and M. Jean. *Nuovo Cimento*, B42:199, 1965.

[9] H. Chen and A. Goswami. *Phys. Lett.*, B24:257, 1967.

[10] A.L. Goodman, G. Struble, and A. Goswami. *Phys. Lett.*, B26:260, 1968.

[11] A.L. Goodman. *Nucl. Phys.*, A186:475–492, 1972.

[12] B.H. Flowers and S. Szpikowski. *Proc. Phys. Soc. Jpn.*, 84:193, ibid. 673, 1964.

[13] J.N. Ginocchio. *Nucl. Phys.*, 74:321, 1965.

[14] J.P. Elliot and A.P. White. *Phys. Lett.*, 97B:169, 1980.

[15] J.P. Elliot and J.A. Evans. *Phys. Lett.*, 101B:216, 1981.

[16] C-H. Yu, C. Baktash, J. Dobaczewski, J.A. Cameron, C. Chitu, M. Devlin, J. Eberth, A. Galindo-Uribarri, D.S. Haslip, D.R. LaFosse, T.J. Lampman, I-Y. Lee, F. Lerma, A.O. Macchiavelli, S.D. Paul, D.C. Radford, D. Rudolph, D.G. Sarantites, C.E. Svensson, J.C. Waddington, and J.N. Wilson. *Phys. Rev.*, C60:031305, 1999.

[17] C. Andreoiu, D. Rudolph, C.E. Svensson, A.V. Afanasjev, J. Dobaczewski, I. Ragnarsson, C. Baktash, J. Eberth, C. Fahlander, D.S. Haslip, D.R. LaFosse, S.D. Paul, D.G. Sarantites, H.G. Thomas, J.C. Waddington, W. Weintraub, J.N. Wilson, and C-H. Yu. *Phys. Rev.*, C62:051301, 2000.

[18] M. Pfützner, E. Badura, C. Bingham, B. Blank, M. Chartier, H. Geissel, J. Giovinazzo, L.V. Grigorenko, R. Grzywacz, M. Hellstrm, Z. Janas, J. Kurcewicz, A.S. Lalleman, C. Mazzocchi, I. Mukha, G. Mnzenberg, C. Plettner, E. Roeckl, K.P. Rykaczewski, K. Schmidt, R.S. Simon, M. Stanoiu, and J.-C. Thomas. *Eur. Phys. J.*, A14:279, 2002.

[19] J. Giovinazzo, B. Blank, M. Chartier, S. Czajkowski, A. Fleury, M. J. Lopez Jimenez, M. S. Pravikoff, J.-C. Thomas, F. de Oliveira Santos, M. Lewitowicz, V. Maslov, M. Stanoiu, R. Grzywacz, M. Pfützner, C. Borcea, and B. A. Brown. *Phys. Rev. Lett.*, 89:102501, 2002.

[20] B. Blank, A. Bey, G. Canchel, C. Dossat, A. Fleury, J. Giovinazzo, I. Matea, N. Adimi, F. De Oliveira, I. Stefan, G. Georgiev, S. Grevy, J. C. Thomas, C. Borcea, D. Cortina, M. Caamano, M. Stanoiu, F. Aksouh, B. A. Brown, F. C. Barker, and W. A. Richter. *Phys. Rev. Lett.*, 94:232501, 2005.

[21] www.ganil.fr/research/developments/spiral2.

[22] www.ganil.fr/eurisol.

[23] http://www-w2k.gsi.de/agata.

[24] http://greta.lbl.gov.

[25] P. Vogel. *Nucl. Phys.*, A662:148–154, 2000.

[26] A.O. Macchiavelli, P. Fallon, R.M. Clark, M. Cromaz, M.A. Deleplanque, R.M. Diamond, G.J. Lane, I.Y. Lee, F.S. Stephens, C.E. Svensson, K. Vetter, and D. Ward. *Phys. Rev.*, C61:041303, 2000.

[27] E. Perlińska, S.G. Rohoziński, J. Dobaczewski, and W. Nazarewicz. *Phys. Rev.*, C69:014316, 2004.

[28] F. Simkovic, Ch. C. Moustakidis, L. Pacearescu, and A. Faessler. *Phys. Rev.*, C68:044302, 2003.

[29] W. Satuła and R. Wyss. *Nucl. Phys.*, A676:120–142, 2000.

[30] J. Terasaki, R. Wyss, and P.-H. Heenen. *Phys. Rev. Lett.*, B437:1, 1998.

[31] N. Pillet, P. Quentin, and J. Libert. *Nucl. Phys.*, A697:141–163, 2002.

[32] I. Kelson. *Phys. Rev.*, 132:2189, 1963.

[33] M. Goeppert-Mayer and A.S. Jensen. *Elementary theory of nuclear shell structure.* John Wiley & sons, New York, 1955.

[34] S.G. Nilsson. *Mat. Fys. Medd. Dan. Vid. Selsk.*, 29:no 16, 1955.

[35] S.G. Nilsson, C. F. Tsang, A. Sobiczewski, Z. Szymański, C. Wycech, C. Gustafsson, I.-L. Lamm, P. Möller, and B. Nilsson. *Nucl. Phys.*, A131:1, 1969.

[36] R. D. Woods and D. S. Saxon. *Phys. Rev.*, 95:577–578, 1954.

[37] J. Dobaczewski. Interactions, symmetry breaking, and effective fields from quarks to nuclei. Proceedings of Joliot-Curie International School, Maubuisson, 2002.

[38] D.J. Rowe. *Nuclear collective motion.* Methuen and Co., London, 1970.

[39] P. Ring and P. Schuck. *The nuclear many-body problem.* Springer-Verlag, Berlin, 1980.

[40] H.A. Bethe and J. Goldstone. *Proc. Roy. Soc.*, A238:551, 1957.

[41] K.A. Brueckner. *Phys. Rev.*, 97:1353, 1955.

[42] K.A. Brueckner, J.L. Gammel, and H. Weitzner. *Phys. Rev.*, A238:551, 1957.

[43] J.W. Negele. *Phys. Rev.*, C1:1260, 1970.

[44] J.W. Negele. *Lecture Notes in Physics 40.* Springer-Verlag, Berlin, 1975.

[45] J. Dechargé and D. Gogny. *Phys. Rev.*, C21:1586, 1979.

[46] T.H.R. Skyrme. *Phil. Mag.*, 1:1043, 1956.

[47] T.H.R. Skyrme. *Nucl. Phys.*, 9:615, 1959.

[48] D. Vautherin and D.M. Brink. *Phys. Rev.*, C5:626, 1972.

[49] D. Vautherin and D.M. Brink. *Phys. Rev.*, C7:296, 1973.

[50] M. Beiner, H. Flocard, N. Van Giai, and P. Quentin. *Nucl. Phys.*, A238:29, 1975.

[51] H. Krivine, J. Treiner, and O. Bohigas. *Nucl. Phys.*, A336:155, 1980.

[52] J. Bartel, P. Quentin, M. Brack, C. Guet, and H.B. Hakansson. *Nucl. Phys.*, A386:79, 1982.

[53] F. Tondeur, M. Brack, M. Farine, and J.M. Pearson. *Nucl. Phys.*, A420:297, 1984.

[54] J. Dobaczewski, H. Flocard, and J. Treiner. *Nucl. Phys.*, A422:103, 1984.

[55] E. Chabanat, P. Bonche, P. Heansel, J. Meyer, and R. Schaeffer. *Phys. Scripta*, T56:231, 1994.

[56] J.C. Slater. *Phys. Rev.*, C81:85, 1951.

[57] P. Gombas. *Ann. Phys.*, 10:253, 1952.

[58] C. Titin-Schnaider and P. Quentin. *Phys. Lett.*, B49:397, 1974.

[59] W. D. Myers and W. J. Swiatecki. *Ann. Phys. (N.Y.)*, 84:186–210, 1974.

[60] H.J. Krappe, J.R. Nix, and A.J. Sierk. *Phys. Rev.*, C20:992, 1979.

[61] P. Möller, J.R. Nix, W.D. Myers, and W.J. Swiatecki. *At. Data and Nucl. Data Tables*, 59:185, 1995.

[62] P. Möller, J.R. Nix, and K.L Kratz. *At. Data and Nucl. Data Tables*, 66:131, 1997.

[63] K. Pomorski and J. Dudek. *Phys. Rev.*, C67:044316, 2003.

[64] S. Goriely, M. Samyn, P.H. Heenen, J.M. Pearson, and F. Tondeur. *Nucl. Phys.*, A700:142, 2002.

[65] S. Goriely, M. Samyn, P.H. Heenen, J.M. Pearson, and F. Tondeur. *Phys. Rev.*, C66:024326, 2002.

[66] W. Satuła, D.J. Dean, J. Gary, S. Mizutori, and W. Nazarewicz. *Phys. Lett.*, B407:103–107, 1997.

[67] A. Poves and G. Martinez-Pinedo. *Phys. Lett.*, B430:203–208, 1998.

[68] W. Satuła and R. Wyss. *Phys. Rev. Lett.*, B393:1–6, 1997.

[69] R.R. Chasman. *Phys. Lett.*, B577:47–53, 2003.

[70] D.S. Brenner, R.B. Cakirli, and R.F. Casten. *Phys. Rev.*, C73:034315, 2006.

[71] J. Jänecke and T.W. O'Donell. *Phys. Lett.*, B605:87–94, 2005.

[72] D.J. Dean, S.E. Koonin, K. Langanke, and P.B. Radha. *Phys. Lett.*, B399:1–7, 1997.

[73] G. de Angelis, C. Fahlander, A. Gadea, E. Farnea, W. Gelletly, A. Aprahamian, D. Bazzacco, F. Becker, P.G. Bizzeti, A. Bizetti-Sona, F. Brandolini, D. de Acuna, M. de Poli, J. Eberth, D. Foltescu, S.M. Lenzi, S. Lunardi, T. Martinez, D.R. Napoli, P. Pavan, C.M. Petrache, C. Rossi Alvarez, D. Rudolph, B. Rubio, W. Satuła, S. Skoda, P. Spolaore, H.G. Thomas, C.A. Ur, and R. Wyss. *Phys. Lett.*, B415:217, 1997.

[74] S.M. Fischer, C.J. Lister, D.P. Balamuth, R. Bauer, J.A. Becker, L.A. Bernstein, M.P. Carpenter, J. Durell, N. Fotiades, S.J. Freeman, P.E. Garett, P.A. Hausladen, R.V.F. Janssess, D. Jenkins, M. Leddy, J. Ressler, J. Schwartz, D. Svelyns, D.G. Sarantines, D. Seweryniak, B.J Varley, and R. Wyss. *Phys. Rev. Lett.*, 87:132501, 2001.

[75] R. Wyss and W. Satuła. *Acta Phys. Polonica*, B32:2457, 2001.

[76] S. Frauendorf and J.A. Sheikh. *Phys. Rev.*, C59:1400, 1999.

[77] A.L. Goodman. *Phys. Rev.*, C63:044325, 2001.

[78] J. Dobaczewski, J. Dudek, and R. Wyss. *Phys. Rev.*, C67:034308, 2003.

[79] K. Zając. *Acta Phys. Pol.*, B34:2241, 2003.

[80] K. Zając. *Int. J. Mod. Phys.*, E13:103–106, 2004.

[81] J. Engel, M. Bender, J. Dobaczewski, W. Nazarewicz, and R. Surman. *Phys. Rev.*, C60:014302, 1999.

[82] F. Simkovic, J. Schwieger, M. Veselsky, G. Pantis, and A. Faessler. *Phys. Lett.*, B393:267, 1997.

[83] J. Engel, S. Pittel, M. Stoitsov, P. Vogel, and J. Dukelsky. *Phys. Rev.*, C55:1781, 1997.

[84] F. Simkovic, M. Nowak, W.A. Kamiński, A.A. Raduta, and A. Faessler. *Phys. Rev.*, C64:035501, 2001.

[85] P. Sarriguren, E. Moya de Guerra, L. Pacearescu, A. Faessler, F. Simkovic, and A.A. Raduta. *Phys. Rev.*, C67:044313, 2003.

[86] E.P. Wigner. *Phys. Rev.*, 51:106, 1937.

[87] W. D. Myers. *Droplet model of atomic nuclei.* Plenum Press, New York, 1977.

[88] G. Audi, O. Bersillon, J. Blachot, and A.H. Wapstra. *Nucl. Phys.*, A729:3, 2003.

[89] D. G. Madland and R. Nix. New model of average neutron and proton pairing gaps. *Nucl. Phys.*, A476:1–38, 1988.

[90] J. Dobaczewski, P. Magierski, W. Nazarewicz, W. Satuła, and Z. Szymański. *Phys. Rev.*, C63:024308, 2001.

[91] W. Satuła, J. Dobaczewski, and W. Nazarewicz. *Phys. Rev. Lett*, 81:3599, 1998.

[92] A. Bohr and B.R. Mottelson. *Nuclear Structure.* Benjamin, New York, 1969.

[93] P. Vogel, B. Jonson, and P.G. Hansen. *Phys. Lett.*, B139:227, 1984.

[94] A.L. Goodman. *Adv. Nuc. Phys.*, 11:263–366, 1979.

[95] D. Gogny. Proceedings of the International Conference on Nuclear Selfonsistent fields, Trieste, 1975, 1975.

[96] P.J. Borycki, J. Dobaczewski, W. Nazarewicz, and M. Stoitsov. *Phys. Rev.*, C73:044319, 2006.

[97] M. Green and S.A. Moszkowski. *Phys. Rev.*, 139:B790, 1965.

[98] R.R. Chasman. *Phys. Rev.*, C14:1935, 1976.

[99] F. Tondeur. *Phys. Rev.*, A315:353, 1978.

[100] A.K. Dutta, J.-P. Arcoragi, J.M. Pearson, R. Behrman, and F. Tondeur. *Nucl. Phys.*, A548:77, 1986.

[101] F. Tondeur, A.K. Dutta, J.-P. Arcoragi, J.M. Pearson, and R. Behrman. *Nucl. Phys.*, A470:93, 1987.

[102] S.J. Krieger, P. Bonche, H. Flocard, P. Quentin, and M.S. Weiss. *Nucl. Phys.*, A517:275, 1990.

[103] A. Bulgac and Y. Yu. *Phys. Rev. Lett.*, 88:042504, 2003.

[104] A. Baran and K. Sieja. *Acta Phys. Polonica*, B35:1291, 2004.

[105] P. Quentin. *Journal de Physique*, 33:457, 1972.

[106] J.N. Ginocchio and J Weneser. *Phys. Rev.*, 170:859, 1968.

[107] O. Civitarese, P.O. Hess, J.G. Hirsch, and M. Reboiro. *Phys. Rev.*, C59:194, 1999.

[108] A.A. Raduta and E. Moya de Guerra. *Ann. Phys. (N.Y.)*, 284:134, 2000.

[109] W. Satuła and R. Wyss. *Phys. Rev. Lett.*, 86:4488, 2001.

[110] S. Głowacz, W. Satuła, and R. Wyss. nucl-th/0212086, 2002.

[111] I. Unna and J. Weneser. *Phys. Rev.*, 137:B1455, 1965.

[112] A. Kerman, R. Lawson, and M. Macfarlane. *Phys. Rev.*, 124:162, 1961.

[113] A. Góźdź, K. Pomorski, M. Brack, and E. Werner. *Nucl. Phys.*, A442:26–49, *ibid.* 50–67, 1985.

[114] A. Góźdź and K. Pomorski. *Nucl. Phys.*, A451:1–10, 1986.

[115] K. Sieja, A. Baran, and K. Pomorski. *Eur. Phys. J*, A20:413–418, 2004.

[116] K. Dietrich, H.J. Mang, and J.H Pradal. *Phys. Rev.*, 135:B22, 1964.

[117] H.J Lipkin. *Ann. Phys. (N.Y.)*, 9:272, 1960.

[118] Y. Nogami. *Phys. Rev.*, 134:B313, 1964.

[119] L. Bennour, P-H. Heenen, P. Bonche, J. Dobaczewski, and H. Flocard. *Phys. Rev.*, C40:2834, 1989.

[120] P. Quentin, N. Redon, J. Meyer, and M. Meyer. *Phys. Rev.*, C41:341, 1990.

[121] P. Magierski, S. Ćwiok, J. Dobaczewski, and W. Nazarewicz. *Phys. Rev.*, C48:1686, 1993.

[122] W. Satuła, R. Wyss, and P. Magierski. *Nucl. Phys.*, A578:45–61, 1993.

[123] H. Chandra and M.L. Rustgi. *Phys. Lett.*, B36:85, 1971.

[124] H. Chandra and M.L. Rustgi. *Phys. Rev.*, C4:874, 1971.

[125] P. Möller and J.R. Nix. *At. Data Nucl. Data Tables*, 26:165, 1981.

[126] R. Bengtsson and W. Nazarewicz. Proc. XIX Winter School of Physics, Zakopane 1984, 1984.

[127] J. Dobaczewski, W. Nazarewicz, J. Skalski, and T. Werner. *Phys. Rev. Lett.*, 60:2254, 1988.

[128] E. A. Stefanova, I. Stefanescu, G. de Angelis, D. Curien, J. Eberth, E. Farnea, A. Gadea, G. Gersch, A. Jungclaus, K. P. Lieb, T. Martinez, R. Schwengner, T. Steinhardt, O. Thelen, D. Weisshaar, and R. Wyss. *Phys. Rev.*, C63:014301, 2001.

[129] D. Ward, C.E. Svensson, I. Ragnarsson, C. Baktash, M.A. Bentley, M.P. Cameron, J.A. Carpenter, R.M. Clark, M. Cromaz, M.A. Deleplanque, M. Devlin, R.M. Diamond, P. Fallon, S. Flibotte, A. Galindo-Uribarri, D.S. Haslip, R.V.F. Janssens, T. Lampman, G.J. Lane, I.Y. Lee, F. Lerma, A.O. Macchiavelli, S.D. Paul, D. Radford, D. Rudolph, D.G. Sarantites, B. Schaly, D. Seweryniak, F.S. Stephens, O. Thelen, K. Vetter, J.C. Waddington, J.N. Wilson, and C.-H. Yu. *Phys. Rev.*, C63:014301, 2001.

[130] L. Chaturvedi, X. Zhao, A.V. Ramaya, J.H. Hamilton, J. Kormicki, S. Zhu, C. Girit, H. Xie, W.-B. Gao, Y.-R. Jiang, A. Petrovici, K.W. Schmid, A. Faessler, N.R. Johnson, C. Baktash, I. Y. Lee, F.K. McGowan, M.L. Halbert, M.A. Riley, J. H. McNeill, M.O. Kortelahti, J.D. Cole, R.B. Piercey, and H.Q. Jin. *Phys. Rev.*, C43:2541, 1991.

[131] A.P. de Lima, A.V. Ramaya, J.H. Hamilton, B. Van Nooijen, R.M. Ronningen, H. Kawakami, R.B. Piercey, E. de Lima, R. L. Robinson, H. J. Kim, L.K. Peker, F.A. Rickey, R. Popli, A.J. Caffrey, and J.C. Wells. *Phys. Rev.*, C23:213, 1981.

[132] L. Cleenman, J. Eberth, W. Neumann, N. Wiehl, and V. Zobel. *Nucl. Phys.*, A334:157, 1980.

[133] K. Kaneko, M. Hasegawa, and T. Mizusaki. *Phys. Rev.*, C71:044301, 2004.

[134] P. Sarriguren, E. Moya de Guerra, and A. Escuderos. *Nucl. Phys.*, A658:13, 1999.

[135] P.J. Ennis, C.J. Lister, W. Gelletly, H.G. Price, B.J. Varley, P.A. Butler, T. Hoare, S. Ćwiok, and W. Nazarewicz. *Nucl. Phys.*, A535:392, 1991.

[136] W. Nazarewicz, J. Dudek, R. Bengtsson, T. Bengtsson, and I. Ragnarsson. *Nucl. Phys.*, A435:397, 1985.

[137] H. Flocard, P. Quentin, A.K. Kerman, and D. Vautherin. *Nucl. Phys.*, A203:433–472, 1972.

[138] L. Bonneau and P. Quentin. *Phys. Rev.*, C72:014311, 2005.

[139] K. Sieja, A. Baran, and P. Quentin. *Physica Scripta*, T125:220–221, 2006.

[140] O. Civitarese, M. Reboiro, and P. Vogel. *Phys. Rev.*, C56:1840, 1996.

[141] A.V. Afanasjev and S. Frauendorf. *Phys. Rev.*, 2004.

[142] A. Baran and K. Sieja. *Int. J. Mod. Phys.*, E14:445–450, 2005.

[143] O. Civitarese and M. Reboiro. *Phys. Rev.*, C56:1179, 1996.

[144] J. Engel, K. Langanke, and P. Vogel. *Phys. Lett.*, B389:211–216, 1996.

[145] K. Sieja and A. Baran. *Acta Phys. Pol.*, B37:107–113, 2006.

[146] J. Aboussir, J.M. Pearson, A.K. Dutta, and F. Tondeur. *Atomic Data and Nuclear Data Tables*, 59:185, 1995.

[147] A. Baran, Z. Łojewski, and K. Sieja. nucl-th/0610101, 2007.

[148] M.V. Stoitsov, J. Dobaczewski, J. Kirchner, W. Nazarewicz, and J. Terasaki. nucl-th/0610061.

[149] M. Samyn, S. Goriely, P.H. Heenen, M. Bender, and J.M. Pearson. *Phys. Rev.*, C70:044309, 2004.

[150] M.K. Pal. *Theory of nuclear structure.* Paperback, 1983.

[151] N. Pillet. *PhD thesis, Universite Bordeaux 1.* 2000.

[152] T.L. Ha. *PhD thesis, Universite Bordeaux 1.* 2004.

[153] P. Quentin, H. Laftchiev, D. Samsoen, I.N. Mikhailov, and J. Libert. *Nucl. Phys.*, A734:477–480, 2004.

[154] J.Y. Zeng, T.H. Jin, and Z.J. Zhao. *Phys. Rev.*, C50:1388, 1994.

[155] O. Burglin and N. Rowley. *Nucl. Phys.*, A602:21, 1996.

[156] H. Molique and J. Dudek. *Phys. Rev.*, C56:1795, 1997.

[157] A. Volya, B.A. Brown, and V. Zelevinsky. *Phys. Lett.*, B509:37–42, 2001.

[158] C. Lanczös. *J. Res. Nat.*, B45:255, 1950.

[159] B.N. Parlett and D.S. Scott. *Math. Comp.*, 33(145):217, 1979.

[160] Kamila Sieja. presented at XXVIII Mazurian Lakes Conference on Physics, Piaski 2005, unpublished.

[161] B.H. Flowers and M. Vujicić. *Nucl. Phys.*, 49:586, 1963.

[162] K. Sieja, T.L. Ha, P. Quentin, and A. Baran. *Int. J. Mod. Phys.*, E16, 2007.

[163] D.R. Tuerpe, W.H. Bassichis, and A.K. Kerman. *Nucl. Phys.*, A142:49, 1970.

[164] R. Chasman and S. Wahlborn. *Nucl. Phys.*, A90:401, 1967.

[165] A. Baran and K. Sieja. in preparation.

Résumé

Récemment avec les nouvelles possibilitées d'études expérimentales de noyaux exotiques riches en proton, un regain d'intérêt s'est porté sur la problématique des correlations d'appariement proton-neutron. Ce travail a pour but l'étude des corrélations au delà du champ moyen et en particulier du pairing proton-neutron isoscalaire et isovecteur pour différents isotopes de Germanium $N \sim Z$. Nous avons d'abord traité l'approche BCS classique avec l'approximation Lipkin-Nogami (LN) de projection sur le bon nombre de particules en utilisant une interaction résiduelle de type contact. Ensuite dans une approche appelée Higher Tamm-Dancoff Approximation (HTDA) les corrélations proton-neutron ont été traitées en conservant explicitement le nombre de particules. Dans les deux cas, nous avons développé les codes numériques correspondants pour traiter les couplages proton-neutron. Les résultats des applications numériques pour quelques noyaux sont discutés et comparés dans les deux approches BCS(LN) et HTDA avec pairing isoscalaire et isovecteur. Nous avons montré que les deux approches donnent une description semblable des correlations du fondamental mais que la méthode HTDA est plus efficace dans le régime de faible pairing. Nous avons mis en evidence le rôle crucial de la conservation du nombre de particules pour la description des corrélations d'appariement proton-neutron. La prise en compte du pairing $T = 0$ genère une énergie de liaison supplémentaire pour les noyaux $N = Z$ conntribuant au terme d'énergie de Wigner.

Mots-clés : calculs microscopiques, champ moyen, approximation de Hartree-Fock, appariement proton-neutron, approximation de BCS, approximation Lipkin-Nogami, conservation de nombre de particules, noyaux exotiques

---

Abstract

Recently a revival of the interest on the subject of the proton-neutron pairing is taking place due to the experimental possibilities of extensive studying of exotic, proton-rich nuclei. The present work aims at investigating the correlations beyond the mean-field, especially isoscalar and isovector pairing in several $N \sim Z$ Ge nuclei. The studies were performed in the well-known BCS approach improved by the approximate Lipkin-Nogami (LN) projection onto a good particle number with the contact two-body force to account for the residual interaction. Then the approach explicitly conserving particle number called Higher Tamm-Dancoff Approximation (HTDA) was extended to take into account proton-neutron correlations. In both cases the numerical codes were rebuilt to include the possibility of the proton-neutron coupling. The results of numerical calculations obtained in BCS(LN) and HTDA approaches with isoscalar and isovector pairing for several nuclei are presented, discussed and compared. It is shown that both approaches give a similar picture of ground state correlations but the HTDA method is as well effective in low pairing regimes. The crucial role of the particle number conservation in the description of proton-neutron pairing correlations is confirmed. The inclusion of the $T = 0$ pairing lead to the appearance of the extra binding in the vicinity of the $N = Z$ nucleus which may be recognized as a contribution to the Wigner cusp.

Keywords: microscopic calculations, mean field, Hartree-Fock approximation, proton-neutron pairing, BCS approximation, Lipkin-Nogami method, particle number conservation, exotic nuclei